# The interplay between pathogenic bacteria and bacteriophage Chi: New directions in motility and phage-host interactions in Enterobacterales

Nathaniel C. Esteves

Dissertation submitted to the faculty of the Virginia Polytechnic Institute and State University in partial fulfillment of the requirements for the degree of

Doctor of Philosophy
In
Biological Sciences

Birgit E. Scharf, Chair
Clayton C. Caswell
Bryan B. Hsu
Brandon L. Jutras

April 5th, 2024
Blacksburg, VA

Keywords: phage, flagella, motility, pathogenic bacteria, virulence, phage therapy

**The interplay between pathogenic bacteria and bacteriophage Chi: New directions in motility and phage-host interactions in Enterobacterales**

Nathaniel C. Esteves

**Abstract**

The bacterial flagellum is a rotary motor that propels motile bacteria through their surroundings via swimming motility, or on surfaces via swarming motility. The flagellum is a key virulence factor for motile pathogenic bacteria. Viruses that infect bacteria via this appendage are known as flagellotropic or flagellum-dependent bacteriophages. Much like other phages, flagellotropic phages are of interest for clinical applications as antibacterial agents, particularly against multidrug resistant (MDR) bacteria. Bacteriophage χ is a flagellotropic phage that infects multiple species of motile pathogens. In the projects described below, we characterized several aspects of the complex interactions between χ and two of its hosts: *Salmonella enterica* and *Serratia marcescens*. In Chapter I, we describe in detail the existing knowledge on flagellum-dependent bacteriophages, pathogenic bacteria, and the flagellar motility system. We also expand significantly on flagellotropic phage χ. In Chapter II, we describe our discovery of *S. enterica* cellular components other than motility that are crucial for bacteriophage χ infection, making the key discovery that the AcrABZ-TolC multi-drug efflux system is required for infection to proceed. We additionally found that the host molecular chaperone trigger factor is important for the χ phage lifecycle. In Chapter III, we outline our characterization of the initial binding interaction between χ and the flagellum, determining that of flagellin's seven domains, C-terminal domain D2 is the most important for χ adsorption. In Chapter IV, we expand on this by discussing our work that determined that the χ tail fiber protein is encoded by the gene CHI_31, purification of this recombinantly-expressed protein, and demonstration of its direct interaction with the flagellar filament. Lastly, in Chapter V, our findings indicate that *S. marcescens* is able

to detect χ infection and lysis in the surroundings and alter gene expression, resulting in an increase in the production of the red pigment prodigiosin. Overall, our hypothetical model for χ infection is as follows: χ binds to the flagellum of its host using its single tail fiber, composed of monomers of the CHI_31 gene product gp31. This tail fiber interacts with CTD2 of flagellin, and the rotation of the flagellum brings the phage to the cell surface, where it interacts with AcrABZ-TolC to inject its genetic material into the host cytoplasm. At some point during the process of production of phage particles and subsequent cell lysis, the host molecular chaperone trigger factor likely assists with proper folding of χ proteins. After cell lysis, cells in the surroundings are capable of detecting lysis and responding accordingly, at least in the case of *S. marcescens*. This research is clinically relevant for a number of reasons. Phage therapy, the use of bacteriophages as antibacterial agents, requires knowledge of phage infection pathways for optimal implementation. The fact that the flagellum and a complex mediating MDR are both essential for χ infection leads to particular interest in χ for this application. Knowledge of the host-determining factors between χ and *Salmonella* may lead to the ability to alter the χ phage genome to target specific pathogenic *Salmonella* or *Escherichia coli* strains while avoiding disruption of beneficial bacterial communities.

# The interplay between pathogenic bacteria and bacteriophage Chi: New directions in motility and phage-host interactions in Enterobacterales

Nathaniel C. Esteves

## General audience abstract

Bacteriophages (phages) are viruses that only infect bacteria. They do not harm animal cells or the human body, despite being highly effective predators of bacteria. As such, they have applications in the medical field as antibacterial agents, similar to antibiotics. Phages that infect pathogenic bacteria like *Salmonella* are of particular interest for scientific research. Bacteriophage χ (Chi) infects bacteria by binding to their flagella, propeller-like appendages that a bacterial cell uses to swim through its surroundings. In many bacterial species, flagella and the ability to swim are closely involved in human infection. Due to this, flagellotropic (flagellum-dependent) phages like χ may be particularly useful as antibiotics. Throughout this project, we characterized the χ phage infection process, including exploring how it attaches to flagella, interactions it has on the surface of and inside *Salmonella* cells, and the largely unexplored relationship with *Serratia marcescens*, another bacterial species that causes illness in humans and is highly antibiotic resistant. Overall, our research contributes to the medical field, and indicates that χ may serve as a highly effective antibacterial treatment.

**Acknowledgments**

I acknowledge first and foremost Dr. Birgit Scharf for many years of guidance throughout my studies, and for providing me with the resources and direction I needed for success. I additionally thank Dr. Scharf for being a key inspiration for me in regard to my career plans, and for her many connections that opened doors for me that wouldn't have been possible otherwise.

My advisory committee members Drs. Clayton Caswell, Bryan Hsu, and Brandon Jutras in addition to Dr. Scharf exhibited great professionalism and gave me valuable guidance and feedback on my work, for which I am eternally grateful.

I deeply appreciate Dr. Floricel Gonzalez for her guidance and advice through my time as an undergraduate researcher and during the beginning of my graduate studies, as well as for being a good friend. Had Floricel not taken a chance by choosing me as an undergraduate assistant, I certainly would not be where I am today.

I also thank former graduate students Drs. Katie Broadway, Tim Arapov, Richard Sobe, Alfred Agbekudzi, and Lieutenant Dr. Karl Compton for help and support during my time in the Scharf lab, in addition to current lab members Foster Agyei, Abbey Horton, Dr. Nisha Dhiman, and Jackson Wood who have assisted me with various experiments and/or been very pleasant colleagues.

Sharat and Idella, I wish you the best during your transition to graduate school.

I am grateful for the help I received from the several talented undergraduate students that I mentored in the Scharf lab. Joshua Yoon and Rebecca Kelly greatly assisted me with characterizing the host range of bacteriophage χ. Danielle Bigham was very helpful in constructing and testing *Salmonella enterica* flagellin mutants' interactions with χ. Abbey Horton has done a good job studying flagellotropic phage Milano and has continued her time in

the Scharf lab as a master's student. Tony Samson and Bryce Brunelli helped further our knowledge on the χ phage tail fiber, and the interactions between χ and *Serratia marcescens*, respectively.

Ph.D. rotation students and mentees Marcel Shams Eddin, Rita Mahklouf, Manali Pathwardhan, Jackson Wood, and Chad Artman each explored new directions within my projects during their rotations in the Scharf lab, which I am grateful for. Jackson has since joined the lab and I am confident that he will make key discoveries that further our knowledge of χ (no pressure).

I am grateful to each of our current and former collaborators, including Edward Egelman (University of Virginia), James Smyth (Virginia Tech FBRI), Michael McClelland (UC Irvine), Karen Fahrner (Harvard), Clayton Caswell (Virginia Tech), and Richard Helm (Virginia Tech).

Thank you to Virginia Tech CeZAP and the Graduate Review Committee for selecting me to receive several research grants, scholarships, and fellowships.

Thank you to my parents, grandparents, and other family and close friends for constant support over the years. And to Amber: I could not have done all of this without you. Thank you for always being there for me and for these years of unwavering moral support.

**Attribution**

Chapters II and III constitute published journal articles that involved work that was aided by several colleagues.

Chapter II: Michael McClelland and Steffen Porwollik, Professor and Research Scientist at University of California Irvine, respectively, assisted with writing and revising the manuscript. They also assisted with certain experiments involving the construction of mutants and mutant libraries.

Chapter III: Danielle N. Bigham assisted in performing experiments, namely quantitative motility assays.

Table of Contents

Chapter I

# Introduction

Adapted from: Flagellotropic bacteriophages: Opportunities and challenges for antimicrobial applications

Published in: *International Journal of Molecular Sciences* (MDPI)

Nathaniel C. Esteves and Birgit E. Scharf

Department of Biological Sciences, Virginia Polytechnic Institute and State University,

Blacksburg, VA 24061, USA

Esteves NC, Scharf BE. Flagellotropic Bacteriophages: Opportunities and Challenges for Antimicrobial Applications. Int J Mol Sci. 2022 Jun 25;23(13):7084. doi: 10.3390/ijms23137084. PMID: 35806089; PMCID: PMC9266447.

ABSTRACT

Bacteriophages (phages) are the most abundant biological entities in the biosphere. As viruses that solely infect bacteria, phages have myriad healthcare and agricultural applications including phage therapy and antibacterial treatments in the foodservice industry. Phage therapy has been explored since the turn of the twentieth century but was no longer prioritized following the invention of antibiotics. As we approach a post-antibiotic society, phage therapy research has experienced a significant resurgence for usage against antibiotic-resistant bacteria, a growing concern in modern medicine. Phages are extraordinarily diverse, as are their host receptor targets. Flagellotropic (flagellum-dependent) phages begin their infection cycle by attaching to the flagellum of their motile host, however, later stages of the infection process of most of these phages remain elusive. Flagella are helical appendages required for swimming and swarming motility and are also of great importance for virulence in many pathogenic bacteria of clinical relevance. Not only is bacterial motility itself frequently important for virulence, as it allows pathogenic bacteria to move toward their host and find nutrients more effectively, flagella can also serve additional functions including mediating bacterial adhesion to surfaces. Flagella are also a potent antigen recognized by the human immune system. Phages utilizing the flagellum for infection are of particular interest due to the unique evolutionary tradeoff they force upon their hosts: by downregulating or abolishing motility to escape infection by a flagellotropic phage, a pathogenic bacterium would also likely attenuate its virulence. This factor may lead to flagellotropic phages becoming especially potent antibacterial agents. Bacteriophage χ, infecting three different genera of Enterobacterales pathogens, is no exception. In this Chapter, we discuss bacteriophages, flagella, flagellotropic phages, bacteriophage χ, and χ host bacteria.

## Phages among us

With an estimated total population of $10^{31}$, bacteriophages are by far the most abundant biological entities on earth, more than all others combined [1]. Within their diversity lies one of phages' greatest strengths as potential antibacterial agents: a bacteriophage-based treatment can be specifically tailored to an individual organism [2, 3], avoiding disruption of the natural bacterial flora. While a physician proposing the use of viruses as beneficial therapeutic agents to patients can be seen as suspicious to the layman, broadening knowledge in the field of phages will likely improve public opinion regarding phage therapy.

The majority of discovered bacteriophages and the vast majority of well-studied ones belong to the order *Caudovirales* [4], known also as tailed dsDNA phages encoding the HK97-fold major capsid protein [5]. This order is subdivided into three major families: *Myoviridae* (long contractile tails), *Siphoviridae* (long non-contractile tails), and *Podoviridae* (short non-contractile tails), all of which have distinct structural characteristics [4].

## Broader applications of the viruses of bacteria

Phage therapy is far from a new concept [6-8]. Frederick Twort and Felix d'Herelle are both credited with discovering phages independently of each other in 1915 and 1917, respectively. While Twort was unsure about the nature of the entity causing bacterial lysis, d'Herelle correctly characterized them as viruses parasitizing bacteria [7]. Immediately after their discovery near the turn of the 20$^{th}$ century, phages were used to treat bacterial infections [9]. D'Herelle himself cured bacterial dysentery multiple times using a phage treatment. Later, d'Herelle alongside George Eliava successfully employed phage treatments against *Vibrio cholerae* and *Yersinia*

*pestis* [7]. Phage therapy was utilized for decades, however with the discovery and popularization of antibiotics a few decades later, phages were largely forgotten as therapeutics [10]. As rates of antibiotic-resistant bacterial infections continue to rise precipitously, phage therapy research has regained its popularity [11-15]. Antibiotic resistance is a growing problem, with many multi-drug resistant (MDR) bacteria emerging every year, including the appearance of so called “pan-resistant” strains, which are resistant to all or nearly all antibiotics on the market [16-19]. A major downside of antibiotics when compared to phages is limited options. While the number of antibiotics on the market is a large but finite number, the number of phages in the world is practically infinite [1, 20, 21]. The fact that most phages are discovered in locations such as bodies of water, sewage, and infected animals is a testament to the number of new phages that can be found in these niches, which can potentially be isolated and applied in a useful context. The self-replicating nature of phages makes their isolation simple and straightforward [22, 23], with propagation being fairly trivial as well [24]. Their remarkable host specificity is an additional benefit, although this may also pose a drawback for broad-spectrum therapies [25, 26]. Upon identification of the bacterial pathogen causing an infection, a tailored phage treatment can be designed to target solely this species or serotype. However, host-phage specificity requires that the pathogenic species has been identified before treatment can be started. Antibiotics do not have this issue as broad-spectrum compounds are available [27-29]. This comes at a cost; broad-spectrum drugs such as the carbapenem class of antibiotics are known for their side effects, mostly due to the elimination of the natural bacterial flora [30-32]. Disruption of the delicate balance of organisms that live within us can lead to superinfections, where a single pathogen can take over following antibiotic treatment [33-35]. A tailored phage treatment would not eliminate natural flora, as phage specificity could avoid killing beneficial

organisms. Phages can also be genetically engineered to exhibit broad spectrum antimicrobial activity [26, 36-39], as this is necessary for the swift treatment of unknown and potentially lethal infections. Phage therapy is legal and commonly employed in several countries, including Georgia, Poland, and Russia [40], while it can only be used as a last resort in other countries including the United States, Australia, and a number of western European nations [12, 40].

Another applied use for phages is in the foodservice industry, where they are frequently used to protect produce from spoilage and to clean surfaces as preventive measure against particularly virulent pathogenic bacteria. Candidates for this application include pathogens such as *Listeria monocytogenes*, *Shigella dysenteriae*, Shiga-toxigenic *Escherichia coli*, *Salmonella enterica* serotype Typhi, and *Clostridium botulinum* [41-43]. Since phage-based products used in the foodservice industry are not used directly in live humans, these products are not subject to the strict FDA requirements that is a current roadblock to phage therapy [44].

**An exploitable evolutionary tradeoff**

An evolutionary tradeoff for bacteria refers to a stressful condition that cannot be easily avoided without introducing a different stressful condition [45-49]. Perhaps the most straightforward example in phage biology is infection via an antibiotic-resistance complex, such as an efflux pump. For instance, phage OMKO1 infects *Pseudomonas aeruginosa* via a multi-drug efflux system that mediates MDR [46]. The simplest way for the bacterium to develop resistance to OMKO1 is by repression of antibiotic pump gene transcription. This leads to reduced prevalence of the complex and thus results in the phage having more difficulty infecting the cells. If the efflux system mutates to become entirely non-functional, the mutant cell is completely resistant

to OMKO1. The tradeoff arises from the fact that by downregulating or mutating this multi-drug efflux pump, the bacterial cells become more susceptible to the substrates of the pump. In the case of OMKO1, this factor has been found to be exploitable by introducing phage and antibiotic simultaneously [46, 50].

The tradeoff for flagellotropic phages is quite a bit simpler. Flagellar motility is a crucial virulence factor for most motile pathogens, and abolishment of motility results in partial or sometimes complete attenuation of many organisms [51-55]. When a flagellotropic phage is present, there is huge selective pressure for the bacterial cells to repress motility. If motility is abolished, they become completely resistant to the phage posing a threat. However, this has the unintended and exploitable side effect of reducing virulence. Flagellotropic phages that additionally utilize other virulence factors as secondary receptors may be of particular interest.

**The flagellotropic phage niche – Phages and their myriad host receptors**

The infection processes of different phages are complex and distinct from one another. However, all phages must begin their infection by attaching to a receptor [56]. Bacterial phage receptors are as diverse as the viruses themselves, as are the receptor binding proteins (RBPs) produced by the phages [57, 58]. A receptor is a cellular component that a phage utilizes to attach to the cell. The receptor can also serve as a mechanism for ejection of viral DNA into its host, although this is not always the case [59-62]. It behooves a phage to utilize a receptor that is indispensable, or at least important, for its host [48, 63]. Otherwise, all a host cell must do to develop resistance is to no longer express the receptor that is being hijacked by the phage [63, 64]. It is for this reason that phages targeting crucial cellular components or virulence factors are of particular interest for

antimicrobial applications. Examples of virulence factors hijacked by bacteriophages include antibiotic efflux systems [46, 65], capsules [66], flagella [67], lipopolysaccharide (LPS) [66, 68], and pili [67].

**The bacterial flagellum**

The bacterial flagellum is a corkscrew-shaped appendage that is responsible for bacterial swimming and swarming motility, during which the flagellum rapidly rotates at speeds of greater than 1,000 Hz in genera such as *Vibrio*, with 100-300 Hz being a more typical rotation speed for most bacterial species [69]. In the archetypal flagellar assembly conserved across multiple phyla, the flagellar motor is a nanomachine powered by the proton motive force (PMF) or a $Na^+$ ion gradient which allows the cells to travel many cell-lengths per second [69-71]. The *E. coli* motor is bi-directional, capable of counterclockwise (CCW) and clockwise (CW) rotation [72-74]. When flagella rotate CCW, they form a tight flagellar bundle that propels the cell in a straight direction known as a run [73-75]. When any of the bundled flagella rotate CW, the bundle falls apart and the cell undergoes a tumble, during which it reorients itself randomly, altering its swimming direction. In contrast, some species of bacteria such as the alfalfa symbiont *Sinorhizobium* (*Ensifer*) *meliloti* have a unidirectional speed-variable motor that functions similarly; a sharp decrease in rotational speed, rather than switching the direction of rotation, results in a tumble [76]. Bacteria have mechanisms for sensing their environment, as it benefits them greatly to move toward nutrients and away from potential repellents. This is accomplished through a complex system known as chemotaxis, which allows bacterial cells to sense attractants or repellants in their environment via chemoreceptors and respond appropriately by biasing the

rotational direction or speed of the flagellum [77-81]. Effective chemotaxis in addition to motility are important virulence factors for many species of bacteria [52, 53].

The flagellum is composed of three main structures: the basal body, the flexible hook, and the corkscrew-shaped filament [54, 70, 82, 83]. The basal body serves as a structural anchor, polymerization platform, and secretion channel, and is required for torque generation and rotation. The filament is the "propeller" which pushes the bacterium through the medium, and the hook is the joint that connects the filament to the basal body [54, 84]. Different species of bacteria synthesize diverse numbers of flagella and organize them differently on the cell. Some produce numerous flagella while others produce a single flagellum. Some bacteria produce either one flagellum at one pole or one at each pole (polar) [85], distribute them randomly on the cell surface (peritrichous) [85], or in a single or in multiple clumps (lophotrichous) [86]. Flagellotropic bacteriophages are diverse but share the common trait of attachment to the filament of the flagellum being their initial infection step [87, 88]. The flagellar filament is composed of monomers of flagellin [54, 89]. These monomers polymerize into a helical pattern, forming the filament [90]. A single filament may contain up to 30,000 individual flagellin monomers [90] and can be 10-15 mm in length[54, 90], many times the length of the cell itself. Flagellin structure is highly variable yet shares important similarities across species [90]. Flagellin is typically composed of seven domains: two D0, D1, and D2 domains on the C- and N-terminal ends, and a hypervariable D3 domain in the center [89, 90]. When flagellin monomers are assembled into the flagellum, the D2 domains and the D3 domain face outward and form the major antigenic region, while the other domains are more conserved and interact with one another to form the filament [89]. Even within a given species, domains may have very low sequence conservation between strains and serotypes, can vary in length by up to 1,000

amino acid residues, or even be absent altogether [90]. Flagellin is also frequently modified post-translationally in various bacterial species. Types of modifications include glycosylation [91-93] and methylation [94]. There is also the important distinction between sheathed and unsheathed flagella. The sheath refers to a section of membrane that is wrapped around the entire flagellar filament [95, 96]. In organisms with sheathed flagella, the flagellar filament does not pierce the outer membrane of the cell, instead the membrane is secured at the base of the filament by a ring and envelops the entire flagellum [95, 96].

**Distinct advantages of the flagellotropic lifestyle**

Apart from the aforementioned evolutionary tradeoff, there are other advantages afforded to phages that utilize flagella as their receptors. Flagellar motility is a very costly process for the bacterial cell. The motor consistently utilizes the PMF generated by proton export from cellular metabolic processes [97-99]. This takes away from PMF energy that could otherwise be used for other crucial cellular functions. For this reason, flagellum production and function are very tightly regulated [74, 100-102]. Most bacteria alter expression of flagellar components in response to their environment. Factors such as reduced nutrient availability [103] and sub-optimal temperatures [104] frequently cause repression of motility, as the cell must save its energy for more essential processes for survival. Cells will generally not be motile if it would cause a significant fitness deficit to do so. For this reason, the flagellotropic phage lifestyle specifically selects for hosts that are ideal for viral replication. A cell with a fitness deficit that would result in reduced viral replication would also likely be non-motile. This reduces the likelihood that a flagellotropic phage will inadvertently infect a sub-optimal host.

Since phages have no motility, interaction with their hosts must occur randomly. The flagellum is a large appendage, frequently many times the length of the cell itself [90]. Therefore, the target for flagellotropic phages is much larger than for most other phages, such as those that use LPS or an outer membrane channel as receptors.

**Phage χ and its host bacteria**

Bacteriophage χ (sometimes referred to as ΦX prior to 1967 [105]) is probably the most well characterized flagellotropic phage. Bacteriophage χ was the first phage determined to be flagellum dependent, infecting multiple genera of Enterobacterales. Sertic & Boulgakov discovered χ in 1936 as a phage specific to flagellated bacteria [106]. Phage χ was then characterized much more in-depth in the 1960s by Elinor Meynell and Julius Adler [87, 105, 107]. Its most frequently studied host is *S. enterica*, of the family *Enterobacteriaceae*. *S. enterica* is an incredibly diverse species, and only some of its many serotypes are susceptible to phage χ. The closely related *Enterobacteriaceae* organism *E. coli* is also infected by χ [87], and this is also strain-dependent. Lastly, the more distantly related organism *Serratia marcescens* of the *Yersiniaceae* family is a host for χ [108]. Due to the diversity of its host range, it is certainly possible that χ may be capable of infecting other species of bacteria. This virulent S*iphoviridae* phage uses its approximately 220-nm long tail fiber to attach to the host flagellum by wrapping the fiber around the filament and using rotation to translocate to the cell surface [87, 109]. As a siphophage, χ has a long (~230 nm), non-contractile tail and an icosahedral capsid with a diameter of approximately 66 nm [110]. It has a 59,407-bp genome with 75 open reading frames [110], most of which have no annotated function. The tail fiber protein likely serves as a RBP for attachment to the main receptor, the flagellum. The flagellum is one of the main differences

between the unique serovars of *Salmonella* [111], so subtle variations in flagellar structure likely contribute to phage χ's selective host range. It is thought that the multi-substrate efflux system AcrAB/TolC serves as a secondary receptor for χ [65].

*Salmonella* is a ubiquitous genus of Gram-negative enteric bacteria, well known for causing gastroenteritis associated with foods such as raw chicken [112, 113]. *Salmonella* is the most common infectious agent triggering bacterial gastroenteritis [113]. In addition, certain Salmonellae can be highly virulent and invasive [114, 115], potentially reaching the bloodstream from the intestine and resulting in deadly bacteremia. *S. enterica* is a very broad species, containing over 2,500 individual serotypes [111], each with distinct phenotypes. These include serotypes such as Typhimurium, Enteritidis, and Newport, each of which cause gastroenteritis in humans but can be commensal in livestock. This is in contrast to serotype Typhi, a highly adapted human-specific pathogen causing Typhoid fever [116]. *Salmonella* is also the most comprehensively sequenced bacterial genus [117]. Many flagellotropic phages infecting *Salmonella* have been found, including the archetypal phage χ [105]. This phage has traditionally been studied in conjunction with the *S. enterica* serotype Typhimurium, one of the most common causes of gastroenteritis and a well-studied model organism. Strain ATCC 14028s is a pathogenic laboratory strain of *S.* Typhimurium. Pathogenic non-typhoidal Salmonellae like ATCC 14028s produce virulence factors including LPS and flagella [114, 118, 119]. S. Typhimurium is motile due to its flagella, and its flagellar motility system is well characterized and very similar to the *E. coli* system [120]. A unique feature of the *S. enterica* flagellar system is that many serotypes, including Typhimurium, have two flagellin genes, and express only one at a time. This is due to a inversible promoter that changes direction randomly due to the Hin invertase [121]. This inversion allows the *S.* Typhimurium cell to switch between producing the

phase 1 flagellin FliC, or the phase 2 flagellin FljB. *S.* Typhimurium flagellin is also methylated on lysine residues by the flagellin lysine methyltransferase FliB, a factor that has implications in virulence [122].

In addition to *S. enterica*, the related *Enterobacteriaceae* species *Escherichia coli* is also infected by χ. Most notably, the strain K-12 and its derivatives are hosts [87], provided they are motile. The host range of χ among other *E. coli* strains has not been explored. While K-12 is largely harmless to humans, some *E. coli* strains like the widespread O157:H7 are highly virulent intestinal pathogens producing severe and sometimes lethal illness in human hosts [123]. Virulence factors like Shiga toxin, flagella, and LPS can be found in certain pathogenic *E. coli* strains [124-126]. *Serratia marcescens*, a somewhat more distant relative of *S. enterica* and a member of the *Yersiniaceae* family, is the third known χ host species. This interaction is highly understudied, and only one publication characterizing χ infection of *S. marcescens* exists [108]. *S. marcescens* is distinct from the other two hosts as it is not a typical foodborne pathogen, and is generally incapable of infecting immunocompetent hosts. However, its robust biofilm formation [127] and frequent MDR [128] gives it a high mortality rate in the immunocompromised. *S. marcescens* is known for its vibrant red color due to the production of the red pigment prodigiosin [130].

Overall, flagellotropic phages have a unique infection pathway that leads to promising applications in healthcare. Their requirement for motility imposes an exploitable evolutionary tradeoff. Mechanisms of flagellotropic phage interactions with host bacteria are understudied, and significant work remains before applications can be realized.

REFERENCES


1. Clokie, M.R.; Millard, A.D.; Letarov, A.V.; and Heaphy, S., Phages in Nature. *Bacteriophage*, **2011**. 1(1): p. 31-45.

2. d'Herelle, F., Bacteriophage as a Treatment in Acute Medical and Surgical Infections. *Bull N Y Acad Med*, **1931**. 7(5): p. 329-48.

3. Romero-Calle, D.; Guimaraes Benevides, R.; Goes-Neto, A.; and Billington, C., Bacteriophages as Alternatives to Antibiotics in Clinical Care. *Antibiotics (Basel)*, **2019**. 8(3).

4. Ackermann, H.W., Tailed Bacteriophages: The Order Caudovirales. *Adv Virus Res*, **1998**. 51: p. 135-201.

5. Suhanovsky, M.M. and Teschke, C.M., Nature's Favorite Building Block: Deciphering Folding and Capsid Assembly of Proteins with the Hk97-Fold. *Virology*, **2015**. 479-480: p. 487-497.

6. Rehman, S.; Ali, Z.; Khan, M.; Bostan, N.; and Naseem, S., The Dawn of Phage Therapy. *Rev Med Virol*, **2019**. 29(4): p. e2041.

7. Chanishvili, N., Phage Therapy--History from Twort and D'herelle through Soviet Experience to Current Approaches. *Adv Virus Res*, **2012**. 83: p. 3-40.

8. Summers, W.C., The Strange History of Phage Therapy. *Bacteriophage*, **2012**. 2(2): p. 130-133.

9. d'Hérelle, F., *Le Bactériophage: Son Role Dans L'immunité*. 1921: Masson et cie.

10. Aminov, R.I., A Brief History of the Antibiotic Era: Lessons Learned and Challenges for the Future. *Front Microbiol*, **2010**. 1: p. 134-134.

11. Kortright, K.E.; Chan, B.K.; Koff, J.L.; and Turner, P.E., Phage Therapy: A Renewed Approach to Combat Antibiotic-Resistant Bacteria. *Cell Host Microbe*, **2019**. 25(2): p. 219-232.

12. Aswani, V.H. and Shukla, S.K., An Early History of Phage Therapy in the United States: Is It Time to Reconsider? *Clin Med Res*, **2021**. 19(2): p. 82-89.

13. Gelman, D.; Eisenkraft, A.; Chanishvili, N.; Nachman, D.; Coppenhagem Glazer, S.; and Hazan, R., The History and Promising Future of Phage Therapy in the Military Service. *J Trauma Acute Care Surg*, **2018**. 85(1S Suppl 2): p. S18-s26.

14. Steele, A.; Stacey, H.J.; de Soir, S.; and Jones, J.D., The Safety and Efficacy of Phage Therapy for Superficial Bacterial Infections: A Systematic Review. *Antibiotics (Basel)*, **2020**. 9(11).

15. Golkar, Z.; Bagasra, O.; and Pace, D.G., Bacteriophage Therapy: A Potential Solution for the Antibiotic Resistance Crisis. *J Infect Dev Ctries*, **2014**. 8(2): p. 129-36.

16. Maltezou, H.C., Metallo-Beta-Lactamases in Gram-Negative Bacteria: Introducing the Era of Pan-Resistance? *Int J Antimicrob Agents*, **2009**. 33(5): p. 405.e1-7.

17. Maseda, E.; Mensa, J.; Valía, J.C.; Gomez-Herreras, J.I.; Ramasco, F.; Samso, E.; Chiveli, M.A.; Pereira, J.; González, R.; Aguilar, G., et al., Bugs, Hosts and Icu Environment: Countering Pan-Resistance in Nosocomial Microbiota and Treating Bacterial Infections in the Critical Care Setting. *Rev Esp Anestesiol Reanim*, **2014**. 61(3): p. e1-e19.

18. Bathoorn, E.; Tsioutis, C.; da Silva Voorham, J.M.; Scoulica, E.V.; Ioannidou, E.; Zhou, K.; Rossen, J.W.; Gikas, A.; Friedrich, A.W.; and Grundmann, H., Emergence of Pan-Resistance in Kpc-2 Carbapenemase-Producing Klebsiella Pneumoniae in Crete, Greece: A Close Call. *J Antimicrob Chemother*, **2016**. 71(5): p. 1207-12.

19. Lv, F.; Cai, J.; He, Q.; Wang, W.; Luo, Y.; Wang, X.; Mi, N.; Zhao, Z.; Li, G.; and Luo, W., Overexpression of Efflux Pumps Mediate Pan Resistance of Klebsiella Pneumoniae Sequence Type 11. *Microb Drug Resist*, **2021**. 27(10): p. 1405-1411.

20. Dion, M.B.; Oechslin, F.; and Moineau, S., Phage Diversity, Genomics and Phylogeny. *Nat Rev Microbiol*, **2020**. 18(3): p. 125-138.

21. Jurczak-Kurek, A.; Gąsior, T.; Nejman-Faleńczyk, B.; Bloch, S.; Dydecka, A.; Topka, G.; Necel, A.; Jakubowska-Deredas, M.; Narajczyk, M.; and Richert, M., Biodiversity of Bacteriophages: Morphological and Biological Properties of a Large Group of Phages Isolated from Urban Sewage. *Sci Rep*, **2016**. 6(1): p. 1-17.

22. Aghaee, B.L.; Mirzaei, M.K.; Alikhani, M.Y.; and Mojtahedi, A., Sewage and Sewage-Contaminated Environments Are the Most Prominent Sources to Isolate Phages against Pseudomonas Aeruginosa. *BMC Microbiology*, **2021**. 21(1): p. 1-8.

23. Pelzek, A.J.; Schuch, R.; Schmitz, J.E.; and Fischetti, V.A., Isolation of Bacteriophages from Environmental Sources, and Creation and Functional Screening of Phage DNA Libraries. *Current protocols essential laboratory techniques*, **2013**. 7(1): p. 13.3. 1-13.3. 35.

24. Bonilla, N.; Rojas, M.I.; Netto Flores Cruz, G.; Hung, S.-H.; Rohwer, F.; and Barr, J.J., Phage on Tap-a Quick and Efficient Protocol for the Preparation of Bacteriophage Laboratory Stocks. *PeerJ*, **2016**. 4: p. e2261-e2261.

25. Koskella, B. and Meaden, S., Understanding Bacteriophage Specificity in Natural Microbial Communities. *Viruses*, **2013**. 5(3): p. 806-823.

26. Ross, A.; Ward, S.; and Hyman, P., More Is Better: Selecting for Broad Host Range Bacteriophages. *Front Microbiol*, **2016**. 7: p. 1352-1352.

27. Singh, S.B.; Young, K.; and Silver, L.L., What Is an "Ideal" Antibiotic? Discovery Challenges and Path Forward. *Biochem Pharmacol*, **2017**. 133: p. 63-73.

28. Picconi, P.; Hind, C.K.; Nahar, K.S.; Jamshidi, S.; Di Maggio, L.; Saeed, N.; Evans, B.; Solomons, J.; Wand, M.E.; Sutton, J.M., et al., New Broad-Spectrum Antibiotics Containing a Pyrrolobenzodiazepine Ring with Activity against Multidrug-Resistant Gram-Negative Bacteria. *J Med Chem*, **2020**. 63(13): p. 6941-6958.

29. Richter, M.F. and Hergenrother, P.J., The Challenge of Converting Gram-Positive-Only Compounds into Broad-Spectrum Antibiotics. *Ann N Y Acad Sci*, **2019**. 1435(1): p. 18-38.

30. Sun, Q.; Wang, Z.L.; Liu, X.C.; Ji, Y.C.; He, Y.; Ai, Q.; and Li, L.Q., Effect of the Course of Treatment with Broad-Spectrum Antibiotics on Intestinal Flora and Short-Chain Fatty Acids in Feces of Very Low Birth Weight Infants: A Prospective Study. *Zhongguo Dang Dai Er Ke Za Zhi*, **2021**. 23(10): p. 1008-1014.

31. Angelucci, F.; Cechova, K.; Amlerova, J.; and Hort, J., Antibiotics, Gut Microbiota, and Alzheimer's Disease. *J Neuroinflammation*, **2019**. 16(1): p. 108.

32. van Werkhoven, C.H.; Ducher, A.; Berkell, M.; Mysara, M.; Lammens, C.; Torre-Cisneros, J.; Rodríguez-Baño, J.; Herghea, D.; Cornely, O.A.; Biehl, L.M., et al., Incidence and Predictive Biomarkers of Clostridioides Difficile Infection in Hospitalized Patients Receiving Broad-Spectrum Antibiotics. *Nat Commun*, **2021**. 12(1): p. 2240.

33. Tan, Y.X.; Wong, G.W.; and Tan, Y.H., Superinfection Associated with Prolonged Antibiotic Use in Non-Ventilator Associated Hospital-Acquired Pneumonia. *Int J Clin Pharm*, **2021**. 43(6): p. 1555-1562.

34. Al Muqati, H.; Al Turaiki, A.; Al Dhahri, F.; Al Enazi, H.; and Althemery, A., Superinfection Rate among the Patients Treated with Carbapenem Versus Piperacillin/Tazobactam: Retrospective Observational Study. *J Infect Public Health*, **2021**. 14(3): p. 306-310.

35. Verdugo, F.; Laksmana, T.; and Uribarri, A., Systemic Antibiotics and the Risk of Superinfection in Peri-Implantitis. *Arch Oral Biol*, **2016**. 64: p. 39-50.

36. Dunne, M.; Prokhorov, N.S.; Loessner, M.J.; and Leiman, P.G., Reprogramming Bacteriophage Host Range: Design Principles and Strategies for Engineering Receptor Binding Proteins. *Curr Opin Biotechnol*, **2021**. 68: p. 272-281.

37. Holtzman, T.; Globus, R.; Molshanski-Mor, S.; Ben-Shem, A.; Yosef, I.; and Qimron, U., A Continuous Evolution System for Contracting the Host Range of Bacteriophage T7. *Sci Rep*, **2020**. 10(1): p. 307.

38. Yehl, K.; Lemire, S.; Yang, A.C.; Ando, H.; Mimee, M.; Torres, M.T.; de la Fuente-Nunez, C.; and Lu, T.K., Engineering Phage Host-Range and Suppressing Bacterial Resistance through Phage Tail Fiber Mutagenesis. *Cell*, **2019**. 179(2): p. 459-469.e9.

39. Dunne, M.; Rupf, B.; Tala, M.; Qabrati, X.; Ernst, P.; Shen, Y.; Sumrall, E.; Heeb, L.; Plückthun, A.; Loessner, M.J., et al., Reprogramming Bacteriophage Host Range through Structure-Guided Design of Chimeric Receptor Binding Proteins. *Cell Rep*, **2019**. 29(5): p. 1336-1350.e4.

40. Cesta, N.; Di Luca, M.; Corbellino, M.; Tavio, M.; Galli, M.; and Andreoni, M., Bacteriophage Therapy: An Overview and the Position of Italian Society of Infectious and Tropical Diseases. *Infez Med*, **2020**. 28(3): p. 322-331.

41. Sillankorva, S.M.; Oliveira, H.; and Azeredo, J., Bacteriophages and Their Role in Food Safety. *Int J Microbiol*, **2012**. 2012: p. 863945-863945.

42. Moye, Z.D.; Woolston, J.; and Sulakvelidze, A., Bacteriophage Applications for Food Production and Processing. *Viruses*, **2018**. 10(4): p. 205.

43. Endersen, L. and Coffey, A., The Use of Bacteriophages for Food Safety. *Current Opinion in Food Science*, **2020**. 36: p. 1-8.

44. Sarhan, W.A. and Azzazy, H.M., Phage Approved in Food, Why Not as a Therapeutic? *Expert Rev Anti Infect Ther*, **2015**. 13(1): p. 91-101.

45. Burmeister, A.R.; Fortier, A.; Roush, C.; Lessing, A.J.; Bender, R.G.; Barahman, R.; Grant, R.; Chan, B.K.; and Turner, P.E., Pleiotropy Complicates a Trade-Off between Phage Resistance and Antibiotic Resistance. *Proc Natl Acad Sci U S A*, **2020**. 117(21): p. 11207-11216.

46. Chan, B.K.; Sistrom, M.; Wertz, J.E.; Kortright, K.E.; Narayan, D.; and Turner, P.E., Phage Selection Restores Antibiotic Sensitivity in Mdr Pseudomonas Aeruginosa. *Sci Rep*, **2016**. 6(1): p. 26717.

47. Dessau, M.; Goldhill, D.; McBride, R.L.; Turner, P.E.; and Modis, Y., Selective Pressure Causes an Rna Virus to Trade Reproductive Fitness for Increased Structural and Thermal Stability of a Viral Enzyme. *PLoS Genetics*, **2012**. 8(11): p. e1003102.

48. Burmeister, A.R.; Sullivan, R.M.; and Lenski, R.E., Fitness Costs and Benefits of Resistance to Phage Lambda in Experimentally Evolved Escherichia Coli, in Evolution in Action: Past, Present and Future. 2020, Springer. p. 123-143.

49. Goldhill, D.H. and Turner, P.E., The Evolution of Life History Trade-Offs in Viruses. *Curr Opin Virol*, **2014**. 8: p. 79-84.

50. Chan, B.K.; Turner, P.E.; Kim, S.; Mojibian, H.R.; Elefteriades, J.A.; and Narayan, D., Phage Treatment of an Aortic Graft Infected with Pseudomonas Aeruginosa. *Evolution, Medicine, and Public Health*, **2018**. 2018(1): p. 60-66.

51. Gu, H., Role of Flagella in the Pathogenesis of *Helicobacter Pylori*. *Curr Microbiol*, **2017**. 74(7): p. 863-869.

52. Duan, Q.; Zhou, M.; Zhu, L.; and Zhu, G., Flagella and Bacterial Pathogenicity. *J Basic Microbiol*, **2013**. 53(1): p. 1-8.

53. Jonson, A.B.; Normark, S.; and Rhen, M., Fimbriae, Pili, Flagella and Bacterial Virulence. *Contrib Microbiol*, **2005**. 12: p. 67-89.

54. Zhou, M.; Yang, Y.; Chen, P.; Hu, H.; Hardwidge, P.R.; and Zhu, G., More Than a Locomotive Organelle: Flagella in *Escherichia Coli*. *Appl Microbiol Biotechnol*, **2015**. 99(21): p. 8883-90.

55. Stevenson, E.; Minton, N.P.; and Kuehne, S.A., The Role of Flagella in Clostridium Difficile Pathogenicity. *Trends Microbiol*, **2015**. 23(5): p. 275-82.

56. Bertozzi Silva, J.; Storms, Z.; and Sauvageau, D., Host Receptors for Bacteriophage Adsorption. *FEMS Microbiol Lett*, **2016**. 363(4): p. fnw002.

57. Dowah, A.S.A. and Clokie, M.R.J., Review of the Nature, Diversity and Structure of Bacteriophage Receptor Binding Proteins That Target Gram-Positive Bacteria. *Biophys Rev*, **2018**. 10(2): p. 535-542.

58. Shin, H.; Lee, J.H.; Kim, H.; Choi, Y.; Heu, S.; and Ryu, S., Receptor Diversity and Host Interaction of Bacteriophages Infecting *Salmonella Enterica* Serovar Typhimurium. *PLoS One*, **2012**. 7(8): p. e43392.

59. Grayson, P. and Molineux, I.J., Is Phage DNA 'Injected' into Cells--Biologists and Physicists Can Agree. *Curr Opin Microbiol*, **2007**. 10(4): p. 401-9.

60. Rossmann, M.G.; Mesyanzhinov, V.V.; Arisaka, F.; and Leiman, P.G., The Bacteriophage T4 DNA Injection Machine. *Curr Opin Struct Biol*, **2004**. 14(2): p. 171-80.

61. Watanabe, K.; Ishibashi, K.; Nakashima, Y.; and Sakurai, T., A Phage-Resistant Mutant of Lactobacillus Casei Which Permits Phage Adsorption but Not Genome Injection. *J Gen Virol*, **1984**. 65 ( Pt 5): p. 981-6.

62. Garcia-Doval, C. and van Raaij, M.J., Bacteriophage Receptor Recognition and Nucleic Acid Transfer. *Subcell Biochem*, **2013**. 68: p. 489-518.

63. Stern, A. and Sorek, R., The Phage-Host Arms Race: Shaping the Evolution of Microbes. *Bioessays*, **2011**. 33(1): p. 43-51.

64. Burmeister, A.R. and Turner, P.E., Trading-Off and Trading-up in the World of Bacteria–Phage Evolution. *Current Biology*, **2020**. 30(19): p. R1120-R1124.

65. Esteves, N.C.; Porwollik, S.; McClelland, M.; and Scharf, B.E., The Multi-Drug Efflux System Acrabz-Tolc Is Essential for Infection of *Salmonella* Typhimurium by the Flagellum-Dependent Bacteriophage Chi. *J Virol*, **2021**. 95(11).

66. Gong, Q.; Wang, X.; Huang, H.; Sun, Y.; Qian, X.; Xue, F.; Ren, J.; Dai, J.; and Tang, F., Novel Host Recognition Mechanism of the K1 Capsule-Specific Phage of Escherichia Coli: Capsular Polysaccharide as the First Receptor and Lipopolysaccharide as the Secondary Receptor. *J Virol*, **2021**. 95(18): p. e0092021.

67. Tittes, C.; Schwarzer, S.; and Quax, T.E.F., Viral Hijack of Filamentous Surface Structures in Archaea and Bacteria. *Viruses*, **2021**. 13(2).

68. Gonzalez, F.; Helm, R.F.; Broadway, K.M.; and Scharf, B.E., More Than Rotating Flagella: Lipopolysaccharide as a Secondary Receptor for Flagellotropic Phage 7-7-1. *J Bacteriol*, **2018**. 200(19).

69. Magariyama, Y.; Sugiyama, S.; and Kudo, S., Bacterial Swimming Speed and Rotation Rate of Bundled Flagella. *FEMS Microbiol Lett*, **2001**. 199(1): p. 125-9.

70. Nakamura, S. and Minamino, T., Flagella-Driven Motility of Bacteria. *Biomolecules*, **2019**. 9(7).

71. Berry, R.M. and Armitage, J.P., The Bacterial Flagella Motor. *Adv Microb Physiol*, **1999**. 41: p. 291-337.

72. Morehouse, K.A.; Goodfellow, I.G.; and Sockett, R.E., A Chimeric N-Terminal Escherichia Coli--C-Terminal Rhodobacter Sphaeroides Flig Rotor Protein Supports Bidirectional E. Coli Flagellar Rotation and Chemotaxis. *J Bacteriol*, **2005**. 187(5): p. 1695-701.

73. Kumar, M.S. and Philominathan, P., The Physics of Flagellar Motion of E. Coli During Chemotaxis. *Biophys Rev*, **2010**. 2(1): p. 13-20.

74. Fukuoka, H.; Inoue, Y.; and Ishijima, A., Coordinated Regulation of Multiple Flagellar Motors by the Escherichia Coli Chemotaxis System. *Biophysics (Nagoya-shi)*, **2012**. 8: p. 59-66.

75. Sarkar, M.K.; Paul, K.; and Blair, D., Chemotaxis Signaling Protein Chey Binds to the Rotor Protein Flin to Control the Direction of Flagellar Rotation in Escherichia Coli. *Proc Natl Acad Sci U S A*, **2010**. 107(20): p. 9370-5.

76. Scharf, B. and Schmitt, R., Sensory Transduction to the Flagellar Motor of Sinorhizobium Meliloti. *J Mol Microbiol Biotechnol*, **2002**. 4(3): p. 183-6.

77. Lux, R. and Shi, W., Chemotaxis-Guided Movements in Bacteria. *Crit Rev Oral Biol Med*, **2004**. 15(4): p. 207-20.

78. Vladimirov, N. and Sourjik, V., Chemotaxis: How Bacteria Use Memory. *Biol Chem*, **2009**. 390(11): p. 1097-104.

79. Tola, Y.H.; Fujitani, Y.; and Tani, A., Bacteria with Natural Chemotaxis Towards Methanol Revealed by Chemotaxis Fishing Technique. *Biosci Biotechnol Biochem*, **2019**. 83(11): p. 2163-2171.

80. Jakuszeit, T.; Lindsey-Jones, J.; Peaudecerf, F.J.; and Croze, O.A., Migration and Accumulation of Bacteria with Chemotaxis and Chemokinesis. *Eur Phys J E Soft Matter*, **2021**. 44(3): p. 32.

81. Adler, J., Chemotaxis in Bacteria. *Annu Rev Biochem*, **1975**. 44: p. 341-56.

82. Grognot, M. and Taute, K.M., More Than Propellers: How Flagella Shape Bacterial Motility Behaviors. *Curr Opin Microbiol*, **2021**. 61: p. 73-81.

83. Silverman, M. and Simon, M.I., Bacterial Flagella. *Annu Rev Microbiol*, **1977**. 31: p. 397-419.

84. Samatey, F.A.; Matsunami, H.; Imada, K.; Nagashima, S.; Shaikh, T.R.; Thomas, D.R.; Chen, J.Z.; Derosier, D.J.; Kitao, A.; and Namba, K., Structure of the Bacterial Flagellar Hook and Implication for the Molecular Universal Joint Mechanism. *Nature*, **2004**. 431(7012): p. 1062-8.

85. Fujii, M.; Shibata, S.; and Aizawa, S., Polar, Peritrichous, and Lateral Flagella Belong to Three Distinguishable Flagellar Families. *J Mol Biol*, **2008**. 379(2): p. 273-83.

86. Constantino, M.A.; Jabbarzadeh, M.; Fu, H.C.; Shen, Z.; Fox, J.G.; Haesebrouck, F.; Linden, S.K.; and Bansil, R., Bipolar Lophotrichous Helicobacter Suis Combine Extended and Wrapped Flagella Bundles to Exhibit Multiple Modes of Motility. *Sci Rep*, **2018**. 8(1): p. 14415.

87. Schade, S.Z.; Adler, J.; and Ris, H., How Bacteriophage χ Attacks Motile Bacteria. *J Virol*, **1967**. 1(3): p. 599.

88. Yen, J.Y.; Broadway, K.M.; and Scharf, B.E., Minimum Requirements of Flagellation and Motility for Infection of Agrobacterium Sp. Strain H13-3 by Flagellotropic Bacteriophage 7-7-1. *Appl Environ Microbiol*, **2012**. 78(20): p. 7216-22.

89. Fedorov, O.V. and Kostyukova, A.S., Domain Structure of Flagellin. *FEBS Lett*, **1984**. 171(1): p. 145-8.

90. Beatson, S.A.; Minamino, T.; and Pallen, M.J., Variation in Bacterial Flagellins: From Sequence to Structure. *Trends Microbiol*, **2006**. 14(4): p. 151-5.

91. Logan, S.M., Flagellar Glycosylation - a New Component of the Motility Repertoire? *Microbiology (Reading)*, **2006**. 152(Pt 5): p. 1249-1262.

92. Merino, S. and Tomás, J.M., Gram-Negative Flagella Glycosylation. *Int J Mol Sci*, **2014**. 15(2): p. 2840-57.

93. Twine, S.M.; Paul, C.J.; Vinogradov, E.; McNally, D.J.; Brisson, J.R.; Mullen, J.A.; McMullin, D.R.; Jarrell, H.C.; Austin, J.W.; Kelly, J.F., et al., Flagellar Glycosylation in Clostridium Botulinum. *FEBS J*, **2008**. 275(17): p. 4428-44.

94. Wang, C.; Nehls, C.; Baabe, D.; Burghaus, O.; Hurwitz, R.; Gutsmann, T.; Bröring, M.; and Kolbe, M., Flagellin Lysine Methyltransferase Flib Catalyzes a [4fe-4s] Mediated Methyl Transfer Reaction. *PLOS Pathog*, **2021**. 17(11): p. e1010052.

95. Zhu, S.; Nishikino, T.; Hu, B.; Kojima, S.; Homma, M.; and Liu, J., Molecular Architecture of the Sheathed Polar Flagellum in Vibrio Alginolyticus. *Proc Natl Acad Sci U S A*, **2017**. 114(41): p. 10966-10971.

96. Fuerst, J.A., Bacterial Sheathed Flagella and the Rotary Motor Model for the Mechanism of Bacterial Motility. *J Theor Biol*, **1980**. 84(4): p. 761-74.

97. Chen, M.T. and Lo, C.J., Using Biophysics to Monitor the Essential Protonmotive Force in Bacteria. *Adv Exp Med Biol*, **2016**. 915: p. 69-79.

98. Konings, W.N.; Hellingwerf, K.J.; and Elferink, M.G., The Interaction between Electron Transfer, Proton Motive Force and Solute Transport in Bacteria. *Antonie Van Leeuwenhoek*, **1984**. 50(5-6): p. 545-55.

99. Iqbal, A.; Panta, P.R.; Ontoy, J.; Bruno, J.; Ham, J.H.; and Doerrler, W.T., Chemical or Genetic Alteration of Proton Motive Force Results in Loss of Virulence of Burkholderia Glumae, the Cause of Rice Bacterial Panicle Blight. *Appl Environ Microbiol*, **2021**. 87(18): p. e0091521.

100. Soutourina, O.A. and Bertin, P.N., Regulation Cascade of Flagellar Expression in Gram-Negative Bacteria. *FEMS Microbiol Rev*, **2003**. 27(4): p. 505-23.

101. Barembruch, C. and Hengge, R., Cellular Levels and Activity of the Flagellar Sigma Factor Flia of Escherichia Coli Are Controlled by Flgm-Modulated Proteolysis. *Mol Microbiol*, **2007**. 65(1): p. 76-89.

102. McCarter, L.L., Regulation of Flagella. *Curr Opin Microbiol*, **2006**. 9(2): p. 180-6.

103. Thomason, M.K.; Fontaine, F.; De Lay, N.; and Storz, G., A Small Rna That Regulates Motility and Biofilm Formation in Response to Changes in Nutrient Availability in Escherichia Coli. *Mol Microbiol*, **2012**. 84(1): p. 17-35.

104. Rudenko, I.; Ni, B.; Glatter, T.; and Sourjik, V., Inefficient Secretion of Anti-Sigma Factor Flgm Inhibits Bacterial Motility at High Temperature. *iScience*, **2019**. 16: p. 145-154.

105. MEYNELL, E.W., A Phage, Øχ, Which Attacks Motile Bacteria. *Microbiology*, **1961**. 25(2): p. 253-290.

106. Sertić, V. and Boulgakov, N.A. Bacteriophages Specific for Flagellated Forms of Bacteria. 1936.

107. Schade, S. and Adler, J., Purification and Chemistry of Bacteriophage Chi. *J Virol*, **1967**. 1(3): p. 591-8.

108. Iino, T. and Mitani, M., Infection of *Serratia Marcescens* by Bacteriophage Chi. *J Virol*, **1967**. 1(2): p. 445-447.

109. Samuel, A.D.; Pitta, T.P.; Ryu, W.S.; Danese, P.N.; Leung, E.C.; and Berg, H.C., Flagellar Determinants of Bacterial Sensitivity to Chi-Phage. *Proc Natl Acad Sci U S A*, **1999**. 96(17): p. 9863-9866.

110. Hendrix, R.W.; Ko, C.-C.; Jacobs-Sera, D.; Hatfull, G.F.; Erhardt, M.; Hughes, K.T.; and Casjens, S.R., Genome Sequence of *Salmonella* Phage X. *Genome Announc*, **2015**. 3(1): p. e01229-14.

111. Grimont, P.A. and Weill, F.-X., Antigenic Formulae of the *Salmonella* Serovars.

112. Ahmer, B.M.M. and Gunn, J.S., Interaction of *Salmonella* Spp. With the Intestinal Microbiota. *Frontiers in microbiology*, **2011**. 2: p. 101-101.

113. Jajere, S.M., A Review of *Salmonella Enterica* with Particular Focus on the Pathogenicity and Virulence Factors, Host Specificity and Antimicrobial Resistance Including Multidrug Resistance. *Vet World*, **2019**. 12(4): p. 504-521.

114. Dos Santos, A.M.P.; Ferrari, R.G.; and Conte-Junior, C.A., Virulence Factors in *Salmonella* Typhimurium: The Sagacity of a Bacterium. *Curr Microbiol*, **2019**. 76(6): p. 762-773.

115. Huang, K.-Y.; Wang, Y.-H.; Chien, K.-Y.; Janapatla, R.P.; and Chiu, C.-H., Hyperinvasiveness of *Salmonella Enterica* Serovar Choleraesuis Linked to Hyperexpression of Type Iii Secretion Systems in Vitro. *Sci Rep*, **2016**. 6: p. 37642-37642.

116. Marchello, C.S.; Hong, C.Y.; and Crump, J.A., Global Typhoid Fever Incidence: A Systematic Review and Meta-Analysis. *Clin Infect Dis*, **2019**. 68(Suppl 2): p. S105-s116.

117. Amoutzias, G.D.; Nikolaidis, M.; and Hesketh, A., The Notable Achievements and the Prospects of Bacterial Pathogen Genomics. *Microorganisms*, **2022**. 10(5): p. 1040.

118. Licht, T.R.; Krogfelt, K.A.; Cohen, P.S.; Poulsen, L.K.; Urbance, J.; and Molin, S., Role of Lipopolysaccharide in Colonization of the Mouse Intestine by Salmonella Typhimurium Studied by in Situ Hybridization. *Infect Immun*, **1996**. 64(9): p. 3811-7.

119. Sivasankar, C.; Lloren, K.K.S.; and Lee, J.H., Deciphering the Interrelationship of Arnt Involved in Lipid-a Alteration with the Virulence of Salmonella Typhimurium. *Int J Mol Sci*, **2024**. 25(5).

120. Aizawa, S.I., Flagellar Assembly in Salmonella Typhimurium. *Mol Microbiol*, **1996**. 19(1): p. 1-5.

121. Bonifield, H.R. and Hughes, K.T., Flagellar Phase Variation in *Salmonella Enterica* Is Mediated by a Posttranscriptional Control Mechanism. *J Bacteriol*, **2003**. 185(12): p. 3567-3574.

122. Horstmann, J.A.; Lunelli, M.; Cazzola, H.; Heidemann, J.; Kühne, C.; Steffen, P.; Szefs, S.; Rossi, C.; Lokareddy, R.K.; Wang, C., et al., Methylation of *Salmonella* Typhimurium Flagella Promotes Bacterial Adhesion and Host Cell Invasion. *Nat Commun*, **2020**. 11(1): p. 2013.

123. Wachsmuth, I.K.; Griffin, P.M.; and Wells, J.G., *Escherichia Coli* O157:H7, a Cause of Hemorrhagic Colitis and Hemolytic Uremic Syndrome. *Acta Paediatr Jpn*, **1991**. 33(5): p. 603-12.

124. Newell, D.G. and La Ragione, R.M., Enterohaemorrhagic and Other Shiga Toxin-Producing Escherichia Coli (Stec): Where Are We Now Regarding Diagnostics and Control Strategies? *Transbound Emerg Dis*, **2018**. 65 Suppl 1: p. 49-71.

125. Wolfson, E.B.; Elvidge, J.; Tahoun, A.; Gillespie, T.; Mantell, J.; McAteer, S.P.; Rossez, Y.; Paxton, E.; Lane, F.; Shaw, D.J., et al., The Interaction of Escherichia Coli O157:H7 and Salmonella Typhimurium Flagella with Host Cell Membranes and Cytoskeletal Components. *Microbiology (Reading)*, **2020**. 166(10): p. 947-965.

126. Youn, M.; Lee, K.M.; Kim, S.H.; Lim, J.; Yoon, J.W.; and Park, S., Escherichia Coli O157:H7 Lps O-Side Chains and Po157 Are Required for Killing Caenorhabditis Elegans. *Biochem Biophys Res Commun*, **2013**. 436(3): p. 388-93.

127. Ray, C.; Shenoy, A.T.; Orihuela, C.J.; and González-Juarbe, N., Killing of *Serratia Marcescens* Biofilms with Chloramphenicol. *Ann Clin Microbiol Antimicrob*, **2017**. 16(1): p. 19.

128. Wilfert, J.N.; Barrett, F.F.; Ewing, W.H.; Finland, M.; and Kass, E.H., *Serratia Marcescens*: Biochemical, Serological, and Epidemiological Characteristics and Antibiotic Susceptibility of Strains Isolated at Boston City Hospital. *Appl Microbiol*, **1970**. 19(2): p. 345-52.

129. O'Rear, J.; Alberti, L.; and Harshey, R.M., Mutations That Impair Swarming Motility in *Serratia Marcescens* 274 Include but Are Not Limited to Those Affecting Chemotaxis or Flagellar Function. *J Bacteriol*, **1992**. 174(19): p. 6125-37.

130. Lin, S.-R.; Chen, Y.-H.; Tseng, F.-J.; and Weng, C.-F., The Production and Bioactivity of Prodigiosin: Quo Vadis? *Drug Discov Today*, **2020**. 25(5): p. 828-836.

FIGURES

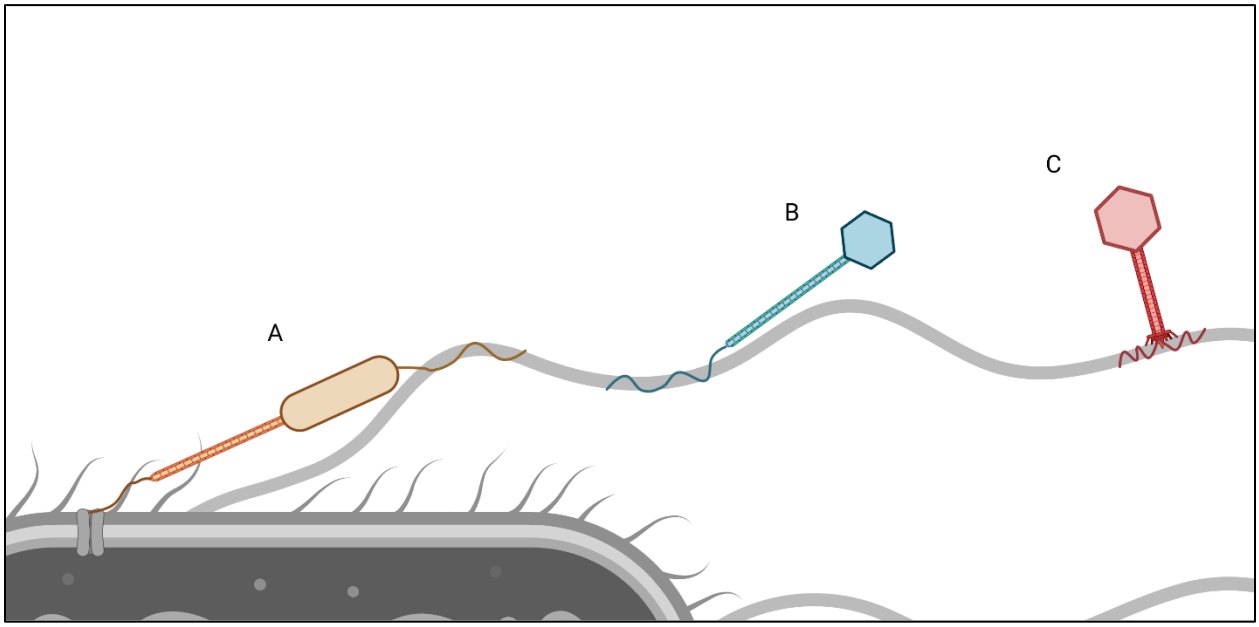


Figure 1.1. Infection mechanisms of various flagellotropic bacteriophages. (A) Phage ΦCbK simultaneously interacts with the *Caulobacter* flagellum using its head fiber and pilus portal protein using its tail fiber. (B) Phage χ uses its single tail fiber to bind to the *Salmonella* flagellum. (C) Phage PBS1 uses its three curled tail fibers to tightly bind to the *Bacillus* flagellum.

Chapter II

# The multi-drug efflux system AcrABZ-TolC is essential for infection of *Salmonella* Typhimurium by the flagellum-dependent bacteriophage Chi

Published in: *Journal of Virology* (American Society for Microbiology)

Nathaniel C. Esteves[a], Steffen Porwollik[b], Michael McClelland[b], and Birgit E. Scharf[a]

[a]Department of Biological Sciences, Virginia Polytechnic Institute and State University, Blacksburg, VA 24061, USA

[b]Department of Microbiology and Molecular Genetics, University of California, Irvine, CA 92697, USA

Running Head: AcrABZ-TolC is required for Chi phage infection

Esteves NC, Porwollik S, McClelland M, Scharf BE. The multi-drug efflux system AcrABZ-TolC is essential for infection of *Salmonella* Typhimurium by the flagellum-dependent bacteriophage Chi. J Virol. 2021 May 10;95(11):e00394-21. doi: 10.1128/JVI.00394-21. Epub 2021 Mar 17. PMID: 33731456; PMCID: PMC8139690.

**ABSTRACT**

Bacteriophages are the most abundant biological entities in the biosphere. Due to their host specificity and ability to kill bacteria rapidly, bacteriophages have many potential healthcare applications, including therapy against antibiotic-resistant bacteria. Infection by flagellotropic bacteriophages requires a properly rotating bacterial flagellar filament. The flagella-dependent phage χ (Chi) infects serovars of the pathogenic enterobacterium *Salmonella enterica*. However, cell surface receptors and proteins involved in other stages of χ infection have not been discovered to date. We screened a multi-gene deletion library of *S. enterica* serovar Typhimurium by spotting mutants on soft agar plates seeded with bacteriophage χ and monitoring their ability to grow and form a swim ring, a characteristic of bacteriophage-resistant motile mutants. Those multi-gene deletion regions identified to be important for χ infectivity were further investigated by characterizing the phenotypes of corresponding single-gene deletion mutants. This way, we identified motile mutants with varying degrees of resistance to χ. Deletions in individual genes encoding the AcrABZ-TolC multi-drug efflux system drastically reduced infection by bacteriophage χ. Furthermore, an *acrABtolC* triple deletion strain was fully resistant to χ. Infection was severely reduced but not entirely blocked by the deletion of the gene *tig* encoding the molecular chaperone trigger factor. Finally, deletion in genes encoding enzymes involved in the synthesis of the antioxidants glutathione (GSH) and uric acid resulted in reduced infectivity. Our findings begin to elucidate poorly understood processes involved in later stages of flagellotropic bacteriophage infection and informs research aimed at the use of bacteriophages to combat antibiotic-resistant bacterial infections.

## IMPORTANCE

Antimicrobial resistance is a large concern in the healthcare field. With more multi-drug resistant bacterial pathogens emerging, other techniques for eliminating bacterial infections are being explored. Among these is phage therapy, where combinations of specific phages are used to treat infections. Generally, phages utilize cell appendages and surface receptors for the initial attachment to their host. Phages that are flagellotropic are of particular interest because flagella are often important in bacterial virulence, making resistance to attachment of these phages harder to achieve without reducing virulence. This study discovered the importance of a multi-drug efflux pump for the infection of *Salmonella enterica* by a flagellotropic phage. In theory, if a bacterial pathogen develops phage resistance by altering expression of the efflux pump then the pathogen would simultaneously become more susceptible to the antibiotic substrates of the pump. Thus, co-administering antibiotics and flagellotropic phage may be a particularly potent antibacterial therapy.

## INTRODUCTION

Bacteriophages, also called phages, are the viruses of bacteria and are the most abundant biological entities in the biosphere (1). Phages generally have very specific host requirements and only infect a small range of bacterial strains and species (2-4). Due to their specificity and ability to kill bacteria efficiently, phages have many potential healthcare applications including phage therapy (5-8). Despite their differences in morphology and genome structure, most phages initiate infection via a receptor on the bacterial cell surface. Receptors include lipopolysaccharides as well as proteins such as channels, porins, pili, or flagella. After attachment, the phage ejects its DNA or RNA genome into the bacterial cell, where the cell machinery is used to replicate phage particles. When a sufficient quantity of phage is produced, the bacterial cell lyses, and the phages diffuse out to infect more host cells (9, 10).

Flagellotropic phages represent a distinct category of phages that infect via adsorption to the bacterial flagellar filament (11-15). It is hypothesized that they attach to the flagellar filament and use its rotation to work their way down to the cell surface like a nut on a bolt with threads in the same orientation (16), although the process of translocation along the flagellum has not been visualized, to date. Bacteriophage χ is a virulent flagellotropic phage that infects some serotypes of enteric, Gram-negative bacteria, most notably from the genera *Escherichia*, *Salmonella*, and *Serratia* (11, 17, 18). It is a double-stranded DNA virus from the *Siphoviridae* family with a genome length of 59 kb, containing an estimate of 75 genes (17). χ has an icosahedral head which is 65 nm in diameter. Its non-contractile tail has a length of 220 nm and a width of 13 nm, and contains a 200 nm single tail fiber (17). The dimensions of the tail fiber suggest that it fits along the right-handed grooves of the helical, left-handed flagellar filament, and that the counter-

clockwise (CCW) rotation of the flagellum forces the phage to follow the grooves to the base of the flagellar filament (16).

Many bacterial motility and chemotaxis genes have been shown to be required for χ to infect cells (19). In particular, absence of the flagellin proteins FliC and FljB causes a χ-resistant phenotype. However, the lack of flagellar filaments is partially offset by the production of polyhooks (20). The deletion of the motility genes *motA* or *motB* also confers resistance to χ underlining the importance of flagellar rotation (16, 19, 21). Additionally, any mutations in chemotaxis genes that lock the flagellar motor in the clockwise (CW) rotating state result in resistance to χ, because the phage is not drawn to the base of the filament (11, 16, 19). Once the phage reaches the cell surface it likely interacts with a secondary receptor (11, 14, 16), but infection processes following phage translocation on a host flagellum are unknown. To date, no host gene products unrelated to motility or chemotaxis have been shown to be involved or required for χ infection.

One biomedically important bacterial species infected by χ is *Salmonella enterica* of the *Enterobacteriaceae* family of Gammaproteobacteria (22). *S. enterica* is a diverse species, containing over 2,500 serovars, many of which are clinically relevant (23). Most pathogenic serovars, including serovar Typhimurium, cause human gastroenteritis and are often collectively referred to as non-typhoidal *Salmonella* (NTS) (22, 24). An NTS infection typically presents itself with severe diarrhea, fever, abdominal pain, and vomiting (22). Some serovars can be invasive, with infections potentially leading to bacteremia, meningitis, and even death in otherwise healthy patients (25). Serovars Typhi and Paratyphi cause typhoid and paratyphoid fever, respectively, which are potentially fatal systemic infections that result in high fever, rash, lethargy, abdominal pain, and vomiting (22). These conditions are a major cause of death in

developing countries. At least 100,000 infections per year in the U.S. are due to antibiotic-resistant *Salmonella*, including those that are resistant to clinically important drugs such as ceftriaxone and ciprofloxacin (26). *S. enterica* subsp. *enterica* serovar Typhimurium 14028s (STM 14028s) is a pathogenic NTS that is susceptible to χ and is often used in laboratory settings.

To decipher the infection process by χ beyond its adhesion to flagella and the importance of flagellar rotation, we screened a library of defined deletion mutants in STM 14028s to identify genes not related to motility that play a role in χ infection.

## RESULTS

### Strategy for the identification of motile *S. enterica* mutants with reduced susceptibility to χ

We hypothesized that χ infection required binding to secondary receptors on the cell surface following interactions with the flagella. We therefore screened a multi-gene deletion (MGD) mutant library of STM 14028s with 449 MGD mutants covering a total of 3,476 genes (27) for motile phage-resistant mutants by spotting mutants onto MSB swim agar containing 1 x $10^7$ pfu of χ. We identified a total of 12 motile χ-resistant MGD library mutants, which informed a selection for further screening of single-gene deletion (SGD) mutants of the individual genes deleted in their respective MGD locus. This resulted in a second screen of 76 SGD mutants, carried out as described above. Phenotypes of χ-resistant SGD mutants were confirmed with a second independent mutant of the same gene disrupted by a different antibiotic cassette. Candidate mutants that retained motility were identified based on the size of their swim ring formed after an 8 h incubation. Phage-susceptible mutants formed very small, approximately 1 to 5 mm swim rings with inconsistent density throughout the ring. This is characteristic of the fact

that χ does not lyse completely on solid media, possibly due to downregulation of flagellar components under extreme selective pressure, resulting in the simultaneous survival and miniscule amount of swimming seen in these spots. Phage-resistant motile mutants formed larger, hazy swim rings of various sizes with more consistent density and shape, as seen in Fig. 2.1A. Motile mutants produced large swim rings of variable sizes on plates lacking phage (Fig. 2.1B) due to minor inconsistencies associated with the high-throughput 96-well pin replicator method of inoculation. Non-motile mutants did not form rings regardless of the presence of phage (Fig. 2.1A and 2.1B).

Next, we validated χ-resistant strains by analyzing newly constructed deletion mutants. We determined that disruption of eight genes negatively impacted susceptibility to χ while maintaining motility. These genes fell into three classes: (1) components of the multi-substrate efflux pump Acr/TolC; (2) the molecular chaperone trigger factor; and (3) enzymes involved in the synthesis of the cellular antioxidants glutathione (GSH) and uric acid (Table 2.1).

**The AcrABZ-TolC multi-drug efflux system**

We found that deletions in genes coding for components of the AcrABZ-TolC multi-substrate efflux system confer high levels of resistance to bacteriophage χ. AcrABZ-TolC is part of the Resistance-Nodulation-Division (RND) family of transporters that is well characterized in *E. coli*. RND efflux systems are tripartite pumps that extend fully across the cell envelope (28-30). They consist of an inner membrane pump, an outer membrane channel, and a periplasmic adaptor protein, and are powered by the proton motive force (PMF) (28, 29). In AcrABZ-TolC, TolC is the outer membrane channel, AcrB is the inner membrane pump, and AcrA is the adaptor protein, which connects AcrB and TolC in the periplasm (28, 29, 31). AcrZ is a small protein

that assists AcrB in exporting certain substrates including chloramphenicol and tetracycline (32). An AcrZ homolog is encoded by the gene STM14_0906 in STM 14028s. AcrABZ-TolC is involved in exporting numerous substrates, including antibiotics like penicillin G and nafcillin, detergents like sodium dodecyl sulfate, bile salts like deoxycholate, and dyes like crystal violet (28). Deletion of components of AcrABZ-TolC in *E. coli* and *S. enterica* increases sensitivity to these toxins (28, 33). To further characterize and quantify mutant phenotypes for their defects in phage infectivity, we performed efficiency-of-plating (EOP) assays (Fig. 2.2A). Deletion of *acrB* caused a reduction in EOP by 95%, whereas the effects of *acrA*, *acrZ*, or *tolC* deletions were more moderate (reductions between 35 and 87%). However, an *acrAB* double deletion strain exhibited a 99% reduction in EOP, and the additional deletion of *tolC* completely abolished infection, resulting in a phage-resistant phenotype.

To verify the involvement of AcrABZ-TolC in χ phage infection, we performed trans-complementation of the genes *acrAacrB*, and *tolC* in the dual gene expression vector pETDuet-1. The genes *acrA* and *acrB* were cloned in MCS1 using the native chromosomal arrangement and *tolC* was cloned in MCS2, yielding plasmid pBS1250. When the Δ*acrABtolC* mutant was complemented with pBS1250 under induction with 1 mM IPTG, the phage-resistant phenotype was restored to an EOP of 85% of wild type (Fig. 2.2A).

To provide further proof of the importance of AcrABZ-TolC in phage infection, we analyzed the effect of modulating its transcriptional regulation. AcrABZ-TolC is part of the complex multi antibiotic resistance (*mar*) regulon, which is conserved across many enteric bacteria. Overexpression of *mar*-regulated genes is associated with multi-drug resistance in enteric pathogens (34-36). Expression of the *mar* regulon is directly controlled by the transcriptional activator MarA. The transcription of *marA* is negatively regulated by MarR through

autorepression of the *marRAB* operon. MarR itself can be inactivated through binding of certain phenolic ligands, such as salicylate. Thus, *marA* transcription is derepressed in the presence of salicylate, which in turn causes increased AcrABZ-TolC expression (37, 38). We hypothesized that overexpression of AcrABZ-TolC will increase the susceptibility of *S. enterica* to χ. Indeed, when wild type STM 14028s was grown in the presence of salicylate, cells exhibited an increased susceptibility to χ phage, showing an EOP of 156% compared to STM 14028s grown in medium lacking salicylate (Fig. 2.2B).

We also discovered that a deletion in *acrF* reduced *S. enterica* susceptibility to χ by 47%. AcrF is a component of the AcrEF-TolC efflux system, a functionally similar multi-substrate efflux pump. However, the STM 14028s SGD mutant in *acrE* did not show a significant χ-resistant phenotype (data not shown). The AcrEF-TolC system has not been studied in as much detail as AcrABZ-TolC, but it has been shown to export certain antibiotics as well as indole compounds from the *E. coli* cell (39, 40). Taking these findings together, we identified the AcrABZ-TolC complex as essential for χ infection and provide preliminary evidence for an involvement of other efflux systems.

**The molecular chaperone trigger factor**

The deletion of *tig*, encoding the molecular chaperone trigger factor, confers 98% resistance to χ (Fig. 2.2). Trigger factor is a ribosome-associated chaperone that has peptidyl-prolyl cis/trans isomerase activity (41). It interacts with polypeptides exiting the ribosome and keeps them in an open conformation so they can be folded properly. It is also abundant as a free protein in the cytosol where it promotes protein refolding (41, 42). The highly compromised infection phenotype of the *tig* mutant implies a major role of this chaperone in χ phage infection. Since the

efflux system AcrABZ-TolC also had a chief impact on χ infection, we tested the possibility that the roles of trigger factor and AcrABZ-TolC are functionally linked. However, lack of trigger factor did not result in a reduction of the MIC of deoxycholate, a known substrate of AcrABZ-TolC (Table 2.2). Thus, trigger factor and AcrABZ-TolC play unrelated roles during χ infection.

**Enzymes involved in the synthesis of cellular antioxidants**

Deletion of *gshA* reduced χ infection of STM 14028s by 54% (Fig. 2.2), whereas a *gshB* deletion mutant showed an EOP of 61% compared to wild type. GshA and GshB are major components of the glutathione synthesis pathway and the lack of either one results in the absence of intracellular glutathione (43-46). Glutathione is an important antioxidant and responsible for maintaining a reducing environment in the cell to prevent damage from reactive oxygen species (ROS) such as superoxide and free radicals (47, 48).

Lack of the hypothetical protein-encoding gene *ylbA* confers a weak χ-resistant phenotype with an 84% EOP compared to wild type (Fig. 2.2). YlbA has no proven function in *S. enterica* and *E. coli*, but homologues have been shown to be involved in the ureide pathway that produces another reducing agent, uric acid (49), allowing for growth in low nitrogen conditions (50, 51). In conclusion, the reduction of cellular levels of two antioxidants resulted in partial resistance to χ.

**Evaluation of cell motility and growth in χ-resistant mutants**

To verify that the observed resistance to χ was not due to reduced motility, we performed quantitative swim plate assays with the SGD mutants. Swim ring diameters after incubation for 8 hours at 37 °C were compared to those of the parental strain STM 14028s. All mutants were

motile, as they formed swim rings at a size of at least 60% of wild type (Fig. 2.3). Motility was also confirmed by observation of cell cultures under a phase contrast microscope (data not shown). It should be noted that all investigated mutants, with the exception of Δ*ylbA* and Δ*acrZ,* exhibited a statistically significant reduction in swim ring diameter. However, since there was no correlation between the degree of resistance to χ and the degree of the motility decrease, we concluded that a modest reduction in motility is not sufficient for a resistant phenotype. To confirm that the χ-resistant phenotype and the reduced motility of any of the investigated mutants was not caused by a growth defect, we assayed growth rates at 37 °C using $OD_{600}$ spectrophotometer readings over a course of 8 hours. No statistically significant differences in growth rates between the deletion mutants and wild type were observed (Fig. 2.4).

## DISCUSSION

In this study, we employed swim plate assays of *S. enterica* serovar Typhimurium deletion mutants to identify genes that are involved in infection by phage χ, beyond those known to be required for flagellar motility. We found motile, phage-resistant mutants that were defective in genes coding for components of the AcrABZ-TolC and AcrEF-TolC efflux systems, the molecular chaperone trigger factor, and enzymes involved in the production of cellular antioxidants such as the glutathione synthesis proteins GshA and GshB, and a hypothetical protein YlbA.

### The putative role of a multi-substrate efflux system in χ infection

Multi-drug resistance in *E. coli* and *S. enterica* is often associated with increased expression of AcrABZ-TolC (28, 33). The outer membrane channel TolC has been shown to be a phage

receptor in other systems (52, 53), but this is the first report of a flagellotropic phage requiring the AcrABZ-TolC efflux system for infection. The exact role of AcrABZ-TolC in χ infection is not known. We hypothesize that the channel formed by AcrB and TolC is involved in the process of phage DNA entry into the host cell. Without production of AcrB, *Salmonella* cells were highly resistant to χ infection. Interestingly, absence of TolC had a lesser effect, showing approximately 75% resistance to χ (Fig. 2.2). It is possible that an outer membrane protein other than TolC can serve as DNA channel into the periplasm, where AcrB then allows DNA entry into the cytoplasm. Since lack of the flagellar filament and hook or the absence of AcrABZ-TolC results in complete resistance to χ, we conclude that both of these structures are essential for the infection process. χ uses the rotating flagellar filament to work its way down to the cell surface (11, 16), and we hypothesize that it then interacts with the AcrABZ-TolC complex to eject its DNA into the host cell. With the exception of the Δ*acrZ* mutant, which was fully motile, deletions of genes encoding components of the AcrABZ-TolC complex had varying mild negative impacts on motility on swim plates. Reduced motility is perhaps due to a decrease in overall fitness caused by the inability of the cells to export toxic substrates (28, 29). It has been shown in other flagellotropic phage systems that even severe reductions in motility and flagellar rotational speed did not result in reductions in phage infection of the magnitude seen in the Δ*acrABtolC* mutant in this study (54). Therefore, we infer that these two behaviors are likely unrelated.

The role of the small protein AcrZ in χ infection is unknown. AcrZ directly associates with AcrB, and its absence results in a reduction in the ability of AcrB to export certain toxic substrates (29, 32). It has been suggested that AcrZ triggers conformational changes in the periplasmic domain of AcrB during the export of certain substrates (30, 32). This could explain

why *acrZ* mutants exhibit an intermediate MIC phenotype (32). We hypothesize that the lack of AcrZ prevents conformational changes in AcrB that are necessary for the AcrABZ-TolC complex to efficiently serve as a phage DNA channel.

**The putative role of a general chaperone in χ infection**

Trigger factor is an important ribosome-associated chaperone (41, 42, 55). Without production of trigger factor, there was a 98% reduction in plating efficiency of host bacteria when infected with χ (Fig 2). Trigger factor has been shown to interact with T4 and T5 phage proteins (56, 57) and is implicated as a chaperone for the gp20 protein of T4 (57). We hypothesize that trigger factor is involved in the proper folding of crucial χ phage proteins. The absence of trigger factor would result in an aborted production of phage particles, and thus, a resistant phenotype. Alternatively, trigger factor could be responsible for the folding of one or more bacterial proteins required during the phage infection cycle, such as cell surface receptors. The absence of trigger factor also caused a reduction in swim ring diameter, suggesting that trigger factor possibly plays a role in the folding of certain motility and/or chemotaxis proteins. Finally, it is conceivable that the resistance of the *tig* mutant to χ is influenced by multiple other factors, because trigger factor is a chaperone for a wide array of proteins (55). However, it does not serve as a chaperone for proteins of the AcrABZ-TolC system, because the deoxycholate minimum inhibitory concentration (MIC) of the *tig* mutant was equal to that observed in wild type, whereas *acrB* and *acrABtolC* deletion mutants exhibited drastic MIC reductions (Table 2.2). Therefore, the effect of trigger factor appears to be independent from that of the AcrABZ-TolC complex.

**Involvement of host antioxidants in χ infection**

Glutathione (GSH) or L-γ-glutamyl-L-cysteinylglycine acts as a crucial antioxidant in prokaryotic as well as eukaryotic cells (46-48). This tripeptide maintains a reducing environment in the cell, neutralizing reactive oxygen species (ROS) such as superoxide, peroxides, and free radicals that would otherwise have the potential to damage cellular components (43, 46-48). GshA is a glutamate-cysteine ligase that conducts one branch of the GSH synthesis pathway, while the glutathione synthetase GshB conducts the final step of GSH production. Absence of either of these proteins results in abolished GSH production (44-46). The lack of GSH in a host cell caused by the deletion of *gshA* or *gshB* had a negative effect on the χ infection process (Fig. 2.2). A reducing environment may be just as important for the protection of phage proteins as it is for its bacterial host proteins. The lack of GSH seems to be more deleterious to the χ infection process than it is to the overall growth of its host under non-stress growth conditions. A reducing cellular environment has been shown to be beneficial in other phage systems, with high levels of oxidation being potentially inhibitory to infection (58). We hypothesize that this is also the case for χ. However, the reduced infectivity of the *gshA* and *gshB* mutants was more moderate than that of the two previously discussed classes, the efflux pump and the *tig* chaperone. Thus, reduction of ROS by GSH improves the ability of χ to infect and lyse its host, but it is not essential for phage propagation.

The role of YlbA in *S. enterica* is unknown, but a close homolog functions as (S)-ureidoglycine aminohydrolase in the ureide pathway of leguminous plants and prokaryotes, where it catabolizes purines to be used as an energy source in environments with low available nitrogen (50, 51). An (S)-ureidoglycine aminohydrolase enzyme is also present in *Bacillus subtilis* (59) and *Klebsiella pneumoniae* (60), and YlbA in *S. enterica* and *E. coli* likely performs the same

function. The impact of a *ylbA* deletion on χ infection was relatively small (>80% EOP, Fig. 2.2) but sufficient to be detected in our screens. A link between the ureide pathway and phage infection has not been previously reported. This pathway ultimately produces allantoin from uric acid (50). Uric acid, similar to GSH, is an antioxidant (49). Absence of YlbA may therefore result in altered levels of uric acid in the cell, although this function has not been confirmed.

**Potential applications and future studies**

The phage-seeded swim plate assay is a powerful method to screen mutant libraries and can be expanded to the studies of other flagellotropic phage systems. By screening only for mutants that resist the phage and remain motile, the high prevalence of motility-related gene disruptions can be ignored. Since swim ring formation also relies on chemotaxis in addition to motility (61), chemotaxis-related gene disruptions are also disregarded.

χ has a broad host range that includes several clinically relevant human pathogenic species of enterobacteria (11, 16, 18), including at least three genera in two different families, *Enterobacteriaceae* and *Yersiniaceae*. The necessity of an antibiotic efflux system in its host infection process makes χ an attractive potential future candidate for phage therapy. Wang-Kan *et al.* showed that *Salmonella* strains with an *acrB* deletion are unable to colonize the mouse intestine, thus significantly reducing virulence, because AcrABZ-TolC exports toxic bile salts such as cholate and deoxycholate (28, 33). The inclusion of χ in a phage cocktail against NTS would likely create selective pressure for pathogenic bacteria to reduce expression of a component of the AcrABZ-TolC system. The subset of resistance mutants that reduce expression would be more sensitive to bile salts, therefore lowering their virulence in the human intestine, as well as lowering resistance to certain antibiotics. A similar trade-off has been successfully

exploited by Chan *et al.* in the *Pseudomonas aeruginosa* phage OMKO1, which also uses a multi-drug efflux system, MexAB, as a cell-surface receptor (62). In this study, phage OMKO1 was co-administered with an antibiotic, forcing a trade-off by the cells, either expressing the *mexAB* operon, resulting in antibiotic resistance and phage susceptibility, or halting expression of the *mexAB* operon, resulting in phage resistance and antibiotic susceptibility (62). We hypothesize that the same phenomenon would occur *in vivo* with *Salmonella* in the mammalian intestine. Without the AcrABZ-TolC complex, *Salmonella* is resistant to χ, but highly susceptible to deoxycholate (63) (Table 2.2). However, its flagellotropic nature makes χ an even better additive to a phage cocktail against NTS. Non-flagellated *Salmonella* strains would be resistant to χ but have sacrificed flagellin as a virulence factor (22, 24, 64, 65). The virulence of *Salmonella* would be significantly reduced when downregulating flagellin or AcrABZ-TolC expression to develop resistance against χ.

The results obtained in this work allow for a myriad of opportunities for future studies. The role of the AcrABZ-TolC system in the infection process can be investigated by disrupting the function of this pump. The aspartate residue in position 408 in AcrB is crucial for proton translocation (33, 66, 67). A mutant strain with an Asp408Ala substitution has an antibiotic MIC profile equivalent to that of an *acrB* knockout strain (33, 67). An infectivity assay of an Asp408Ala mutant would therefore determine whether sensitivity to χ is affected by a functional AcrB pump.

While it is known that the single tail fiber of χ wraps around the flagellar filament of its host cell (11), phage protein(s) that interact with receptors on the cell surface have not been determined. With the identification of AcrABZ-TolC as putative cell surface receptor for χ, it is now possible to identify phage proteins that interact with this receptor.

One of the main features of phage therapy compared to conventional antibiotic administration is the specific customization of the treatment to the disease-causing species. Bacteriophage χ targets several prevalent pathogenic species, which makes it a good candidate for an antibacterial phage cocktail. However, certain serovars of *Salmonella enterica* subsp. *enterica* do not serve as a host for χ (68). Thus, our findings also open up opportunities to analyze whether variants in serovar antigens, flagella, and/or the AcrABZ-TolC system are determinants of host specificity of this bacteriophage.

## MATERIALS AND METHODS

### Bacterial strains and plasmids

Derivatives of *S. enterica* sv. Typhimurium 14028s (STM 14028s) used in this study are listed in Table 2.3.

### Phage propagation and isolation

To propagate and isolate χ phage particles, an overlay-based method was used. STM 14028s was grown in lysogeny broth (LB) (69) at 37°C to stationary phase. This stationary phase culture was diluted 1:100 in LB and allowed to reach an $OD_{600}$ of 1.0. Exactly 100 µl of culture was mixed with 100 µl of the appropriate serial dilution of χ phage to produce plates with confluent lysis. This mixture was combined with 4 ml of molten LB with 0.35% w/v agar and was poured onto an LB plate for a total of 15 plates. Plaques were allowed to form by incubating for approximately 8 h at 37°C, at which point 5 ml of TM buffer (50 mM Tris/HCl, pH 7.5, 10 mM $MgSO_4$) was poured onto each plate. The plates were placed on a rocking platform overnight at 4°C, rotating at approximately 30 RPM. The TM buffer and soft agar from each plate was pooled

in a centrifuge tube and chloroform was added to a final concentration of 2% v/v. The mixture was centrifuged at 10,000 x g for 30 min at 4°C. The supernatant was collected into a new tube, mixed with polyethylene glycol 8000 to a final concentration of 10% w/v and stirred overnight at 4°C. The mixture was centrifuged at 15,000 x g for 30 min at 4°C, and the pellet containing phage was suspended in TM buffer. This mixture was purified using an OptiPrep™ density gradient. Briefly, the gradient was made with 5 ml each of 50% and 10% OptiPrep™ (Sigma) in flexible polyallomer ultracentrifuge tubes (Beckman Coulter). The concentrated phage in TM buffer was layered on top of the gradient and centrifuged at 200,000 x g for 2 h at 15°C using an SW41 rotor (Beckman-Coulter). The white band containing phage was extracted with a syringe and 25-gauge needle and added to dialysis tubing in TM buffer. This was allowed to stir for 48 hours at 4°C, changing the buffer approximately every 12 h. The TM buffer containing phage was extracted from the dialysis tubing, and the phage suspension was titered for plaque forming units (pfu) by a plaque assay.

**Library screening**

The STM 14028s multi-gene deletion (MGD) library (27) was screened via replica plating onto MSB swim plate medium. MSB medium is a modified lysogeny broth (LB), consisting of 1% Bacto Tryptone, 0.5% yeast extract, 2 mM $CaCl_2$, and 2 mM $MgSO_4$. To make swim plates, agar was added to a final concentration of 0.3%, which allowed motile bacteria to form swim rings. After cooling to 50°C, bacteriophage χ in TM buffer was added to a final concentration of $1x10^7$ pfu/mL. Approximately 40 mL of this molten agar was added to Thermo Scientific™ Nunc 128 x 86 mm 1-well rectangular plates and allowed to solidify. Libraries in 96-well plates were patched into the swim agar in the 1-well plates using a 96-well pin replicator tool (Boekel

Scientific). After an approximately 8 h incubation at 37°C, plates were examined to determine swim ring formation. Colonies that formed swim rings in the presence of phage were investigated further with targeted gene deletions, which were generated by lambda-red mutagenesis.

**Generation of loss-of-function mutants**

We utilized established STM 14028s single-gene deletion (SGD) mutants of regions identified to be of interest in the MGD library screen (27). For *acrAB* and *acrABtolC* mutants, and select SGD mutants identified in Table 2.3, additional targeted mutagenesis was conducted using lambda red mutagenesis, modified from Datsenko and Wanner, 2000 (70). Briefly, plasmid pKD46 (pBAD λ-red) was introduced into wild type (or, in case of *acrABtolC*, a *tolC* SGD) STM 14028s via electroporation, following a protocol modified from Binotto et al., 1991 (71). A 50 μL aliquot of electrocompetent STM 14028s cells was mixed with approximately 200 ng of plasmid pKD46, transferred to an electroporation cuvette with a 2-mm electrode gap (Bio Rad) and electroporated at 2.5 kV, 25μF, 2Ω, yielding a 5-ms exponentially decaying pulse. After recovery in Super Optimal broth with Catabolite repression (SOC; 2% Bacto tryptone, 0.5% yeast extract, 10 mM NaCl, 2.5 mM KCl, 10 mM $MgCl_2$, 10 mM $MgSO_4$, and 20 mM glucose) at 30°C for 1 h, cells were plated onto LB with 100 μg/mL ampicillin and incubated overnight at 30°C. Cells containing plasmid pKD46 were subsequently made electrocompetent, adding 0.2% w/v L-arabinose to activate expression of the lambda red genes on pKD46.

To inactivate individual genes, the 2 kb tetracycline resistance cassette *tetRA* was inserted to replace the targeted region of the bacterial chromosome. Primers were designed with homology to the desired region and to the *tetRA* cassette. A PCR reaction was performed with these custom

primers and chromosomal DNA from *S. enterica* serovar Typhimurium TH2788 as template, which contains a Tn10 insertion in *fliY* (72). This reaction yielded a fragment containing the *tetRA* cassette with ends homologous to the desired region for deletion in *S. enterica* 14028s. The PCR product was purified using a Promega™ gel and PCR cleanup kit, mixed with STM 14028s competent cells and electroporated, as above. After the recovery period, cells were plated on LB with 10 μg/mL tetracycline and incubated overnight at 37°C.

**Construction of *acrABtolC* expression vector and complementation of the Δ*acrABtolC* mutant**

STM 14028s *acrAB* and *tolC* was ligated into pETDuet-1 MCS1 and MCS2 following standard restriction enzyme cloning procedures. Briefly, custom primers were designed with homology to the 5' end of *acrA* and the 3' end of *acrB,* flanked by restriction enzyme recognition sequences. These were used to amplify the entire *acrAB* locus via PCR. A restriction digest of this fragment and the pETDuet-1 vector was performed. This *acrAB* fragment was ligated into MCS1 of pETDuet-1 using T4 DNA ligase (NEB). Procedures were repeated for STM 14028s *tolC,* which was ligated into MCS2 of the plasmid constructed in the previous step. This construct was confirmed via Sanger sequencing and introduced into STM 14028s Δ*acrABtolC* via electroporation. Expression of *acrABtolC* was induced by the addition of 1 mM IPTG to solid and liquid media.

**Quantitative motility assays**

Bacterial cultures were grown in LB at 37°C to an $OD_{600}$ of 1.0. Next, 2.5 μL of culture was spotted in the center of a plate containing MSB swim plate medium. These plates were incubated facing upwards at 37°C. After approximately 5 h, the swim ring diameters were measured. Swim

ring diameters relative to wild type were calculated by using the formula (diameter of swim ring formed by tested strain) / (diameter of swim ring formed by wild type strain).

**Assay of efficiency of plating**

Efficiency of plating (EOP) was determined via plaque assay. Briefly, LB medium was inoculated with a single bacterial colony and grown at 37°C. At an $OD_{600}$ of 1.0, motility was verified via phase contrast microscopy, and 100 µl of this culture was mixed with serial dilutions of bacteriophage χ stock ($1.1x10^{11}$ pfu/ml) in 0.85% w/v NaCl. After an incubation time of 6 min to allow binding, this mixture was added to 4 mL of molten LB agar at 45°C and poured onto an LB agar plate. After an 8 h incubation, plaques were counted to determine pfu/ml. EOP was calculated using the following formula: (pfu/mL deletion mutant) / (pfu/mL wild type). To test the effect of salicylate, 5 mM sodium salicylate was added to all solid and liquid media before performing the EOP assay.

**Determination of bacterial growth rate**

Bacterial cultures were grown in LB broth overnight at 37°C with shaking, then diluted 1:1000 in 50 mL MSB and incubated under the same conditions. A 1 mL aliquot of culture was collected at 30 min intervals for 8 h and the $OD_{600}$ was determined via spectrophotometer.

**Assay of minimum inhibitory concentration (MIC)**

MIC was determined in LB liquid medium. Sodium deoxycholate, a substrate of AcrABZ-TolC, was added to the medium to final concentrations of 1% to 10% (w/v). An overnight liquid culture was added at a dilution of 1:1000 to LB supplemented with sodium deoxycholate and

incubated in a 37°C roller drum for 8 h. MIC was recorded as the lowest concentration of sodium deoxycholate that resulted in no growth.

ACKNOWLEDGMENTS

We thank Saeed Tavazoie for bacteriophage χ, Kelly Hughes for *S. enterica* strain TH2788, and Howard Berg for plasmid pKD46. We thank Weiping Chu for technical assistance. M.M. and S.P. were supported in part by R03 AI139557, USDA 2015-67017-23360, 2017-67015-26085, an NIFA Hatch grant (CA-D-PLS-2327-H), and an NIFA-BARD award (2017-67017-26180).

TABLES

**Table 2.1**: Candidate genes involved in infection of *Salmonella* by χ

| **Gene** | **Gene number** | **Function of gene product** |
|---|---|---|
| *acrB* | STM14_0559 | AcrABZ-TolC multi-substrate efflux system, inner membrane component |
| *acrA* | STM14_0560 | AcrABZ-TolC, periplasmic adaptor protein |
| *tolC* | STM14_3859 | AcrABZ-TolC, outer membrane channel |
| *acrZ** | STM14_0906 | AcrABZ-TolC, AcrB-associated protein |
| *acrF* | STM14_4091 | AcrEF-TolC multi-substrate efflux system, inner membrane component |
| *tig* | STM14_0529 | Trigger factor molecular chaperone |
| *gshA* | STM14_3403 | Glutamate-cysteine ligase |
| *gshB* | STM14_3739 | Glutathione synthetase |
| *ylbA* | STM14_0616 | Putative (S)-ureidoglycine aminohydrolase |

*The AcrZ homolog is encoded by the gene STM14_0906 in STM 14028s.

**Table 2.2**: Minimum inhibitory concentration of sodium deoxycholate on selected deletion mutants

| **Relevant genotype** | **MIC (%w/v deoxycholate) *** |
|---|---|
| Wild type | 8% |
| Δ*acrB* | 2% |
| Δ*acrABtolC* | 2% |
| Δ*tig* | 8% |

* The assay was conducted in liquid medium with an increasing deoxycholate concentration in intervals of 1%. The assay was done in triplicate and resulted in a standard deviation of zero.

**Table 2.3: Strains and plasmids used in this study**

| Strain Name | Parent Strain/Plasmid | Relevant Characteristics | Source |
|---|---|---|---|
| MZ1597 | STM 14028s | Wild type | ATCC |
| MZ1597 multi-gene deletion library | STM 14028s | Multi-gene deletion library, Kan$^r$, Cap$^r$ | (27) |
| TH2788 | *Salmonella enterica* subsp. *enterica* serovar Typhimurium str. LT2 | FliY::Tn10dTc | Gift from Kelly Hughes |
| 14028s Δ*acrA::tet* | STM 14028s | Δ*acrA*, Tet$^r$ | This study |
| 14028s Δ*acrA::kan* | STM 14028s | Δ*acrA*, Kan$^r$ | (17) |
| 14028s Δ*acrAB*::*tet* | STM 14028s | Δ*acrAB*, Tet$^r$ | This study |
| 14028s Δ*acrAB::tet* Δ*tolC::kan* | STM 14028s | Δ*acrAB* Δ*tolC*, Tet$^r$, Kan$^r$ | This study |
| 14028s Δ*acrB::tet* | STM 14028s | Δ*acrB*, Tet$^r$ | This study |
| 14028s Δ*acrB::kan* | STM 14028s | Δ*acrB*, Kan$^r$ | (17) |
| 14028s Δ*acrF::kan* | STM 14028s | Δ*acrF*, Kan$^r$ | (27) |
| 14028s Δ*acrF::cap* | STM 14028s | Δ*acrF*, Cap$^r$ | (27) |
| 14028s Δ*fliC::kan* Δ*fljBA::tet* | STM 14028s | Δ*fliC* Δ*fljBA*, Kan$^r$, Tet$^r$ | This study |
| 14028s Δ*gshA::kan* | STM 14028s | Δ*gshA*, Kan$^r$ | (27) |
| 14028s Δ*gshA::tet* | STM 14028s | Δ*gshA*, Tet$^r$ | This study |
| 14028s Δ*gshB::tet* | STM 14028s | Δ*gshB*, Tet$^r$ | This study |
| 14028s ΔSTM14_0524-0529::*kan* | STM 14028s | ΔSTM14_0524-0529, Kan$^r$ | (27) |
| 14028s ΔSTM14_0904-0923::*kan* | STM 14028s | ΔSTM14_0904-0923, Kan$^r$ | (27) |
| 14028s ΔSTM14_0906::*kan* | STM 14028s | ΔSTM14_0906, Kan$^r$ | (27) |
| 14028s ΔSTM14_0906::*cap* | STM 14028s | ΔSTM14_0906, Cap$^r$ | (27) |
| 14028s ΔSTM14_2324-2359::*kan* | STM 14028s | ΔSTM14_2324-2359, Kan$^r$ | (27) |
| 14028s Δ*tig::tet* | STM 14028s | Δ*tig*, Tet$^r$ | This study |
| 14028s Δ*tig::cap* | STM 14028s | Δ*tig*, Cap$^r$ | (27) |
| 14028s Δ*tolC::kan* | STM 14028s | Δ*tolC*, Kan$^r$ | (17) |
| 14028s Δ*tolC::tet* | STM 14028s | Δ*tolC*, Tet$^r$ | This study |
| 14028s Δ*ylbA::kan* | STM 14028s | Δ*ylbA*, Kan$^r$ | (27) |
| 14028s Δ*ylbA::tet* | STM 14028s | Δ*ylbA*, Kan$^r$ | This study |
| Bacteriophage χ | | Wild type | Gift from Saeed Tavazoie |
| pBS1250 | pETDuet-1 | $p_{lac}$ STM 14028s *acrAB* (MCS1), *tolC* (MCS2), Amp$^r$ | This study |
| pETDuet-1 | | $p_{lac}$ MCS1, MCS2, Amp$^r$ | Novagen |
| pKD46 | pINT-ts | pBAD *gam bet exo*, Amp$^r$ | Gift from Howard C. Berg |

REFERENCES


1. Clokie MR, Millard AD, Letarov AV, Heaphy S. 2011. Phages in nature. Bacteriophage 1:31-45.
2. Koskella B, Meaden S. 2013. Understanding bacteriophage specificity in natural microbial communities. Viruses 5:806-823.
3. de Jonge PA, Nobrega FL, Brouns SJJ, Dutilh BE. 2019. Molecular and evolutionary determinants of bacteriophage host range. Trends Microbiol 27:51-63.
4. Nobrega FL, Vlot M, de Jonge PA, Dreesens LL, Beaumont HJE, Lavigne R, Dutilh BE. 2018. Targeting mechanisms of tailed bacteriophages. 16:760-773.
5. Gordillo Altamirano FL, Barr JJ. 2019. Phage therapy in the postantibiotic era. Clin Microbiol Rev 32:e00066-18.
6. Chanishvili N. 2012. Phage therapy--history from Twort and d'Herelle through Soviet experience to current approaches. Adv Virus Res 83:3-40.
7. Romero-Calle D, Guimaraes Benevides R, Goes-Neto A, Billington C. 2019. Bacteriophages as alternatives to antibiotics in clinical care. Antibiotics (Basel) 8.
8. Hanlon GW. 2007. Bacteriophages: an appraisal of their role in the treatment of bacterial infections. Int J Antimicrob Agents 30:118-128.
9. Stone E, Campbell K, Grant I, McAuliffe O. 2019. Understanding and exploiting phage-host interactions. Viruses 11:567.
10. Rakhuba DV, Kolomiets EI, Dey ES, Novik GI. 2010. Bacteriophage receptors, mechanisms of phage adsorption and penetration into host cell. Pol J Microbiol 59:145-55.
11. Schade SZ, Adler J, Ris H. 1967. How bacteriophage χ attacks motile bacteria. J Virol 1:599.
12. Yen JY, Broadway KM, Scharf BE. 2012. Minimum requirements of flagellation and motility for infection of *Agrobacterium* sp. strain H13-3 by flagellotropic bacteriophage 7-7-1. Appl Environ Microbiol 78:7216-7222.
13. Raimondo LM, Lundh NP, Martinez RJ. 1968. Primary adsorption site of phage PBS1: the flagellum of *Bacillus subtilis*. J Virol 2:256-64.
14. Guerrero-Ferreira RC, Viollier PH, Ely B, Poindexter JS, Georgieva M, Jensen GJ, Wright ER. 2011. Alternative mechanism for bacteriophage adsorption to the motile bacterium *Caulobacter crescentus*. Proc Natl Acad Sci U S A 108:9963-9968.
15. Zhilenkov EL, Popova VM, Popov DV, Zavalsky LY, Svetoch EA, Stern NJ, Seal BS. 2006. The ability of flagellum-specific *Proteus vulgaris* bacteriophage PV22 to interact with *Campylobacter jejuni* flagella in culture. Virol J 3:50.
16. Samuel AD, Pitta TP, Ryu WS, Danese PN, Leung EC, Berg HC. 1999. Flagellar determinants of bacterial sensitivity to chi-phage. Proc Natl Acad Sci U S A 96:9863-9866.
17. Hendrix RW, Ko C-C, Jacobs-Sera D, Hatfull GF, Erhardt M, Hughes KT, Casjens SR. 2015. Genome sequence of *Salmonella* phage χ. Genome Announcements 3:e01229-14.
18. Iino T, Mitani M. 1967. Infection of *Serratia marcescens* by bacteriophage chi. J Virol 1:445-447.
19. Girgis HS, Liu Y, Ryu WS, Tavazoie S. 2007. A comprehensive genetic characterization of bacterial motility. PLOS Genet 3:e154.

20. Kagawa H, Ono N, Enomoto M, Komeda Y. 1984. Bacteriophage chi sensitivity and motility of *Escherichia coli* K-12 and *Salmonella typhimurium* Fla- mutants possessing the hook structure. J Bacteriol 157:649-654.
21. Ravid S, Eisenbach M. 1983. Correlation between bacteriophage chi adsorption and mode of flagellar rotation of *Escherichia coli* chemotaxis mutants. J Bacteriol 154:604-611.
22. Jajere SM. 2019. A review of *Salmonella enterica* with particular focus on the pathogenicity and virulence factors, host specificity and antimicrobial resistance including multidrug resistance. Vet World 12:504-521.
23. Grimont PA, Weill F-X. Antigenic formulae of the *Salmonella* serovars.
24. Marcus SL, Brumell JH, Pfeifer CG, Finlay BB. 2000. *Salmonella* pathogenicity islands: big virulence in small packages. Microbes Infect 2:145-56.
25. Huang K-Y, Wang Y-H, Chien K-Y, Janapatla RP, Chiu C-H. 2016. Hyperinvasiveness of *Salmonella enterica* serovar Choleraesuis linked to hyperexpression of type III secretion systems in vitro. Sci Rep 6:37642-37642.
26. V T Nair D, Venkitanarayanan K, Kollanoor Johny A. 2018. Antibiotic-resistant *Salmonella* in the food supply and the potential role of antibiotic alternatives for control. Foods (Basel, Switzerland) 7:167.
27. Porwollik S, Santiviago CA, Cheng P, Long F, Desai P, Fredlund J, Srikumar S, Silva CA, Chu W, Chen X, Canals R, Reynolds MM, Bogomolnaya L, Shields C, Cui P, Guo J, Zheng Y, Endicott-Yazdani T, Yang HJ, Maple A, Ragoza Y, Blondel CJ, Valenzuela C, Andrews-Polymenis H, McClelland M. 2014. Defined single-gene and multi-gene deletion mutant collections in *Salmonella enterica* sv Typhimurium. PLoS One 9:e99820.
28. Kobylka J, Kuth MS, Müller RT, Geertsma ER, Pos KM. 2020. AcrB: a mean, keen, drug efflux machine. Ann N Y Acad Sci 1459:38-68.
29. Anes J, McCusker MP, Fanning S, Martins M. 2015. The ins and outs of RND efflux pumps in *Escherichia coli*. Frontiers in Microbiology 6:587-587.
30. Du D, Wang Z, James NR, Voss JE, Klimont E, Ohene-Agyei T, Venter H, Chiu W, Luisi BF. 2014. Structure of the AcrAB-TolC multidrug efflux pump. Nature 509:512-515.
31. Elkins CA, Nikaido H. 2003. 3D structure of AcrB: the archetypal multidrug efflux transporter of *Escherichia coli* likely captures substrates from periplasm. Drug Resist Updat 6:9-13.
32. Hobbs EC, Yin X, Paul BJ, Astarita JL, Storz G. 2012. Conserved small protein associates with the multidrug efflux pump AcrB and differentially affects antibiotic resistance. Proc Natl Acad Sci U S A 109:16696-701.
33. Wang-Kan X, Blair JMA, Chirullo B, Betts J, La Ragione RM, Ivens A, Ricci V, Opperman TJ, Piddock LJV. 2017. Lack of AcrB efflux function confers loss of virulence on *Salmonella enterica* serovar Typhimurium. mBio 8.
34. Alekshun MN, Levy SB. 1999. The *mar* regulon: multiple resistance to antibiotics and other toxic chemicals. Trends Microbiol 7:410-3.
35. Thota SS, Chubiz LM. 2019. Multidrug Resistance Regulators MarA, SoxS, Rob, and RamA repress flagellar gene expression and motility in *Salmonella enterica* serovar Typhimurium. J Bacteriol 201.
36. Ferrari RG, Galiana A, Cremades R, Rodríguez JC, Magnani M, Tognim MC, Oliveira TC, Royo G. 2013. Expression of the *marA*, *soxS*, *acrB* and *ramA* genes related to the

AcrAB/TolC efflux pump in *Salmonella enterica* strains with and without quinolone resistance-determining regions *gyrA* gene mutations. Braz J Infect Dis 17:125-30.
37. Vila J, Soto SM. 2012. Salicylate increases the expression of *marA* and reduces in vitro biofilm formation in uropathogenic *Escherichia coli* by decreasing type 1 fimbriae expression. Virulence 3:280-5.
38. Wang T, Kunze C, Dunlop MJ. 2019. Salicylate increases fitness cost associated with MarA-mediated antibiotic resistance. Biophys J 117:563-571.
39. Zhang C-Z, Chang M-X, Yang L, Liu Y-Y, Chen P-X, Jiang H-X. 2017. Upregulation of AcrEF in quinolone resistance development in *Escherichia coli* when AcrAB-TolC function is impaired. Microb Drug Resist 24:18-23.
40. Piñero-Fernandez S, Chimerel C, Keyser UF, Summers DK. 2011. Indole transport across *Escherichia coli* membranes. J Bacteriol 193:1793-1798.
41. Haldar S, Tapia-Rojo R, Eckels EC, Valle-Orero J, Fernandez JM. 2017. Trigger factor chaperone acts as a mechanical foldase. Nat Commun 8:668.
42. Martinez-Hackert E, Hendrickson WA. 2009. Promiscuous substrate recognition in folding and assembly activities of the trigger factor chaperone. Cell 138:923-934.
43. Malki L, Yanku M, Borovok I, Cohen G, Mevarech M, Aharonowitz Y. 2009. Identification and characterization of *gshA*, a gene encoding the glutamate-cysteine ligase in the halophilic archaeon *Haloferax volcanii*. J Bacteriol 191:5196.
44. Smirnova GV, Tyulenev AV, Bezmaternykh KV, Muzyka NG, Ushakov VY, Oktyabrsky ON. 2019. Cysteine homeostasis under inhibition of protein synthesis in *Escherichia coli* cells. Amino Acids 51:1577-1592.
45. Apontoweil P, Berends W. 1975. Mapping of *gshA*, a gene for the biosynthesis of glutathione in *Eschericha coli* K12. Mol Gen Genet 141:91-95.
46. Watanabe K, Yamano Y, Murata K, Kimura A. 1986. The nucleotide sequence of the gene for gamma-glutamylcysteine synthetase of *Escherichia coli*. Nucleic Acids Res 14:4393-400.
47. Forman HJ, Zhang H, Rinna A. 2009. Glutathione: overview of its protective roles, measurement, and biosynthesis. Mol Aspects Med 30:1-12.
48. Ferguson GP, Booth IR. 1998. Importance of glutathione for growth and survival of *Escherichia coli* cells: Detoxification of methylglyoxal and maintenance of intracellular K+. J Bacteriol 180:4314.
49. Glantzounis GK, Tsimoyiannis EC, Kappas AM, Galaris DA. 2005. Uric acid and oxidative stress. Curr Pharm Des 11:4145-51.
50. Kim K, Park J, Rhee S. 2007. Structural and functional basis for (S)-allantoin formation in the ureide pathway. J Biol Chem 282:23457-64.
51. Serventi F, Ramazzina I, Lamberto I, Puggioni V, Gatti R, Percudani R. 2010. Chemical basis of nitrogen recovery through the ureide pathway: formation and hydrolysis of S-ureidoglycine in plants and bacteria. ACS Chem Biol 5:203-14.
52. German GJ, Misra R. 2001. The TolC protein of *Escherichia coli* serves as a cell-surface receptor for the newly characterized TLS bacteriophage. J Mol Biol 308:579-85.
53. Fan F, Li X, Pang B, Zhang C, Li Z, Zhang L, Li J, Zhang J, Yan M, Liang W, Kan B. 2018. The outer-membrane protein TolC of *Vibrio cholerae* serves as a second cell-surface receptor for the VP3 phage. J Biol Chem 293:4000-4013.

54. Yen JY, Broadway KM, Scharf BE. 2012. Minimum requirements of flagellation and motility for infection of *Agrobacterium* sp. strain H13-3 by flagellotropic bacteriophage 7-7-1. Appl Environ Microbiol 78:7216-7222.
55. Ferbitz L, Maier T, Patzelt H, Bukau B, Deuerling E, Ban N. 2004. Trigger factor in complex with the ribosome forms a molecular cradle for nascent proteins. Nature 431:590-6.
56. Depping R, Lohaus C, Meyer HE, Rüger W. 2005. The mono-ADP-ribosyltransferases Alt and ModB of bacteriophage T4: Target proteins identified. Biochem Biophys Res Commun 335:1217-1223.
57. Quinten TA, Kuhn A. 2012. Membrane interaction of the portal protein gp20 of bacteriophage T4. J Virol 86:11107.
58. Loison P, Majou D, Gelhaye E, Boudaud N, Gantzer C. 2016. Impact of reducing and oxidizing agents on the infectivity of Qβ phage and the overall structure of its capsid. FEMS Microbiol Ecol 92.
59. Ramazzina I, Costa R, Cendron L, Berni R, Peracchi A, Zanotti G, Percudani R. 2010. An aminotransferase branch point connects purine catabolism to amino acid recycling. Nat Chem Biol 6:801-6.
60. French JB, Ealick SE. 2010. Biochemical and structural characterization of a ureidoglycine aminotransferase in the *Klebsiella pneumoniae* uric acid catabolic pathway. Biochemistry 49:5975-7.
61. Li X, Gonzalez F, Esteves N, Scharf BE, Chen J. 2020. Formation of phage lysis patterns and implications on co-propagation of phages and motile host bacteria. PLOS Comput Biol 16:e1007236.
62. Chan BK, Sistrom M, Wertz JE, Kortright KE, Narayan D, Turner PE. 2016. Phage selection restores antibiotic sensitivity in MDR *Pseudomonas aeruginosa*. Sci Rep 6:26717-26717.
63. Oswald C, Tam H-K, Pos KM. 2016. Transport of lipophilic carboxylates is mediated by transmembrane helix 2 in multidrug transporter AcrB. Nat Commun 7:13819-13819.
64. Dos Santos AMP, Ferrari RG, Conte-Junior CA. 2019. Virulence factors in *Salmonella* Typhimurium: The sagacity of a bacterium. Curr Microbiol 76:762-773.
65. Metcalfe HJ, Best A, Kanellos T, La Ragione RM, Werling D. 2010. Flagellin expression enhances *Salmonella* accumulation in TLR5-positive macrophages. Dev Comp Immunol 34:797-804.
66. Pos KM. 2009. Drug transport mechanism of the AcrB efflux pump. Biochim Biophys Acta 1794:782-93.
67. Seeger MA, von Ballmoos C, Verrey F, Pos KM. 2009. Crucial role of Asp408 in the proton translocation pathway of multidrug transporter AcrB: evidence from site-directed mutagenesis and carbodiimide labeling. Biochemistry 48:5801-12.
68. Meynell EW. 1961. A phage, *øχ*, which attacks motile bacteria. Microbiology 25:253-290.
69. Bertani G. 1951. Studies on lysogenesis. I. The mode of phage liberation by lysogenic *Escherichia coli*. J Bacteriol 62:293-300.
70. Datsenko KA, Wanner BL. 2000. One-step inactivation of chromosomal genes in *Escherichia coli* K-12 using PCR products. Proc Natl Acad Sci U S A 97:6640-5.
71. Binotto J, MacLachlan PR, Sanderson KE. 1991. Electrotransformation in *Salmonella typhimurium* LT2. Can J Microbiol 37:474-7.

72. Bonifield HR, Hughes KT. 2003. Flagellar phase variation in *Salmonella enterica* is mediated by a posttranscriptional control mechanism. J Bacteriol 185:3567-3574.

FIGURES

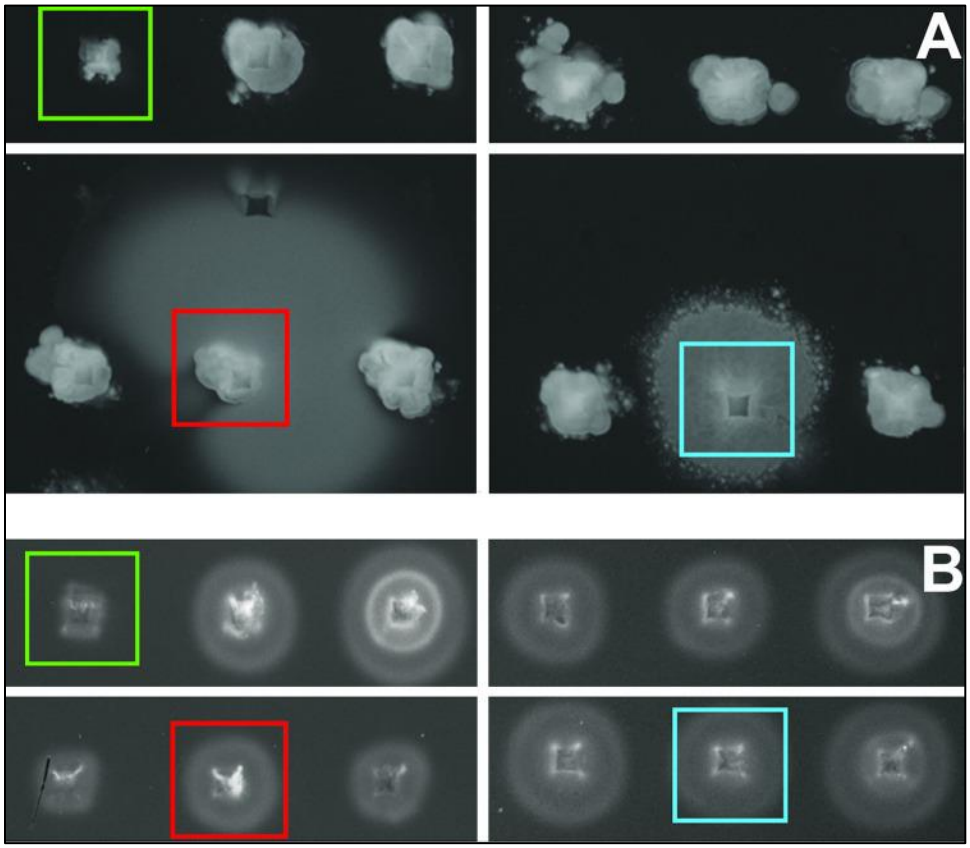


Fig. 2.1. (A) Screen of the STM 14028s MGD library on a rectangular plate containing MSB swim agar with approximately $1x10^7$ pfu/ml χ phage after an 8h incubation at 37°C. The colony highlighted in red is a ΔSTM14_0524-0529 mutant, which is motile and highly χ-resistant. The colony highlighted in blue is a ΔSTM14_0904-0923 mutant, which is motile and χ-resistant to a lesser degree than the red ΔSTM14_0524-0529, with an intermediate phenotype and irregular swim ring shape. The colony highlighted in green is a ΔSTM14_2324-2359 mutant, which includes a deletion in the essential flagellar motor gene *motA* and is non-motile and χ-resistant. The remaining colonies consist of motile χ-susceptible mutants, which only exhibit small amounts of growth and swimming around the initial inoculation point when compared to the non-motile mutant. (B) Screen of the same STM 14028s MGD mutants on a rectangular plate containing MSB swim agar without added phage after a 3h incubation at 37°C. Mutant colonies are highlighted as in Fig. 2.1A. The inconsistent swim ring size is characteristic of the inherent variability when inoculating swim agar using a 96-well pin replicator rather than applying a more controlled inoculation volume via pipet.

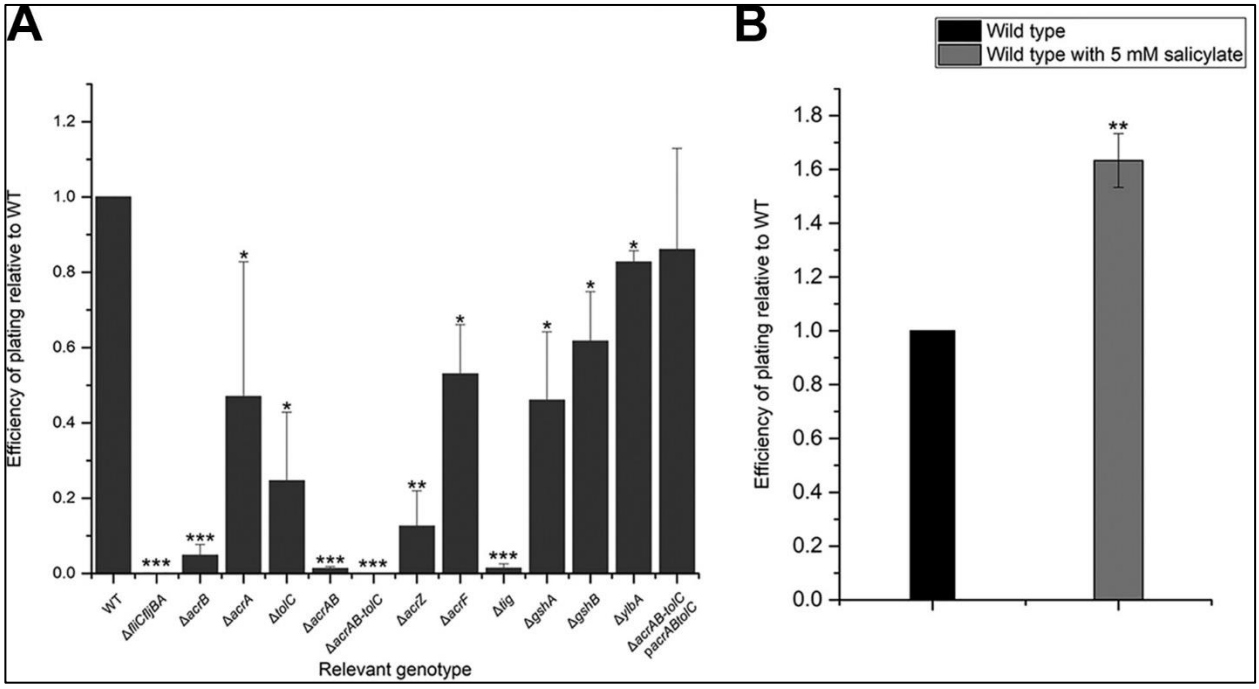


Fig. 2.2. (A) Efficiency of plating (EOP) of *Salmonella enterica* sv Typhimurium 14028s (STM 14028s) mutants compared to wild type. EOP results for all mutants were confirmed with a second deletion mutant constructed with a different antibiotic resistance cassette, with the exception of the Δ*gshB*, Δ*acrAB*, and Δ*acrABtolC* mutants. (B) EOP of wild type STM 14028s grown in medium with and without 5 mM sodium salicylate. EOP is calculated using the formula EOP= (pfu per ml mutant) / (pfu per ml wild type). All data points are composed of three replicates. Error bars represent standard deviation and statistical significance was determined using Student's t-test.

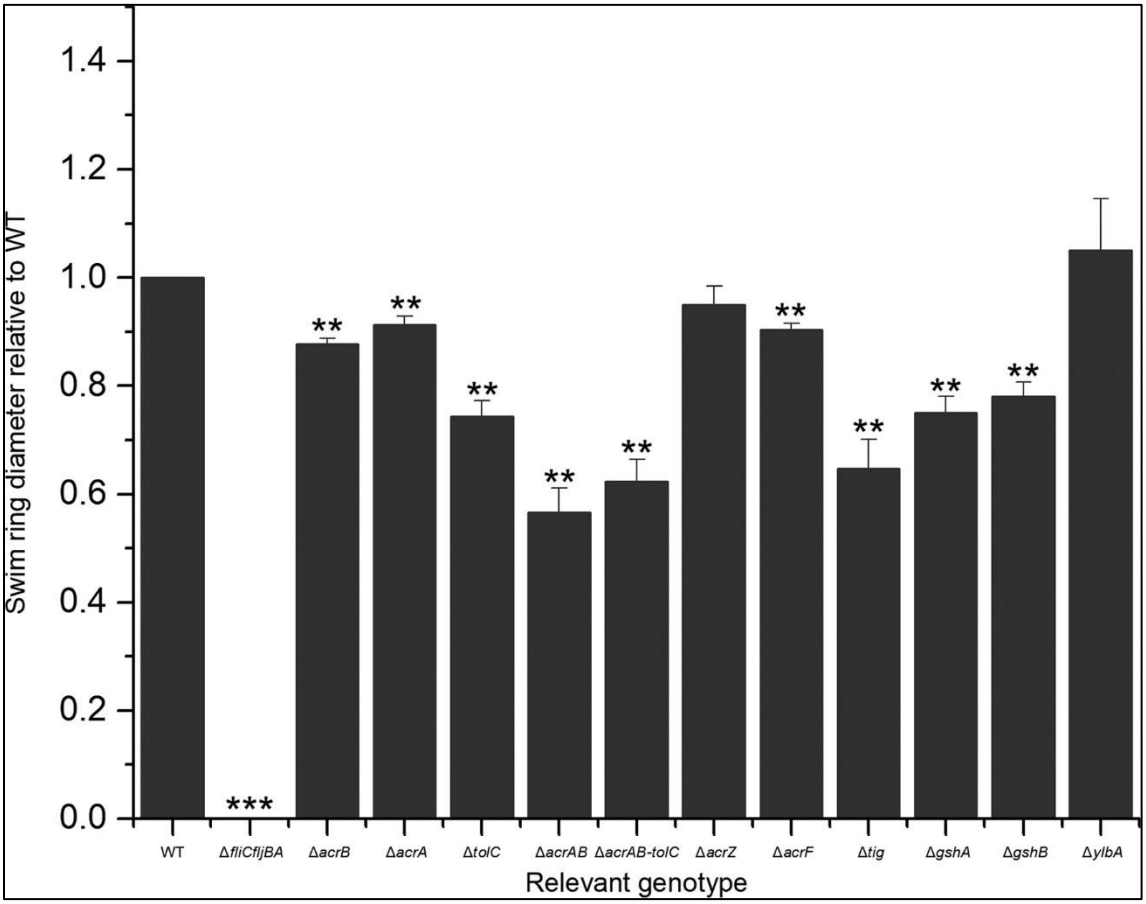


Fig. 2.3. Swim ring diameter of STM 14028s mutants compared to wild type formed on 0.3% MSB agar after 5 h. All data points are composed of three replicates. Error bars represent standard deviation and statistical significance was determined using Student's t-test.

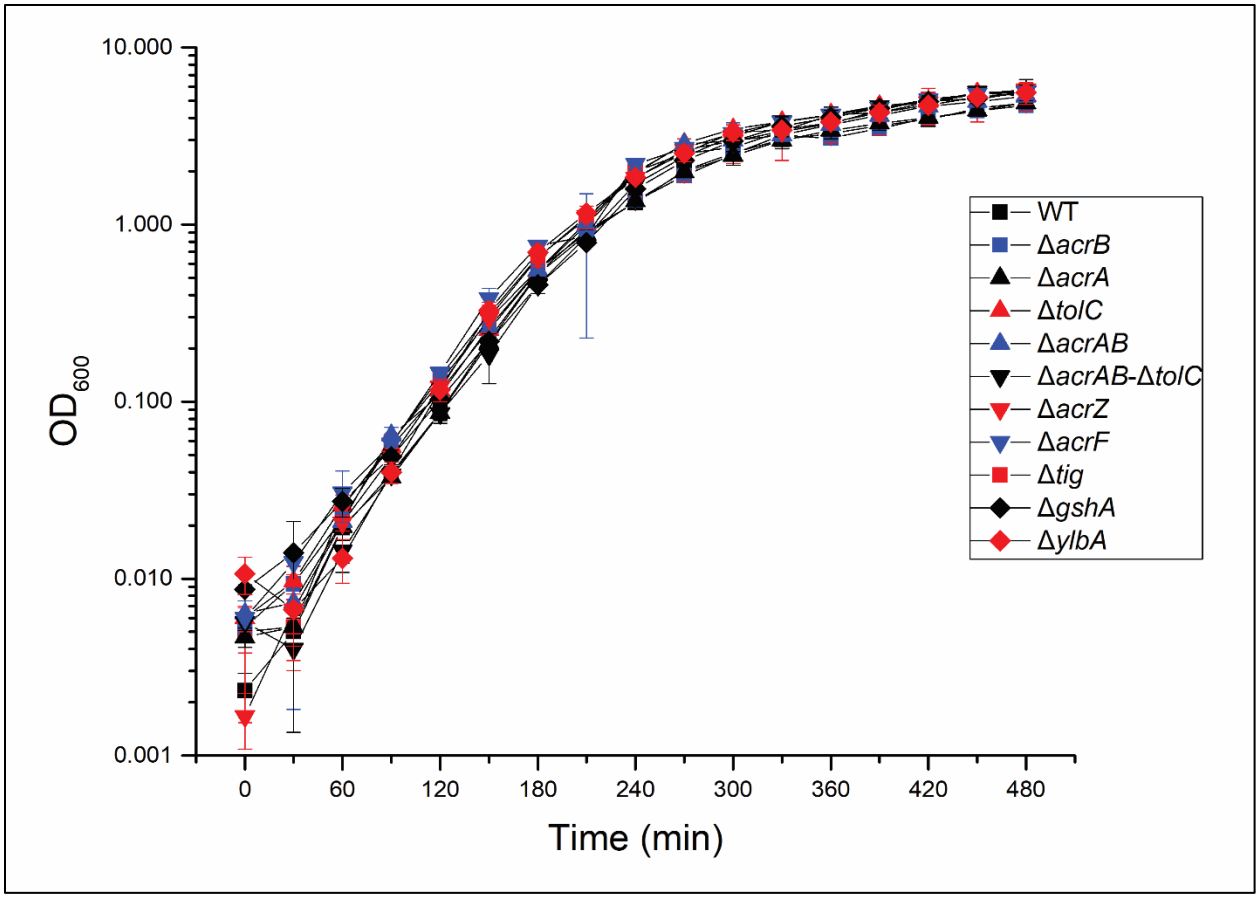


Fig. 2.4. Growth curves of select STM 14028s deletion mutants. All data points are the average of three replicates. Error bars represent standard deviation and statistical significance was determined using Student's t-test.

Chapter III

# Phages on filaments: A genetic screen elucidates the complex interactions between *Salmonella enterica* flagellin and bacteriophage Chi

Published in: *PLOS Pathogens* (Public Library of Science)

Nathaniel C. Esteves, Danielle N. Bigham, Birgit E. Scharf

Department of Biological Sciences, Virginia Polytechnic Institute and State University,

Blacksburg, VA 24061, USA

Esteves NC, Bigham DN, Scharf BE. Phages on filaments: A genetic screen elucidates the complex interactions between *Salmonella enterica* flagellin and bacteriophage Chi. *PLoS Pathog*. 2023 Aug 3;19(8):e1011537. doi: 10.1371/journal.ppat.1011537. PMID: 37535496; PMCID: PMC10399903.

Short title: *Salmonella* FliC antigenic domains are essential for χ phage binding

ABSTRACT

The bacterial flagellum is a rotary motor organelle and important virulence factor that propels motile pathogenic bacteria, such as *Salmonella enterica*, through their surroundings. Bacteriophages, or phages, are viruses that solely infect bacteria. As such, phages have myriad applications in the healthcare field, including phage therapy against antibiotic-resistant bacterial pathogens. Bacteriophage χ (Chi) is a flagellum-dependent (flagellotropic) bacteriophage, which begins its infection cycle by attaching its long tail fiber to the *S. enterica* flagellar filament as its primary receptor. The interactions between phage and flagellum are poorly understood, as are the reasons that χ only kills certain *Salmonella* serotypes while others entirely evade phage infection. In this study, we used molecular cloning, targeted mutagenesis, heterologous flagellin expression, and phage-host interaction assays to determine which domains within the flagellar filament protein flagellin mediate this complex interaction. We identified the antigenic N- and C-terminal D2 domains as essential for phage χ binding, with the hypervariable central D3 domain playing a less crucial role. Here, we report that the primary structure of the *Salmonella* flagellin D2 domains is the major determinant of χ adhesion. The phage susceptibility of a strain is directly tied to these domains. We additionally uncovered important information about flagellar function. The central and most variable domain, D3, is not required for motility in *S.* Typhimurium 14028s, as it can be deleted or its sequence composition can be significantly altered with minimal impacts on motility. Further knowledge about the complex interactions between flagellotropic phage χ and its primary bacterial receptor may allow genetic engineering of its host range for use as targeted antimicrobial therapy against motile pathogens of the χ-host genera *Salmonella*, *Escherichia*, or *Serratia*.

AUTHOR SUMMARY

Multidrug-resistant (MDR) bacteria kill over one million people per year worldwide. For instance, MDR typhoid fever is a significant concern in developing countries. As we precipitously approach a post-antibiotic society, bacteriophage therapy is a promising solution to the antibiotic crisis. Bacteriophage χ is a virus capable of infecting three species of pathogenic bacteria via their flagella, a significant virulence factor. Flagellum-dependent phages exploit an evolutionary tradeoff: a bacterium suppressing motility to avoid infection by such a phage would likely attenuate its own virulence. This makes flagellum-dependent phages of particular interest for potent therapy against MDR pathogens. In this study, we unveil crucial information about the mechanism of infection of *Salmonella enterica* by χ, knowledge which has the potential to lead to genetic modification of χ phage's host range and subsequent clinical applications. Similar studies can be conducted in other phage systems to broaden humanity's repertoire of potent therapeutic bacteriophages.

## INTRODUCTION

*Salmonella enterica* is a very broad species of Proteobacteria responsible for millions of bacterial infections per year worldwide (1). With greater than 2,600 serotypes contained within six subspecies (2), *S. enterica* is an extremely diverse bacterial species. Serotypes are broadly categorized as typhoidal or non-typhoidal. Typhoidal *Salmonellae* cause the potentially deadly disease typhoid fever, which leads to numerous deaths particularly in developing countries (3). Non-typhoidal Salmonellosis (NTS) is a generally self-limiting bacterial gastroenteritis (4), which presents with diarrhea, nausea, and vomiting and carries a slight risk of death from

dehydration or invasive disease, with certain serotypes being more likely than others to be invasive (5). NTS is the leading cause of bacterial foodborne illness worldwide, resulting in an estimated 93 million cases per year and hundreds of thousands of deaths (1, 4). Multidrug resistance (MDR) is a growing concern in *S. enterica* (1, 3, 6). MDR typhoid fever is a particularly serious problem, as people with untreated typhoid infections have a high rate of mortality (6, 7). A potential solution to treat infections caused by increased bacterial antibiotic resistance is bacteriophage therapy (8-10).

Bacteriophages, or phages, are viruses which solely infect bacteria without attacking eukaryotic cells (11). Their host specificity, efficiency of killing, and self-replicating nature make phages remarkable candidates for potent antimicrobial therapy (12-14). In fact, phages have been used for this purpose beginning over a century ago (15), but were largely abandoned with the invention and popularization of antibiotics (12). As we move toward a post-antibiotic era, phage therapy has seen a significant resurgence as a valid medical treatment (13, 16). The host specificity of phages greatly improves their usefulness as therapeutics, as a phage treatment can be specifically tailored to a particular pathogenic bacterium, avoiding disruption of the delicate balance of natural bacterial flora. Phage cocktails, mixtures of phages, can be used when broader spectra of activity are needed (17). More information is required about phage infection mechanisms for the true potential of phage therapy to be realized.

All phages begin their infection cycle by binding to a bacterial-encoded receptor (18, 19). This receptor is recognized and bound to via a phage-encoded receptor binding protein (RBP) (18). Phage receptor diversity is extremely broad, with various phages being capable of utilizing lipopolysaccharide, pili, porins, or other cell membrane components as receptors (19, 20). One unique phage infection mechanism is that of the flagellotropic (flagellum-dependent) phages.

This diverse category of viruses shares the common feature of using the bacterial flagellum as its primary receptor (20).

The bacterial flagellum is a rotary appendage that propels bacteria through their surroundings via swimming motility (21-23) or on surfaces via swarming motility (24). The flagellum is composed of three major subsections: basal body, hook, and filament (25). The basal body is a complex of over twenty proteins, which form the motor responsible for torque generation and the secretion system machinery required for export of flagellar proteins (25). The rod of the motor is attached to the flexible hook (26) which is, in turn, attached to the helical filament (21). The filament is a long, rigid propeller that translates motor rotation into forward propulsion. It is a polymer composed of a protein called flagellin, often designated FliC in organisms such as *Escherichia coli* (27) and *S. enterica* (28). Up to 30,000 individual flagellin monomers polymerize into a helix with eleven-fold radial symmetry to form a single filament (29). Flagella and flagellins are potent virulence factors in many pathogenic bacteria for a multitude of reasons (30-33): (i) motility itself gives bacteria a competitive advantage (34); (ii) flagella play roles in cell invasion, biofilm formation, and adhesion to surfaces (1, 31, 34); and (iii) flagellin is a potent antigen recognized by toll-like receptor 5 in humans (35, 36).

Flagellin proteins are extremely variable between bacterial strains, both by amino acid sequence and length (27, 37). For instance, the hypervariable D3 domains of flagellin share merely 15.5% amino acid sequence identity between the closely related *S. enterica* serotypes Typhimurium and Enteritidis (Table 3.1). Certain bacteria, such as the *Yersiniaceae* species *Serratia marcescens*, have highly truncated FliC proteins (38). In many enteric bacteria, flagellin is composed of seven domains: D0, D1, and D2 at the N- and C-termini, and a single, central D3 (39, 40). In the three-dimensional FliC structure, each N-terminal domain is located adjacent to its C-terminal

counterpart. NTD2, CTD2, and D3 form the antigenic region, facing outward in the assembled flagellar filament (40). These antigenic domains are hypervariable with D3 being the most variable and typically having very little conservation between different serotypes (37). The D2 and D3 domains also greatly vary in length from over 1,000 amino acid residues to essentially lacking these antigenic domains (20, 37). For instance, *Caulobacter crescentus* encodes six different short flagellins, all of which lack D2 and D3 domains (41). Variation in the flagellin antigenic domains likely plays a role in pathogenesis (27). In contrast, structural domains NTD0, NTD1, CTD1, and CTD0 are highly conserved even across different phyla of bacteria and are crucial for filament core formation and filament assembly (37, 40, 41).

In addition to the primary structure, there are other significant differences between the flagellins of various Enterobacterales bacteria. Most *S. enterica* serotypes undergo flagellin phase variation between two flagellins via a unique transcriptional regulatory mechanism (42). The *fljAB* operon is under the control of an inversible promoter, which switches direction mediated by the Hin invertase. When the promoter faces in the antisense direction relative to the *flj* operon, *fljA* and *fljB* are not transcribed. When the promoter faces forwards, *fljA* and *fljB* are transcribed. The gene product FljB is phase 2 flagellin, while FljA is a transcriptional repressor of *fliC*. This ensures that only one flagellin gene is expressed at any given time (42). The inversion is a rare event (42, 43), and under normal circumstances *Salmonella* cells will only produce filaments composed of a single flagellin type at a time. More rarely, some *S. enterica* serotypes produce a third flagellin, generally given the designation FlpA. This third flagellin gene is typically plasmid-borne and can therefore be unstable, may not be consistently present in all strains of a particular serotype, and can be horizontally transferred to other serotypes (44). *E. coli* and *S. marcescens* each typically have only a single flagellin. *E. coli* and *S. marcescens* also lack the

flagellin lysine-N-methyltransferase FliB present in *S. enterica* (45, 46). This enzyme adds methyl groups to lysine residues primarily in the antigenic domains NTD2, CTD2, and D3 of both FliC and FljB (47). Flagellin methylation in *Salmonella* has implications for adhesion, immune evasion, and virulence (47). Similarly to *E. coli* and *S. marcescens*, *S. enterica* has never been shown to post-translationally modify its flagellins in other ways such as glycosylation (48). Bacteriophage χ (Chi) is a flagellum-dependent (flagellotropic) phage infecting multiple species of enteric bacteria (49-51). The infection process of χ is hypothesized to follow a nut-and-bolt mechanism, which postulates that the phage attaches to the filament within the grooves formed by the flagellin monomers and is brought down to the cell surface by the rotation of the flagellum, much like a nut moving down a bolt (20, 52, 53). The requirements for infection by χ are thus very specific. Cells that lack flagella or that have paralyzed flagella are unable to be infected by χ (49). Control of motor rotation through the chemotaxis system has also been shown to be important for χ infection, as cells with flagella that only rotate clockwise are resistant to χ (52). Phage χ is known to infect *S. enterica* (20, 50, 54, 55), *E. coli* (20, 49), and *S. marcescens* (51), all of which are capable of pathogenesis (1, 56, 57). The breadth of the Enterobacterales and relative lack of χ phage research means that other bacterial species may be susceptible as well. The status of flagella and motility as potent virulence factors makes flagellotropic phages of particular interest as powerful antimicrobial agents against clinically significant bacteria (20). Phages targeting virulence factors or antibiotic resistance mechanisms impose an exploitable evolutionary tradeoff: a bacterium which downregulates expression of a virulence factor such as flagellin to avoid infection by a phage would likely attenuate its own virulence (20, 58). Bacteriophage χ has an unusual host range in that it infects bacteria across two families, the *Enterobacteriaceae* and *Yersiniaceae*, but infects only certain serotypes within *S. enterica* subsp.

*enterica*. Subtle differences between *Salmonella* serotypes therefore must determine whether a strain is susceptible or resistant to χ phage. Very little has been uncovered about the factors contributing to this host range, but flagellar structure is a likely candidate. This is because the flagellum is the primary receptor for χ (49, 53), and flagellin antigen is a key differentiating factor between *Salmonella* serotypes (2). We have recently identified a potential secondary cell surface receptor for χ. The multidrug efflux pump AcrABZ-TolC is essential for χ infection as its deletion results in complete abolishment of infection without halting motility (54). The essential nature of an antibiotic resistance mechanism for infection further increases the attractiveness of χ for clinical use, as avoidance of phage infection by mutation of AcrABZ-TolC is an additional evolutionary tradeoff that can possibly be exploited by coadministration of phage and antibiotic (58, 59). In this study, we used targeted mutagenesis and heterologous expression of mutant flagellin to determine which structural domains of the flagellar filament are essential for χ infection, broadening knowledge on a phage with potential clinical applications, in addition to employing motility assays with FliC domain mutants to further understand the function of *Salmonella* flagella.

RESULTS

**Susceptibility phenotypes cannot be determined solely from antigenic formulae**

Table 3.1. Susceptibility phenotypes of a subset of *Salmonella enterica* serotypes and their flagellin (H) antigens (2). The symbol (-) indicates no phase 2 flagellin is produced by that serotype. None of the serotypes listed produce phase 3 flagellin. A comprehensive list of all tested serotypes and their H antigen formulae is found in S1 Table.

| **Serotype** | **Phase 1 H antigen** | **Phase 2 H antigen** | **χ host phenotype** |
|---|---|---|---|
| Abortusovis | c | 1,6 | Resistant |
| Choleraesuis | c | 1,5 | Susceptible |
| Enteritidis | g,m | - | Resistant |
| Heidelberg | r | 1,2 | Resistant |
| Javiana | l,$z_{28}$ | 1,5 | Susceptible |
| Montevideo | g,m,s | - | Resistant |
| Schwarzengrund | d | 1,7 | Susceptible |
| Typhimurium | i | 1,2 | Susceptible |

We tested numerous *S. enterica* serotypes with representative Phase 1 and Phase 2 antigens for χ susceptibility to determine whether a correlation could be found between antigen type and phage susceptibility. We employed qualitative phage spot assays to determine χ susceptibility. A small subset of tested strains indicated that bacteriophage χ is only capable of infecting certain *S. enterica* serotypes (Table 3.1). More comprehensively, our qualitative serotype susceptibility testing (total n=37) demonstrated that approximately half of the tested serotypes (S1 Table) are hosts for χ (n=19), while the other half is resistant (n=18). There are monophasic, biphasic, and triphasic serotypes in both the resistant and susceptible category, ruling out a requirement for multiple flagellins for χ infection. We have noted that strains with the g flagellin antigen, including serotype Enteritidis, are always resistant to χ, in agreement with observations by Meynell (50). Other than that, no clear correlation between serotype and susceptibility was found. It is worth noting that the host range of χ is significantly different from the host range of

the very closely related phage YSD1 (60). Additionally, ser. Typhimurium FliC expressed in ser. Enteritidis does not confer a host phenotype (S1 Table).

Table 3.2. Domain definition of *S. enterica* serotypes Typhimurium and Enteritidis FliC used for *fliC* mutant construction according to ser. Typhimurium literature and sequence homology (40). There is no full consensus on the domain definition in all bacterial species, thus values may vary slightly between literature sources. Amino acid sequence identities and similarities between domains of ser. Typhimurium 14028s FliC and ser. Enteritidis P125109 FliC are given. Identities and similarities were calculated by EMBOSS Needleman-Wunsch algorithm (EMBL-EBI) (61, 62).

| **Domain** | ser. Typhimurium **AAs in 14028s** | ser. Enteritidis **AAs in P125109** | **Identity** | **Similarity** |
|---|---|---|---|---|
| NTD0 | 1-44 | 1-44 | 93.2% | 97.7% |
| NTD1 | 45-177 | 45-177 | 80.5% | 88.0% |
| NTD2 | 178-190 | 178-190 | 16.7% | 16.7% |
| D3 | 191-290 | 191-300 | 15.5% | 20.6% |
| CTD2 | 291-406 | 301-416 | 23.4% | 35.9% |
| CTD1 | 407-453 | 417-463 | 74.5% | 87.2% |
| CTD0 | 454-495 | 464-505 | 95.2% | 100.0% |
| Full length | 1-495 | 1-505 | 52.4% | 61.8% |

**Motility is significantly reduced when *fliC* is expressed from pBS1316**

We constructed numerous flagellin mutants and chimeras (Fig. 3.1) by combining domains from the host serotype Typhimurium and the non-host serotype Enteritidis, as well as introducing deletions of entire domains. These included mutations of the antigenic domains NTD2, D3, and CTD2, as well as the structural NTD0, NTD1, CTD1, and CTD0 domains. FliC sequences are aligned in S1 Figure, and the residue assignments are listed in Table 3.2. Mutant flagellins were first expressed from a novel flagellin expression vector, which is based on plasmid pTrc99a. This vector was constructed to include the entire ser. Typhimurium *fliC* promoter in addition to known regulatory elements in the 5' UTR (28, 63). Despite the use of this vector, motility was significantly reduced with trans-complemented flagellin compared to flagellin expressed from the chromosome. We also noted a greater level of variability in motility. For this reason, we only

report qualitative motility data for the trans-complementation mutants, which are given in the rightmost column of Fig. 3.1, and performed subsequent, quantitative analyses with chromosomal *fliC* mutant strains. Quantification of motility was analyzed on soft agar swim plates, and the data are given in Fig. 3.2. We found that plasmids pFliC4, pFliC5, pFliC7, pFliC9, pFliC10, pFliC12, and pFliC13 did not confer motility to ser. Typhimurium Fla$^-$. Conversely, plasmids pFliC1, pFliC2, pFliC3, pFliC6, pFliC8, and pFliC11 rescued motility in ser. Typhimurium Fla$^-$ to varying degrees on swim plates or when viewed using phase contrast microscopy. Thus, we constructed chromosomal mutants for the latter group. The non-host ser. Enteritidis only possesses FliC, and it is unknown whether the FliB methylase of ser. Typhimurium would methylate ser. Enteritidis flagellin. Therefore, flagellin mutants were constructed in a Δ*fljBA* Δ*fliB* background to eliminate the variables of flagellin phase variation and flagellin methylation (46) (48), and we refer to this strain as WT or FliC1 in the following sections.

### *Salmonella* ser. Typhimurium cells expressing ser. Enteritidis fliC are motile and χ resistant

Strains with chromosomal *fliC* mutations all exhibited increased motility as compared to their plasmid-borne counterparts (Fig. 3.2). This allowed the collection of quantitative EOP and adsorption data. EOP values were calculated as percentage of FliC1 (wild type ser. Typhimurium FliC without expressing FliB or FljB) (Fig. 3.3), and adsorption is given as percentage of phage particles adsorbed after a ten-minute incubation (99% for FliC1) (Fig. 3.4). More importantly, FliC2 (wild type ser. Enteritidis FliC expressed in ser. Typhimurium) exhibits only slightly reduced (86% of FliC1 motility; Fig. 3.2) compared to cells producing native ser. Typhimurium FliC. Despite its high motility, FliC2 was χ resistant, without any plaque formation (EOP = 0)

(Fig. 3.3). The EOP assay is highly sensitive and capable of detecting an EOP approximately $10^8$-fold lower than FliC1. As FliC2 did not allow phage production or even adsorption, flagellar filaments composed of a non-host FliC entirely prevent infection of and binding to an otherwise χ susceptible strain (Fig. 3.4). From this we conclude that production of a flagellar filament composed of FliC from a non-host serotype is sufficient to fully block χ infection in a host serotype, signifying that flagellin structure is a key factor determining host range.

**D3 alone has only a small impact on motility and phage interactions**

After determining that a non-host flagellin gene expressed in a host strain prevents χ binding and infection, we sought to investigate the potential role of FliC D3 as this is the most variable domain. This goal was accomplished by constructing D3 deletion and substitution mutants. Despite the loss of 100 amino acid residues, a strain with a deletion of the central antigenic ser. Typhimurium FliC D3 (FliC3) was only slightly reduced in its motility (84% of FliC1; Fig. 3.2). A similar phenotype was seen when ser. Typhimurium D3 was replaced with D3 from ser. Enteritidis FliC (FliC6), although this strain displayed a more significant reduction in swim ring diameter with 66% of FliC1. More interestingly, both FliC3 and FliC6 remained susceptible to χ phage, with FliC3 exhibiting an EOP statistically indistinguishable from FliC1 and FliC6 being susceptible to a lesser degree (EOP = 34%). FliC3 presented only a modest reduction in phage adsorption (95%), while FliC6 showed a more pronounced reduction to 67%, indicating a reduced quality of binding in the presence of a non-host D3. Since some mutant strains with large motility defects were still χ susceptible, it rules out the possibility that the modest motility defect of FliC2 described above is causing χ resistance. These data lead to the conclusion that while D3 is not required for binding, a non-host D3 can weaken the quality of binding.

**D2 domains are indispensable for motility and determine χ susceptibility**

After determining that D3 is dispensable in χ susceptibility, we next investigated the role of the D2 domains. Deletion and substitution mutants were constructed, with mutations in individual D2 domains, both D2 domains, or D2 and D3 domains combined. The N- and C-terminal D2 antigenic domains are in close proximity in assembled flagellar filaments (40). Interactions between the D2 domains are known to contribute to the overall stability of the filament. *S. enterica* flagellar filaments composed of mutant flagellin monomers lacking portions of the outer domains have been shown to be less stable (64). Additionally, D2 domains transiently interact with each other and with other flagellin domains to overall stabilize the filament (65). As such, we observed complete abolishment of motility when D2 domains alone were deleted or substituted, for example with complementation plasmids pFliC4, 12, and 13 (Fig. 3.1). Consequently, these strains were χ resistant. On the contrary, when both D2 domains and the D3 domain of ser. Typhimurium were exchanged with their ser. Enteritidis FliC counterparts (FliC8), motility was partially rescued (32% of FliC1). Despite its significant motility, FliC8 was fully resistant to χ (EOP = 0%) and also prevented χ adsorption, as its adsorption value of 7% was not statistically significant from that of the χ resistant strains FliC2 or Δ*fliC*. Moreover, the inverse holds true: when both D2 domains and the D3 domains from ser. Enteritidis FliC were replaced by their ser. Typhimurium equivalents (FliC11), χ susceptibility was restored with an EOP of 67% of FliC1. Interestingly, this mutant's EOP was significantly higher than the 34% EOP value of FliC6, which possesses the D0, D1, and D2 domains from the susceptible strain. In contrast, the adsorption value of FliC11 (48%), was lower than that of FliC6 (67%), although this difference was not statistically significant (P=0.09). Although the motility of FliC11 (21% of FliC1) was significantly reduced, it was sufficient to result in χ susceptibility. From these data,

taken together with the comparatively minor effects of D3 mutations, we conclude that the D2 domains play a key role in determining χ susceptibility, as substitution of these domains in conjunction with D3 was sufficient to fully abolish binding and infection while retaining motility.

**All mutants produce their respective mutant flagellins**

After determining mutant motility phenotypes, we analyzed and correlated flagellin production with these phenotypes. Via SDS-PAGE of whole cell lysates, and subsequent Coomassie staining and immunoblotting, we were able to provide evidence that all strains expressed stable flagellins, including those expressing chimeric flagellins (Fig. 3.5). Additionally, the commercially available *Salmonella* anti-H a-z antibody detected all flagellin proteins, including those with reduced antigenic domains. Serotype Typhimurium strain 14028s $FliC_{ON}$ Δ*fliB* (chromosomal mutant FliC1; WT) produced an intense flagellin band with an apparent molecular weight of 50 kDa, close to its calculated molecular weight of 51 kDa. The molecular weight of ser. Enteritidis strain P125109 (Ent.) flagellin is only 2 kDa higher than that of 14028s, however, the corresponding FliC band had an apparent molecular weight of 60 kDa. The 51-kDa band of the pFliC1 mutant appeared less intense than WT, likely corresponding to reduced production of WT flagellin. The pFliC2 mutant produced a band of the same molecular weight compared to Ent. The pFliC3 strain (ΔD3) showed a band at approximately 40 kDa, which is similar to the calculated molecular weight of 42 kDa. The non-motile pFliC4 and pFliC5 mutant strains each produced a band at approximately 37 kDa and 28 kDa, respectively, which is in agreement with the calculated sizes of D2, and D2 and D3 deletion mutant flagellins. A faint band could be identified for the motile pFliC6 strain, exhibiting the same apparent molecular weight as Ent.

FliC. The faint band in the pFliC7 strain exhibited the expected FliC size (51 kDa), although this mutant was non-motile. The motile pFliC8 strain (D2s and D3s replaced with ser. Enteritidis FliC) produced a band with an anomalous apparent molecular weight similar to the one observed for Ent. FliC. The band in the non-motile pFliC9 strain exhibited an increased intensity with a comparable size to WT FliC. The non-motile pFliC10 strain showed a band at the typical ser. Enteritidis FliC molecular weight. A distinct band was identified for the motile pFliC11 mutant strain, migrating at the typical molecular weight of ser. Typhimurium flagellin. Finally, the non-motile pFliC12 and pFliC13 mutant strains, encoding chimeric FliCs with ser. Enteritidis D3, both produced faint bands with the anomalous apparent molecular weight of ser. Enteritidis FliC. Lastly, the *Salmonella* anti-H a-z antibody recognized a 34 kDa band of similar intensity in all sixteen strains, including the non-flagellated Fla$^-$. We identified bands for all mutants that corresponded to FliC or FliC variants. The Coomassie-stained SDS-PAGE gel of whole cell lysates supported our immunoblot findings, although not all flagellin bands were easily discernable from other cellular proteins (S2 Figure). Interestingly, all non-motile strains expressing chimera or domain-deletion flagellin produced variant FliC protein, which excludes the lack of FliC production as the reason for their motility phenotype.

## DISCUSSION

### Strain selection and elimination of phase variation and methylation

In this study, all experiments are conducted in a *fliC*-locked Δ*fliB* ser. Typhimurium 14028s strain. This strain only produces flagellin FliC due to a complete deletion of phase 1 flagellin repressor gene *fljA* and phase 2 flagellin gene *fljB* (42). Deletion of the *fliB* gene ensures that flagellin is not methylated (46). Despite methylation not being crucial for χ phage infection, we

believed this to be an unnecessary variable, as methylation may alter the quality of phage binding. It is also unknown whether mutant flagellin proteins would be methylated by FliB. We determined that ser. Typhimurium cells expressing only *fliC* or only *fljB* are susceptible to χ (S1 Table). The *fliC* promoter is a classical promoter, while the *fljAB* promoter is complex, as it undergoes Hin-mediated inversion for flagellin phase variation (42). For this reason, the experiments in this study were carried out with strains expressing only FliC. Serotype Enteritidis was chosen as a non-host strain for multiple reasons: (i) ser. Enteritidis is a common serotype found in cases of gastroenteritis (66, 67); (ii) it is fully resistant to χ; (iii) it only produces a single flagellin without undergoing phase variation; and (iv) its H antigen type is g,m, with g antigen flagellins having been shown to be χ resistant by Meynell (50) and confirmed by our data (S1 Table). It is worth noting that despite being fully resistant to χ, this serotype allows a very small level of adsorption similar to the Fla$^-$ strain (Fig. 3.4). We hypothesize that this is likely due to χ being able to bind directly to the flagellar hook at extremely high multiplicities of infection. Phage χ has been demonstrated to bind to polyhook mutants (52), which would suggest that it likely can bind to hooks with wild-type length at high concentrations.

**Trans-complementation of flagellin yields poor motility**

We have found that motility is reduced when flagellin is expressed in trans, even when WT *fliC* is expressed from its native ser. Typhimurium $P_{fliC}$ promoter. Bacterial flagellar synthesis, including transcription, export, and assembly, is a complex process with multiple regulatory steps and mechanisms (21, 25, 68). Regulation of flagellin transcription may not function properly during *in trans* flagellin expression. The 5' untranslated region (UTR) of *fliC* has been reported to contain regulatory elements in *S*. Typhimurium (28). In addition, a stem-loop

structure that forms between RNA sequences in the *fliC* 5' UTR and sequences early in the coding region affects translation (69). Our pBS1316 vector includes these known regulatory elements, but there could be additional, undiscovered regulatory elements located outside of the cloned region. An abridged RNA length in the 3' UTR could also possibly reduce mRNA stability, as this has been shown to be a phenomenon in various bacteria (70). Plasmid copy number may also impact expression levels or disrupt the temporal regulation of flagellin expression (71, 72). High copy number may also result in depletion of the flagellar sigma factor, $\sigma^{28}$, and subsequently impact expression of late flagellum and chemotaxis genes. Additionally, heterologously expressed flagellin may not interact optimally with chaperone proteins, impacting folding and thus function. Regardless of the cause, this reduction in motility was significant enough to make quantitative phage-host interaction data unreliable, an issue that was ameliorated by the generation of chromosomal flagellin mutants.

**The involvement of domains D2 and D3 in motility and phage infection**

We showed in this study that deletion of both D2 domains with or without the D3 domain abolishes motility (Fig. 3.1). In addition, these domains cannot be heterologously substituted without the corresponding homologous D3 domain. We hypothesize that interactions between residues within NTD2, D3, and CTD2 mediate folding and assembly of monomers into the flagellar filament. During evolution, these domain interactions developed exclusively within a specific *S. enterica* serotype.

Thus, domains from different serotypes may not interact to support filament assembly, as the antigenic domains are known to play a role in filament stability (64). However, if both NTD2 and CTD2 are substituted along with D3, they can interact with each other to form a functional

filament. These constraints in the experimental approach prohibited us from determining whether NTD2, CTD2, or both are involved in χ infection.

Our experiments allow the conclusion that the central D3 antigenic domain by itself is not essential to determine χ phage susceptibility, despite being the most variable domain between *Salmonella* serotypes, as its deletion only mildly affects χ adsorption and does not disturb infection. Thus, D3 is not required for χ phage interaction. This lack of specificity offers a fitness advantage to χ, as subtle differences in the most variable FliC domain will not impact its capacity to infect a large variety of serotypes. We have also found that loss of D3 only has a minor impact on motility in *S.* Typhimurium. From these results, we infer that D3 is not essential for ser. Typhimurium 14028s filament formation or function, which confirms related studies in *E. coli* and *S.* Typhimurium LT2 (73, 74). Due to the vast diversity of flagellin alleles in the *S. enterica* genus, we cannot exclude the possibility that the D3 domain is essential for motility in certain serotypes or strains. Interestingly, we have found that the presence of non-host D3 in strain FliC6 reduces the quality of χ phage binding and infection without abolishing it.

The structural factors within flagellin that determine χ susceptibility may be inclusionary or exclusionary in nature. Inclusionary would specify that a particular motif within NTD2, D3, or CTD2 is required for χ infection. Exclusionary would indicate that particular motifs block χ infection, and that a strain can be infected as long as its flagellin does not contain one of these exclusionary motifs. Van Asten et al. reported that amino acid residues 258-348 of *S. enterica* serotype Enteritidis FliC form the epitope region determining the “g,m” flagellin antigen type (75). Meynell stated that χ infection in strains with flagellins of the g antigenic group is blocked (50), an observation that we have confirmed. It is therefore likely that certain residues within the “g,m” epitope region of FliC serve as an exclusionary factor preventing χ adsorption. The region

identified by Van Asten et al. lies mostly within CTD2, with 32 residues (aa 327-348) extending into D3. This corroborates our initial hypothesis that the D2 domains are most important for the determination of χ susceptibility, while D3 plays a smaller role. Our detailed domain replacement strategy further supports this hypothesis. We have determined that a strain expressing ser. Enteritidis NTD2, D3, and CTD2 (FliC8) is fully resistant to χ and retains motility. This ser. Enteritidis substitution contains the entirety of the g,m epitope region. Additionally, the inverse mutant (FliC11) is susceptible to χ, as it contains the D2 and D3 domains from ser. Typhimurium with the "i" antigen epitope. This result suggests that the g,m epitope dictates χ susceptibility. We also discovered that substitution of 14028s FliC D3 with its ser. Enteritidis equivalent (FliC6) reduces the quality of phage binding and infectivity without abolishing it completely. Therefore, D3 seems less important than the D2 domains but may still be part of the exclusionary factor. This notion matches well with the fact that only 32 residues of the g.m epitope lie within D3. However, the non-motile phenotype of individual D2 domain mutants and the poorly defined span of most antigenic epitopes, including the "i" epitope of ser. Typhimurium FliC, are prohibitory to further investigations. We have also shown that many non-host serotypes do not produce g type flagellins, and that production of flagellin with a similar host-strain antigen does not guarantee a host phenotype. For instance, the non-host serotype Michigan does not produce g type flagellin and serotype Heidelberg is also a non-host despite producing flagellin of antigen type 1,2. Furthermore, phage χ also binds to the flagellar filament of its host *S. marcescens*, which has an antigenic region that is 136 amino acid residues shorter than the *S.* Typhimurium FliC equivalent (38). In summary, we can conclude that factors within the D2 domains are essential, but we are unable to determine whether they are inclusionary or exclusionary. Furthermore, CTD2, as it compiles most of the epitope region, appears of greater

importance for χ infection than NTD2. Finally, although a direct interaction of χ with the D3 domain is unlikely, exclusionary factors may exist that obstruct binding.

**Factors other than flagella influence host range**

When ser. Enteritidis flagellin is expressed in a ser. Typhimurium Fla$^-$ strain, motility is retained but infection is entirely abolished. However, the expression of ser. Typhimurium flagellin in an ser. Enteritidis Fla$^-$ strain is sufficient to restore motility but the strain remains χ resistant (S1 Table). This implies that factors other than the flagellar filament structure are crucial in determining host susceptibility. Flagellin is by far the most structurally variable motility protein between *S. enterica* serotypes (37). During χ translocation along the flagellum to the cell surface, it will first interact with the filament (FliC or FljB), then with the hook-filament junction (FlgLK), and lastly with the hook (FlgE). The primary sequences of serotypes Typhimurium and Enteritidis FlgK and FlgE are 100% identical, while FlgL differs by only one single residue (76, 77). This high sequence conservation implies that ser. Enteritidis resistance is likely the result of steps secondary to initial attachment and translocation along the flagellum. Recently, we identified that the multi-substrate efflux system AcrABZ-TolC is essential for χ infection of *S.* Typhimurium via a motility-unrelated mechanism (54). We hypothesize that χ interacts with the AcrABZ-TolC complex at the cell surface and may use it as a channel to eject its DNA into the cytoplasm. RND-family inner membrane efflux pump AcrB, accessory protein AcrZ, and periplasmic adaptor AcrA are 100% identical, while the outer membrane channel TolC is 99% identical between the two serotypes. Further investigation is needed to determine whether the subtle differences between TolC of these two serotypes significantly affect susceptibility. We also discovered that the ribosome-associated molecular chaperone trigger factor is critical for χ

phage infection of *S.* Typhimurium (over 95% reduction in EOP when absent), while deletion of the *tig* gene only caused a minor motility defect (54). We hypothesize that trigger factor is involved in the folding of phage proteins, which would result in inefficient virion assembly in the absence of this chaperone. Since trigger factor proteins of both serotypes differ by only one amino acid residue, it is unlikely that this chaperone contributes to the functional differences in their χ resistance. Another significant difference between serotypes of *S. enterica* is the O antigen composition of lipopolysaccharide (LPS), which is a very common phage target. While it is possible that χ-resistant LPS mutants may have evaded our extensive deletion library screen analysis (54), as mutations in LPS are pleiotropic and often negatively affect motility (19, 78, 79), many factors generally disturb successful phage infection such as restriction/modification or CRISPR systems (80). Overall, the χ phage infection process is very complex, and one or many other motility-unrelated distinctions between serotypes Enteritidis and Typhimurium likely play a role in the host phenotypes of these two serotypes.

**Analysis of mutant flagellin production**

The immunoblot in Fig. 3.5 provided evidence that all mutant strains produce their respective flagellin proteins, although it is unknown whether these are exported and assembled into a filament. The immunoblot analysis was successful despite several mutants having significantly altered epitope regions. However, it is worth noting that band intensities for flagellins with altered epitopes cannot be correlated directly with the amount of flagellin produced due to the antibody's potentially reduced affinity for a particular mutant epitope. Interestingly, the non-motile mutants pFliC4, pFliC5, pFliC7, pFliC9, pFliC10, pFliC12, and pFliC13 produced bands not present in the $Fla^-$ strain, indicating that FliC is stably produced, including highly truncated

flagellin variants such as those lacking both D2 domains and additionally D3. We hypothesize that these significantly altered or truncated flagellins cannot be exported by the flagellar Type III export apparatus and/or are unable to form a filament.

While ser. Typhimurium FliC migrated according to its calculated molecular weight of 51 kDa, the 2-kDa larger ser. Enteritidis FliC migrated anomalously with an apparent molecular weight of 60 kDa. Interestingly, as revealed by the analysis of FliC domain variants, this phenomenon is caused specifically by the D3 domain of ser. Enteritidis FliC, as a FliC variant constructed on ser. Enteritidis FliC with D3 from ser. Typhimurium exhibits a migration behavior according to its calculated molecular weight (pFliC9). In contrast, pFliC10, which is ser. Enteritidis FliC containing ser. Typhimurium D2 domains, produces a FliC band that migrates at the anomalous apparent molecular weight of ser. Enteritidis FliC. The D3 domains in the two serotypes differ in length by only 10 residues, which would not cause such a significant apparent molecular weight shift. We can only speculate that this phenomenon is due to small variations in charge, as it is known that electrophoretic migration of methyl-accepting chemotaxis proteins is affected by neutralization of individual residues (81, 82). The ser. Enteritidis D3 domain possesses four additional positively charged and two additional negatively charged residues compared to its ser. Typhimurium equivalent (76, 77).

The 34 kDa cross-reacting band is present in all sixteen samples including the Fla- strain. During antigen preparation, it is possible that another flagellar component had been co-purified with flagellin, allowing the resulting antiserum to recognize this protein. We hypothesize that this band corresponds to the hook-filament junction protein FlgL, which is 34.2 kDa in ser. Typhimurium, while the other proteins forming the hook and filament junction do not match this apparent molecular weight (25).

**Further studies, applications, and potential setbacks**

Advanced knowledge about the interaction between χ and its host is necessary to eventually allow its inclusion in phage therapy cocktails. We have shown that the D2 domains of flagellin likely mediate the interaction with χ, possibly alongside D3. However, the domains or motifs within the χ receptor binding protein that are required for attachment to flagella are unknown. CHI_31, the putative tail fiber protein gene, could be mutagenized in a similar way as we have done for flagellin, to analyze the function of individual domains. It has not been shown experimentally that χ tail fiber consists of CHI_31, although the tail fiber protein has been shown to act as the RBP in the related phage YSD1 (60). Furthermore, a high-resolution structure of the χ tail fiber is lacking, which would aid in the identification of potential targets for mutagenesis. An additional problem is the inherent difficulty in constructing targeted mutants of lytic bacteriophages. A CRISPR/Cas-based method is one of the currently utilized techniques to successfully mutagenize lytic phages (83). Alternatively, a directed evolutionary approach may be effective and more straightforward. Such approaches have been applied to isolate host range mutants of bacteriophages (84). Alternatively, chemical mutagens like ethyl methanesulfonate or 5-bromouracil could be used to mutate phage DNA (85, 86). UV mutagenesis could also be attempted, as this has been applied to *E. coli* phage λ (87).

In this study, we have characterized part of the complex interaction between flagellotropic phage χ and *S. enterica* flagellin. We have demonstrated that alteration of certain FliC domains is sufficient to fully block χ infection. Our data, combined with previous knowledge about the flagellin g antigen epitope region, lead to our hypothesis that CTD2 is the most crucial domain for χ binding. Domains D3 and NTD2 are likely also significant but less important factors. Since g antigen flagellins block χ infection (50), we believe that exclusionary factors exist within

CTD2 or the C-terminal end of D3, which are part of the g epitope. Our data support this hypothesis, as exchange of both D2 domains and the D3 domain leads to a complete switch of the χ susceptibility phenotype, but alteration of solely D3 has a comparatively minor effect. However, we realize that there are numerous serotypes expressing non-g flagellins that are also entirely χ resistant (S1 Table), so there are clearly more factors involved in determining host range. Multiple studies have shown that mutagenesis can be used to alter a phage's host range (84, 88). This has clear potential in clinical applications. We now know that subtle changes in flagellin structure can significantly alter the ability of χ to bind flagella and subsequently kill its host. Findings of this study will move research in the direction of genetically modified phage treatments in clinical applications, a promising technique that has only recently come to fruition.

## MATERIALS AND METHODS

Table 3.3. Plasmids, bacterial strains, and bacteriophage used in this study. Figure 3.1 provides further detail on flagellin domain mutants. *S. enterica* serotypes tested for qualitative χ susceptibility are not included in this table and are listed comprehensively in S1 Table.

| **Strain/plasmid** | **Parent strain/plasmid** | **Genotype/ Relevant characteristics** | **Source** |
|---|---|---|---|
| pTrc99a | pBR322 | $P_{lac}$; MCS; pBR322 ori; $amp^r$ | Howard C. Berg |
| pBS1316 | pTRC99a | $P_{fliC(14028s)}$; MCS; pBR322 ori; $amp^r$ | This study |
| pFliC1 | pBS1316 | See Figure 3.1 | This study |
| pFliC2 | pBS1316 | See Figure 3.1 | This study |
| pFliC3 | pBS1316 | See Figure 3.1 | This study |
| pFliC4 | pBS1316 | See Figure 3.1 | This study |
| pFliC5 | pBS1316 | See Figure 3.1 | This study |
| pFliC6 | pBS1316 | See Figure 3.1 | This study |
| pFliC7 | pBS1316 | See Figure 3.1 | This study |
| pFliC8 | pBS1316 | See Figure 3.1 | This study |
| pFliC9 | pBS1316 | See Figure 3.1 | This study |
| pFliC10 | pBS1316 | See Figure 3.1 | This study |
| pFliC11 | pBS1316 | See Figure 3.1 | This study |

| | | | |
|---|---|---|---|
| pFliC12 | pBS1316 | See Figure 3.1 | This study |
| pFliC13 | pBS1316 | See Figure 3.1 | This study |
| pWRG730 | pSIM5 | $P_L$ *redαβγ*; $P_{tet}$ I-SceI; ori $SC101_{TS}$; $chl^r$ | Roman Gerlach |
| pWRG717 | pBluescript II | kan/I-SceI cassette template plasmid; $kan^r$ | Roman Gerlach |
| 14028s | *Salmonella enterica* subsp. *enterica* serotype Typhimurium 14028s | Wild type | Michael McClelland |
| 14028s Δ*fliB* | 14028s | Δ*fliB* | This study |
| 14028s Δ*fliB* pWRG730 | 14028s | Δ*fliB;* pWRG730; $chl^r$ | This study |
| 14028s $fliC_{ON}$ Δ*fliB* | 14028s | Δ*fliB;* Δ*fljBAhin*::*tetRA*; $tet^r$ | This study |
| 14028s $fliC_{ON}$ Δ*fliB* pWRG730 | 14028s | Δ*fliB;* Δ*fljBAhin*::*tetRA*; pWRG730; $chl^r$ $tet^r$ | This study |
| FliC1 | 14028s $fliC_{ON}$ Δ*fliB* | See Figure 3.1 | This study |
| FliC2 | 14028s $fliC_{ON}$ Δ*fliB* | See Figure 3.1 | This study |
| FliC3 | 14028s $fliC_{ON}$ Δ*fliB* | See Figure 3.1 | This study |
| FliC6 | 14028s $fliC_{ON}$ Δ*fliB* | See Figure 3.1 | This study |
| FliC8 | 14028s $fliC_{ON}$ Δ*fliB* | See Figure 3.1 | This study |
| FliC11 | 14028s $fliC_{ON}$ Δ*fliB* | See Figure 3.1 | This study |
| 14028s $Fla^-$ | 14028s | Δ*fliC::kan* Δ*fljBAhin*::*tetRA*; $tet^r$; $kan^r$ | (54) |
| P125109 | *Salmonella enterica* subsp. *enterica* serotype Enteritidis | Wild type | Michael McClelland |
| TH2788 | *Salmonella* Typhimurium LT2 | *fliY*::Tn10dTc; $tet^r$ | Kelly T. Hughes |
| DH5α | *Escherichia coli* K12 | $F^-$ *endA1 glnV44 thi-1 recA1 relA1 gyrA96 deoR nupG purB20* φ80d*lacZ*ΔM15 Δ(*lacZYA-argF*)U169, *hsdR17*($r_K^- m_K^+$), $\lambda^-$ | Howard C. Berg |
| Bacteriophage χ | - | Wild type | Saeed Tavazoie |

**Construction of cloning vector pBS1316**

Flagellin expression vector pBS1316 was constructed using Gibson assembly (89). Oligonucleotides (Invitrogen) were designed to amplify plasmid pTrc99a, retaining its multiple cloning site. Additional primers were designed to amplify the 146 bases immediately upstream of the ser. Typhimurium *fliC* ATG start codon, ensuring coverage of the entirety of the *fliC* promoter and known regulatory elements (28, 63). Primers additionally included 40-bp of flanking homology to the ends of the linearized pTRC99a. These purified PCR products were assembled using NEB 2x Gibson Assembly Master Mix and *E. coli* DH5α was subsequently transformed with the assembled reaction mixture and plated on lysogeny broth (LB) plates (90) (10 g/l tryptone, 5 g/l yeast extract, 5 g/l NaCl, 15 g/l agar) with 100 µg/ml ampicillin (LB amp). The plasmid construct was verified by Sanger sequencing.

**Trans-complementation of flagellin in 14028s**

The *fliC* mutant inserts were generated by PCR. Domains from either *S.* Typhimurium 14028s or *S.* Enteritidis P125109 were amplified and fused together by overlap extension PCR using outer primers with BamHI and SalI restriction enzyme sites. Some more complex mutants required multiple overlap extension steps. Plasmid pBS1316 and each completed insert were digested with these enzymes, purified via 1% TAE-agarose gel electrophoresis and subsequent kit purification (Thermo Scientific GeneJet), and ligated using T4 DNA ligase (New England Biolabs). *E. coli* DH5α was transformed with the ligation mixtures and constructs were verified by Sanger sequencing. Electrocompetent *S.* Typhimurium 14028s Fla$^-$ cells were prepared by first growing bacteria at 37°C until an $OD_{600}$ of 0.3-0.5 was reached. Cells were then chilled on ice for 15 minutes and centrifuged at 8,000 x g for 10 minutes at 4°C. The supernatant was

discarded and cells were washed twice with 1/2 volume of ice-cold 10% glycerol, then resuspended in 1/100$^{th}$ volume of 10% glycerol. Electrotransformation was performed by first adding 100 ng of pBS1316 construct plasmid DNA to a 50 µl aliquot of electrocompetent cells. This was transferred to a 0.2 cm electroporation cuvette (Bio-Rad) and electrotransformed via a 5 ms exponential-decay pulse at 2.5 kV, 25 µF, 200 Ω. One ml of chilled SOC medium (20 g/l tryptone, 5 g/l yeast extract, 10 mM NaCl, 2.5 mM KCl, 10 mM $MgCl_2$, 10 mM $MgSO_4$, 20 mM glucose) was immediately added and the cell suspension was plated on LB amp after a 1-hour recovery at 37°C. Motility of these Fla$^-$ pFliC mutants was qualitatively determined via microscopy.

**Mutant construction**

Trans-complementation was used to decide which mutations to construct chromosomally. A corresponding chromosomal mutant was not constructed for plasmid mutants that were entirely non-motile. Trans-complementation mutants found to be motile had their mutant alleles amplified from the plasmid and inserted into the chromosome using the lambda-red recombineering system and I-SceI nuclease counterselection essentially as described previously (91). Fresh electrocompetent cells were prepared for each transformation. Plasmid pWRG730 ($P_L$ λred; $P_{tet}$ I-SceI; ori $SC101_{TS}$) (91) was introduced into ser. Typhimurium 14028s by electroporation and cells were recovered in 1 ml terrific broth (20 g/l tryptone, 24 g/l yeast extract, 0.4% v/v glycerol, 17 mM $KH_2PO_4$, 72 mM $K_2HPO_4$) for 60 minutes at 30°C. The cell suspension was spread plated on LB with 10 µg/ml chloramphenicol (LB $chl_{10}$) and incubated overnight at 30°C.

For *fliC* allelic exchange, oligonucleotides were designed with 40-bp flanking homology to sequences within *fliC* and 20-bp of homology to template plasmid pWRG717 (91). PCR was used to amplify the kan/I-SceI cassette from pWRG717 using Phusion DNA polymerase (New England Biolabs). This cassette contains the aminoglycoside phosphotransferase gene conferring kanamycin resistance, and the I-SceI nuclease recognition site TAGGGATAACAGGGTAAT. Strain 14028s with pWRG730 was grown at 30°C until an $OD_{600}$ of 0.5 was reached. This culture was then transferred to a 42°C shaking water bath incubator for 15 minutes to induce expression of lambda-red genes under the λ $P_L$ promoter, followed by immediately transferring the culture to ice. Cells were made electrocompetent as described above, and the kan/I-SceI cassette with 40 bp *fliC* flanking homology was introduced by electroporation followed by recovery in terrific broth at 30°C for 1 hour and plating on LB with 50 µg/ml kanamycin and 10 µg/ml chloramphenicol (LB kan/$chl_{10}$) at 30°C to select for insertion mutants and retain plasmid pWRG730. Kan/chl-resistant colonies were isolated and *fliC*::kan/I-SceI insertion in one colony was verified by colony PCR. Mutant *fliC* DNA was amplified from the respective pBS1316 template plasmid and electrocompetent 14028s *fliC*::kan/I-SceI strain was transformed with the mutant *fliC* PCR product and recovered at 30°C in terrific broth for 1 hour. Serial 1:10 dilutions were prepared and $10^{-1}$ through $10^{-4}$ were spread plated on LB with 30 µg/ml chloramphenicol and 0.5 µg/ml anhydrotetracycline (aTc) (LB $chl_{30}$/aTc) at 30°C. After overnight incubation, large colonies were streaked for isolation on LB $chl_{30}$/aTc and subsequently streaked on LB kan/$chl_{10}$ to confirm loss of kanamycin resistance. $Kan^s$ colony *fliC* genotypes were then verified by colony PCR and Sanger sequencing. To eliminate the variable of flagellin lysine methylation, the flagellin methylase gene *fliB* was deleted scarlessly in the same manner. The kan/I-SceI cassette was inserted into the *fliB* gene and subsequently crossed out with the second step

cassette consisting of a fusion of 500 bp immediately up and downstream of the *fliB* gene followed by selection on LB $chl_{30}$/aTc plates. The absence of the *fliB* gene was confirmed by colony PCR and Sanger sequencing. To eliminate flagellin phase variation, the genes *fljB* and *fljA* were inactivated by insertion of a single *tetRA* cassette amplified from TH2788 (*S.* Typhimurium LT2 *fliY*::Tn10dTc) with flanking homology to the beginning of *fljB* and the end of *fljA* and subsequent selection on LB with 10 µg/ml tetracycline (LB tet). After mutagenesis was complete, pWRG730 was cured from the strain by overnight incubation at 42°C on LB tet, followed by confirmation of the $chl^s/kan^s/tet^r$ phenotype.

**Verification and quantification of motility**

Motility of cells grown to an $OD_{600}$ of 2.0 was verified using phase contrast microscopy. Quantitative motility assays were conducted on soft agar swim plates containing MSB swim medium (1% tryptone, 0.5% yeast extract, 0.3% agar, and 2 mM each of $MgSO_4$ and $CaCl_2$). Each *S. enterica* strain was inoculated into 10 ml of LB and placed into a 37°C shaking incubator at 220 RPM overnight. A 2.5 µl drop of the stationary phase bacterial culture was pipetted onto the center of a soft agar swim plate. This was repeated in technical triplicate for each of three biological replicates. The plates were incubated at 37°C and measured at two different time points, after eight and 16 hours.

**Spot assays for qualitative determination of phage susceptibility**

*Salmonella* serotypes of interest were grown in LB medium until an $OD_{600}$ of 2.0 was reached. Cell motility was verified via phase contrast microscopy. Non-motile strains were not tested; all non-motile bacteria are completely χ resistant because rotating flagella must be present for

infection to proceed (49). Next, 100 µl of motile cell suspension was mixed with 4 ml of molten 0.5% agar LB and immediately poured onto a 1.5% agar LB plate. Agar was allowed to solidify and serial 1:10 dilutions of χ phage were prepared in 0.85% NaCl. Ten microliters of each dilution were spotted onto the soft agar lawn and plates were left on the benchtop until fully dry, then flipped, and incubated at 37°C overnight. Zones of clearing indicated phage-mediated cell lysis and thus susceptibility.

**Plaque assays for calculation of EOP**

Plaque assays were performed using standard procedures. Briefly, cells were grown to an $OD_{600}$ of 2.0 and verified motile via phase contrast microscopy as described above. Bacteriophage χ was diluted 1:10 serially in 0.85% NaCl. One hundred microliters of motile cells in LB were mixed with 100 µl of phage dilutions and allowed to incubate for six minutes to allow binding. Next, 4 ml of molten 0.5% agar LB was mixed with the cell-phage mixture, which was then poured onto 1.5% agar LB plates and allowed to solidify. Plaques were counted after overnight incubation at 37°C. EOP was calculated using the formula EOP = (pfu/ml mutant)/(pfu/ml WT)*100%.

**Assay of phage adsorption**

To determine adsorption percentage, the *Salmonella* strain of interest was grown in triplicate in 10 ml LB with 220 RPM shaking at 37°C to an $OD_{600}$ of 2.0. Culture motility was verified by phase contrast microscopy. A 10 ml LB control with no cells was also prepared. Next, $10^6$ pfu of χ phage was added to each culture. The cultures were returned to shaking for ten minutes to allow binding to occur. One ml of each culture was centrifuged at 15,000 x g for 3 minutes at

4°C. Supernatants were removed without disturbing the cell pellets and serial 1:10 dilutions were immediately prepared. Phages present in supernatants were titered via plaque assay, using *S.* Typhimurium 14028s as indicator strain. Adsorption percentage was calculated using the formula: (1 – (pfu supernatant with cells/pfu control) * 100%).

**Gel electrophoresis and immunoblot analysis for determination of flagellin production**

Immunoblot analysis was employed to determine whether flagellin is produced by a particular pFliC mutant. In addition, whole cell lysates were also visualized on SDS-PAGE gels stained with Coomassie brilliant blue R250 (S2 Figure). First, pFliC mutant strains were grown to an $OD_{600}$ of 2.0. Motility was verified by phase contrast microscopy for the strains that were known to be motile. Next, 15 µl of each culture was mixed with 15 µl of 2x Laemmli loading buffer (65.8 mM Tris pH 6.8, 2.1% SDS, 26.3% glycerol, 0.01% bromophenol blue, 5% β-mercaptoethanol) and boiled for 10 minutes, before loading on a Criterion TGX 10% polyacrylamide gel (Bio-Rad). Precision Plus Protein dual-color molecular weight marker (Bio-Rad) was loaded to determine protein size. After gel electrophoresis, proteins were transferred to a 0.45 µm nitrocellulose membrane (Cytiva). The membrane was blocked overnight by incubating in a solution of 5% nonfat dry milk in phosphate-buffered saline with Tween 20 (PBS-T; 80 mM $Na_2HPO_4$, 20 mM $NaH_2PO_4$, 100mM NaCl, 0.1% v/v Tween 20) on a rocking platform. BD Difco *Salmonella* H Antiserum a-z was added to freshly-prepared blocking solution at a ratio of 1:5,000 and this mixture was incubated with the membrane for two hours under gentle agitation. The membrane was washed four times with PBS-T and incubated with freshly-prepared blocking solution containing 1:2,500 secondary StarBright Blue 700 Goat Anti-Rabbit IgG (Bio-Rad) for one hour, agitating gently. After four washes with PBS-T, the blot was

imaged with a Bio-Rad Chemidoc instrument. Controls consisted of ser. Typhimurium 14028s $FliC_{ON}$/Δ*fliB* (FliC1), ser. Enteritidis P125109 WT, and ser. Typhimurium 14028s $Fla^-$.

ACKNOWLEDGMENTS

We thank Roman Gerlach for lambda-red plasmids pWRG730 and pWRG717. We acknowledge Michael McClelland for providing the numerous *Salmonella* strains mentioned in S1 Table for testing. We thank the late Howard C. Berg for *E. coli* DH5α and pTrc99a, Saeed Tavazoie for bacteriophage χ, and Kelly Hughes for *S. enterica* LT2 strain TH2788. We thank Rebecca Kelly and Joshua Yoon for testing *Salmonella* strains for χ susceptibility.

REFERENCES

1. Jajere SM. A review of *Salmonella enterica* with particular focus on the pathogenicity and virulence factors, host specificity and antimicrobial resistance including multidrug resistance. Veterinary world. 2019;12(4):504-21.
2. Grimont PA, Weill F-X. Antigenic formulae of the *Salmonella* serovars.
3. Marchello CS, Hong CY, Crump JA. Global Typhoid Fever Incidence: A Systematic Review and Meta-analysis. Clin Infect Dis. 2019;68(Suppl 2):S105-s16.
4. Majowicz SE, Musto J, Scallan E, Angulo FJ, Kirk M, O'Brien SJ, et al. The global burden of nontyphoidal *Salmonella* gastroenteritis. Clin Infect Dis. 2010;50(6):882-9.
5. Huang K-Y, Wang Y-H, Chien K-Y, Janapatla RP, Chiu C-H. Hyperinvasiveness of *Salmonella enterica* serovar Choleraesuis linked to hyperexpression of type III secretion systems in vitro. Sci Rep. 2016;6:37642-.
6. Hughes MJ, Birhane MG, Dorough L, Reynolds JL, Caidi H, Tagg KA, et al. Extensively Drug-Resistant Typhoid Fever in the United States. Open Forum Infect Dis. 2021;8(12):ofab572.
7. Zaki SA, Karande S. Multidrug-resistant typhoid fever: a review. J Infect Dev Ctries. 2011;5(5):324-37.
8. Golkar Z, Bagasra O, Pace DG. Bacteriophage therapy: a potential solution for the antibiotic resistance crisis. J Infect Dev Ctries. 2014;8(2):129-36.
9. Romero-Calle D, Guimaraes Benevides R, Goes-Neto A, Billington C. Bacteriophages as alternatives to antibiotics in clinical care. Antibiotics (Basel, Switzerland). 2019;8(3).

10. Hanlon GW. Bacteriophages: an appraisal of their role in the treatment of bacterial infections. Int J Antimicrob Agents. 2007;30(2):118-28.
11. Clokie MR, Millard AD, Letarov AV, Heaphy S. Phages in nature. Bacteriophage. 2011;1(1):31-45.
12. Chanishvili N. Phage therapy--history from Twort and d'Herelle through Soviet experience to current approaches. Advances in virus research. 2012;83:3-40.
13. Gordillo Altamirano FL, Barr JJ. Phage therapy in the postantibiotic era. Clin Microbiol Rev. 2019;32(2):e00066-18.
14. Kutter E, De Vos D, Gvasalia G, Alavidze Z, Gogokhia L, Kuhl S, et al. Phage therapy in clinical practice: treatment of human infections. Curr Pharm Biotechnol. 2010;11(1):69-86.
15. d'Herelle F. Bacteriophage as a Treatment in Acute Medical and Surgical Infections. Bull N Y Acad Med. 1931;7(5):329-48.
16. Wu S, Zachary E, Wells K, Loc-Carrillo C. Phage Therapy: Future Inquiries. Postdoc J. 2013;1(6):24-35.
17. Chan BK, Abedon ST. Phage therapy pharmacology phage cocktails. Adv Appl Microbiol. 2012;78:1-23.
18. Dowah ASA, Clokie MRJ. Review of the nature, diversity and structure of bacteriophage receptor binding proteins that target Gram-positive bacteria. Biophys Rev. 2018;10(2):535-42.
19. Shin H, Lee JH, Kim H, Choi Y, Heu S, Ryu S. Receptor diversity and host interaction of bacteriophages infecting *Salmonella enterica* serovar Typhimurium. PloS one. 2012;7(8):e43392.
20. Esteves NC, Scharf BE. Flagellotropic Bacteriophages: Opportunities and Challenges for Antimicrobial Applications. Int J Mol Sci. 2022;23(13).
21. Berry RM, Armitage JP. The bacterial flagella motor. Adv Microb Physiol. 1999;41:291-337.
22. Macnab RM, DeRosier DJ. Bacterial flagellar structure and function. Canadian journal of microbiology. 1988;34(4):442-51.
23. Nakamura S, Minamino T. Flagella-Driven Motility of Bacteria. Biomolecules. 2019;9(7).
24. Harshey RM, Matsuyama T. Dimorphic transition in *Escherichia coli* and *Salmonella typhimurium*: surface-induced differentiation into hyperflagellate swarmer cells. Proceedings of the National Academy of Sciences of the United States of America. 1994;91(18):8631-5.
25. Liu R, Ochman H. Stepwise formation of the bacterial flagellar system. Proceedings of the National Academy of Sciences of the United States of America. 2007;104(17):7116.

26. Samatey FA, Matsunami H, Imada K, Nagashima S, Shaikh TR, Thomas DR, et al. Structure of the bacterial flagellar hook and implication for the molecular universal joint mechanism. Nature. 2004;431(7012):1062-8.
27. Reid Sean D, Selander Robert K, Whittam Thomas S. Sequence Diversity of Flagellin (*fliC*) Alleles in Pathogenic *Escherichia coli*. J Bacteriol. 1999;181(1):153-60.
28. Aldridge P, Gnerer J, Karlinsey JE, Hughes KT. Transcriptional and Translational Control of the *Salmonella fliC* Gene. J Bacteriol. 2006;188(12):4487.
29. Mondino S, San Martin F, Buschiazzo A. 3D cryo-EM imaging of bacterial flagella: Novel structural and mechanistic insights into cell motility. The Journal of biological chemistry. 2022;298(7):102105.
30. Jonson AB, Normark S, Rhen M. Fimbriae, pili, flagella and bacterial virulence. Contrib Microbiol. 2005;12:67-89.
31. Zhou M, Yang Y, Chen P, Hu H, Hardwidge PR, Zhu G. More than a locomotive organelle: flagella in *Escherichia coli*. Appl Microbiol Biotechnol. 2015;99(21):8883-90.
32. Duan Q, Zhou M, Zhu L, Zhu G. Flagella and bacterial pathogenicity. J Basic Microbiol. 2013;53(1):1-8.
33. Gu H. Role of Flagella in the Pathogenesis of *Helicobacter pylori*. Current microbiology. 2017;74(7):863-9.
34. Moens S, Vanderleyden J. Functions of bacterial flagella. Crit Rev Microbiol. 1996;22(2):67-100.
35. Metcalfe HJ, Best A, Kanellos T, La Ragione RM, Werling D. Flagellin expression enhances *Salmonella* accumulation in TLR5-positive macrophages. Developmental and comparative immunology. 2010;34(8):797-804.
36. Savar NS, Bouzari S. In silico study of ligand binding site of toll-like receptor 5. Adv Biomed Res. 2014;3:41.
37. Beatson SA, Minamino T, Pallen MJ. Variation in bacterial flagellins: from sequence to structure. Trends in microbiology. 2006;14(4):151-5.
38. Harshey RM, Estepa G, Hideki Y. Cloning and nucleotide sequence of a flagellin-coding gene (hag) from *Serratia marcescens* 274. Gene. 1989;79(1):1-8.
39. Fedorov OV, Kostyukova AS. Domain structure of flagellin. FEBS Lett. 1984;171(1):145-8.
40. Yonekura K, Maki-Yonekura S, Namba K. Complete atomic model of the bacterial flagellar filament by electron cryomicroscopy. Nature. 2003;424(6949):643-50.
41. Montemayor Eric J, Ploscariu Nicoleta T, Sanchez Juan C, Parrell D, Dillard Rebecca S, Shebelut Conrad W, et al. Flagellar Structures from the Bacterium *Caulobacter crescentus* and Implications for Phage ϕCbK Predation of Multiflagellin Bacteria. J Bacteriol. 2021;203(5):e00399-20.

42. Bonifield HR, Hughes KT. Flagellar phase variation in *Salmonella enterica* is mediated by a posttranscriptional control mechanism. J Bacteriol. 2003;185(12):3567-74.
43. Stocker BA. Measurements of rate of mutation of flagellar antigenic phase in *Salmonella typhimurium*. J Hyg (Lond). 1949;47(4):398-413.
44. Smith NH, Selander RK. Molecular genetic basis for complex flagellar antigen expression in a triphasic serovar of *Salmonella*. Proceedings of the National Academy of Sciences of the United States of America. 1991;88(3):956-60.
45. Burnens AP, Stanley J, Sack R, Hunziker P, Brodard I, Nicolet J. The flagellin N-methylase gene fliB and an adjacent serovar-specific IS200 element in *Salmonella typhimurium*. Microbiology (Reading). 1997;143 ( Pt 5):1539-47.
46. Wang C, Nehls C, Baabe D, Burghaus O, Hurwitz R, Gutsmann T, et al. Flagellin lysine methyltransferase FliB catalyzes a [4Fe-4S] mediated methyl transfer reaction. PLOS Pathog. 2021;17(11):e1010052.
47. Horstmann JA, Lunelli M, Cazzola H, Heidemann J, Kühne C, Steffen P, et al. Methylation of *Salmonella* Typhimurium flagella promotes bacterial adhesion and host cell invasion. Nat Commun. 2020;11(1):2013.
48. De Maayer P, Cowan DA. Flashy flagella: flagellin modification is relatively common and highly versatile among the Enterobacteriaceae. BMC Genomics. 2016;17(1):377.
49. Schade SZ, Adler J, Ris H. How bacteriophage χ attacks motile bacteria. J Virol. 1967;1(3):599.
50. MEYNELL EW. A phage, *øχ*, which attacks motile bacteria. Microbiology. 1961;25(2):253-90.
51. Iino T, Mitani M. Infection of *Serratia marcescens* by bacteriophage chi. J Virol. 1967;1(2):445-7.
52. Samuel AD, Pitta TP, Ryu WS, Danese PN, Leung EC, Berg HC. Flagellar determinants of bacterial sensitivity to chi-phage. Proceedings of the National Academy of Sciences of the United States of America. 1999;96(17):9863-6.
53. Berg HC, Anderson RA. Bacteria Swim by Rotating their Flagellar Filaments. Nature. 1973;245(5425):380-2.
54. Esteves NC, Porwollik S, McClelland M, Scharf BE. The multi-drug efflux system AcrABZ-TolC is essential for infection of *Salmonella* Typhimurium by the flagellum-dependent bacteriophage Chi. J Virol. 2021;95(11).
55. Sertić V, Boulgakov NA, editors. Bacteriophages Specific for Flagellated Forms of Bacteria1936.
56. Khanna A, Khanna M, Aggarwal A. *Serratia marcescens*- a rare opportunistic nosocomial pathogen and measures to limit its spread in hospitalized patients. J Clin Diagn Res. 2013;7(2):243-6.

57. Wachsmuth IK, Griffin PM, Wells JG. *Escherichia coli* O157:H7, a cause of hemorrhagic colitis and hemolytic uremic syndrome. Acta Paediatr Jpn. 1991;33(5):603-12.
58. Chan BK, Sistrom M, Wertz JE, Kortright KE, Narayan D, Turner PE. Phage selection restores antibiotic sensitivity in MDR *Pseudomonas aeruginosa*. Sci Rep. 2016;6:26717-.
59. Burmeister AR, Fortier A, Roush C, Lessing AJ, Bender RG, Barahman R, et al. Pleiotropy complicates a trade-off between phage resistance and antibiotic resistance. Proceedings of the National Academy of Sciences of the United States of America. 2020;117(21):11207-16.
60. Dunstan RA, Pickard D, Dougan S, Goulding D, Cormie C, Hardy J, et al. The flagellotropic bacteriophage YSD1 targets *Salmonella* Typhi with a Chi-like protein tail fibre. Molecular microbiology. 2019;112(6):1831-46.
61. Needleman SB, Wunsch CD. A general method applicable to the search for similarities in the amino acid sequence of two proteins. Journal of molecular biology. 1970;48(3):443-53.
62. Madeira F, Pearce M, Tivey ARN, Basutkar P, Lee J, Edbali O, et al. Search and sequence analysis tools services from EMBL-EBI in 2022. Nucleic acids research. 2022;50(W1):W276-w9.
63. Schaubach OL, Dombroski AJ. Transcription Initiation at the Flagellin Promoter by RNA Polymerase Carrying ς28 from *Salmonella typhimurium*. The Journal of biological chemistry. 1999;274(13):8757-63.
64. Mimori-Kiyosue Y, Yamashita I, Fujiyoshi Y, Yamaguchi S, Namba K. Role of the outermost subdomain of *Salmonella* flagellin in the filament structure revealed by electron cryomicroscopy. Journal of molecular biology. 1998;284(2):521-30.
65. Nedeljković M, Sastre DE, Sundberg EJ. Bacterial Flagellar Filament: A Supramolecular Multifunctional Nanostructure. Int J Mol Sci. 2021;22(14).
66. Perry JJ, Yousef AE. *Salmonella enteritidis* in shell eggs: evolving concerns and innovative control measures. Adv Appl Microbiol. 2012;81:243-74.
67. De Cesare A. *Salmonella* in Foods: A Reemerging Problem. Adv Food Nutr Res. 2018;86:137-79.
68. Jones CJ, Aizawa S. The bacterial flagellum and flagellar motor: structure, assembly and function. Adv Microb Physiol. 1991;32:109-72.
69. Rosu V, Chevance FF, Karlinsey JE, Hirano T, Hughes KT. Translation inhibition of the *Salmonella fliC* gene by the *fliC* 5' untranslated region, *fliC* coding sequences, and FlgM. J Bacteriol. 2006;188(12):4497-507.
70. Menendez-Gil P, Toledo-Arana A. Bacterial 3'UTRs: A Useful Resource in Post-transcriptional Regulation. Front Mol Biosci. 2020;7:617633.

71. Jahn M, Vorpahl C, Hübschmann T, Harms H, Müller S. Copy number variability of expression plasmids determined by cell sorting and Droplet Digital PCR. Microb Cell Factories. 2016;15(1):211.
72. Bolivar F, Rodriguez RL, Betlach MC, Boyer HW. Construction and characterization of new cloning vehicles I. Ampicillin-resistant derivatives of the plasmid pMB9. Gene. 1977;2(2):75-93.
73. Yoshioka K, Aizawa S, Yamaguchi S. Flagellar filament structure and cell motility of *Salmonella typhimurium* mutants lacking part of the outer domain of flagellin. J Bacteriol. 1995;177(4):1090-3.
74. Kuwajima G. Construction of a minimum-size functional flagellin of *Escherichia coli*. J Bacteriol. 1988;170(7):3305-9.
75. van Asten AJ, Zwaagstra KA, Baay MF, Kusters JG, Huis in't Veld JH, van der Zeijst BA. Identification of the domain which determines the g,m serotype of the flagellin of *Salmonella enteritidis*. J Bacteriol. 1995;177(6):1610-3.
76. Jarvik T, Smillie C, Groisman Eduardo A, Ochman H. Short-Term Signatures of Evolutionary Change in the *Salmonella enterica* Serovar Typhimurium 14028 Genome. J Bacteriol. 2010;192(2):560-7.
77. Thomson NR, Clayton DJ, Windhorst D, Vernikos G, Davidson S, Churcher C, et al. Comparative genome analysis of *Salmonella* Enteritidis PT4 and *Salmonella* Gallinarum 287/91 provides insights into evolutionary and host adaptation pathways. Genome Res. 2008;18(10):1624-37.
78. Eriksson U, Lindberg AA. Adsorption of phage P22 to *Salmonella typhimurium*. J Gen Virol. 1977;34(2):207-21.
79. Gonzalez F, Helm RF, Broadway KM, Scharf BE. More than Rotating Flagella: Lipopolysaccharide as a Secondary Receptor for Flagellotropic Phage 7-7-1. J Bacteriol. 2018;200(19).
80. Szczepankowska A. Role of CRISPR/cas system in the development of bacteriophage resistance. Advances in virus research. 2012;82:289-338.
81. Boyd A, Simon MI. Multiple electrophoretic forms of methyl-accepting chemotaxis proteins generated by stimulus-elicited methylation in *Escherichia coli*. J Bacteriol. 1980;143(2):809-15.
82. Kondoh H, Ball CB, Adler J. Identification of a methyl-accepting chemotaxis protein for the ribose and galactose chemoreceptors of *Escherichia coli*. Proceedings of the National Academy of Sciences of the United States of America. 1979;76(1):260-4.
83. Ramirez-Chamorro L, Boulanger P, Rossier O. Strategies for Bacteriophage T5 Mutagenesis: Expanding the Toolbox for Phage Genome Engineering. Front Microbiol. 2021;12:667332.
84. Dunne M, Prokhorov NS, Loessner MJ, Leiman PG. Reprogramming bacteriophage host range: design principles and strategies for engineering receptor binding proteins. Curr Opin Biotechnol. 2021;68:272-81.

85. Dodson LA, Masker WE. Survival and mutagenesis of bacteriophage T7 damaged by methyl methanesulfonate and ethyl methanesulfonate. Mutat Res. 1986;162(2):137-44.
86. Skopek TR, Hutchinson F. DNA base sequence changes induced by bromouracil mutagenesis of lambda phage. Journal of molecular biology. 1982;159(1):19-33.
87. Wood RD, Hutchinson F. Non-targeted mutagenesis of unirradiated lambda phage in *Escherichia coli* host cells irradiated with ultraviolet light. Journal of molecular biology. 1984;173(3):293-305.
88. Dunne M, Rupf B, Tala M, Qabrati X, Ernst P, Shen Y, et al. Reprogramming Bacteriophage Host Range through Structure-Guided Design of Chimeric Receptor Binding Proteins. Cell Rep. 2019;29(5):1336-50.e4.
89. Gibson DG, Young L, Chuang R-Y, Venter JC, Hutchison CA, Smith HO. Enzymatic assembly of DNA molecules up to several hundred kilobases. Nat Methods. 2009;6(5):343-5.
90. Bertani G. Studies on lysogenesis. I. The mode of phage liberation by lysogenic *Escherichia coli*. J Bacteriol. 1951;62(3):293-300.
91. Hoffmann S, Schmidt C, Walter S, Bender JK, Gerlach RG. Scarless deletion of up to seven methyl-accepting chemotaxis genes with an optimized method highlights key function of CheM in *Salmonella* Typhimurium. PloS one. 2017;12(2):e0172630.

FIGURES

| pBS1316 mutant plasmid | Chromosomal mutant | FliC domains | | | | | | | Trans-complementation strain motility |
|---|---|---|---|---|---|---|---|---|---|
| | | NTD0 | NTD1 | NTD2 | D3 | CTD2 | CTD1 | CTD0 | |
| pFliC1 | FliC1 | | | | | | | | motile |
| pFliC2 | FliC2 | | | | | | | | motile |
| pFliC3 | FliC3 | | | | | | | | motile |
| pFliC4 | N/A | | | | | | | | non-motile |
| pFliC5 | N/A | | | | | | | | non-motile |
| pFliC6 | FliC6 | | | | | | | | motile |
| pFliC7 | N/A | | | | | | | | non-motile |
| pFliC8 | FliC8 | | | | | | | | motile |
| pFliC9 | N/A | | | | | | | | non-motile |
| pFliC10 | N/A | | | | | | | | non-motile |
| pFliC11 | FliC11 | | | | | | | | motile |
| pFliC12 | N/A | | | | | | | | non-motile |
| pFliC13 | N/A | | | | | | | | non-motile |

Figure 3.1. Abbreviated names of FliC domain mutants. Both plasmids and their corresponding chromosomal mutants are shown, where applicable. N/A indicates that a corresponding chromosomal mutant was not constructed, as the trans-complementation strain was not motile. The identity of the domains of flagellin in each mutant is color coded, with blue indicating domains from ser. Typhimurium strain 14028s, red indicating domains from ser. Enteritidis strain P125109, and black indicating a deletion of that entire domain. The trans-complementation strain motility phenotypes given in the rightmost column dictated whether a chromosomal mutant was constructed for that particular strain.

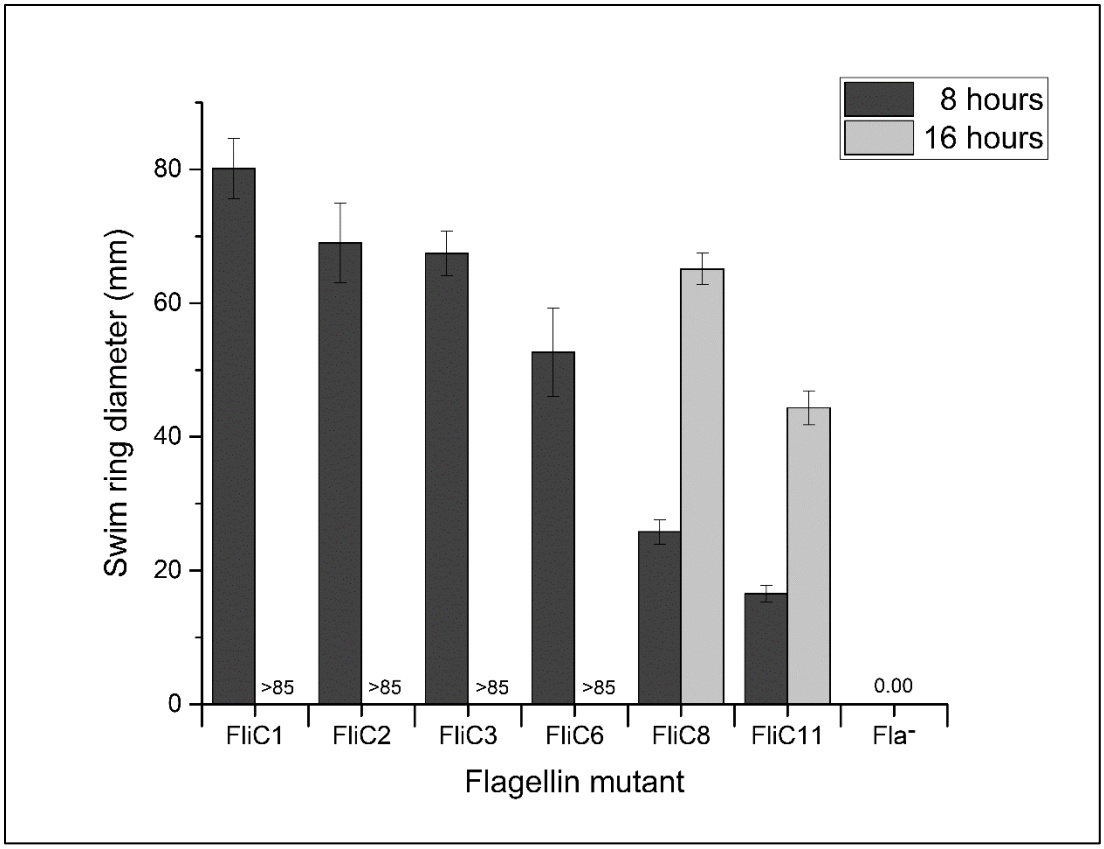


Figure 3.2. Swimming motility of flagellin mutants quantified on 0.3% agar MSB swim plates. Values are given as swim ring diameter in millimeters. Swim rings were measured at 8 hours and 16 hours post-inoculation. Each mutant's swim ring data are representative of three technical replicates for each of three biological replicates. Swim rings for strains FliC1, FliC2, FliC3, and FliC6 reached the edge of their respective plates (85 mm) prior to the second time point and were therefore not measured at 16 hours and are marked as >85. Negative control Fla$^-$ is marked with 0.00, as this strain is non-flagellated and formed no swim ring after the full 16 hours of incubation. All mutants' motility defects are statistically significant compared to FliC1, calculated using Student's T-Test.

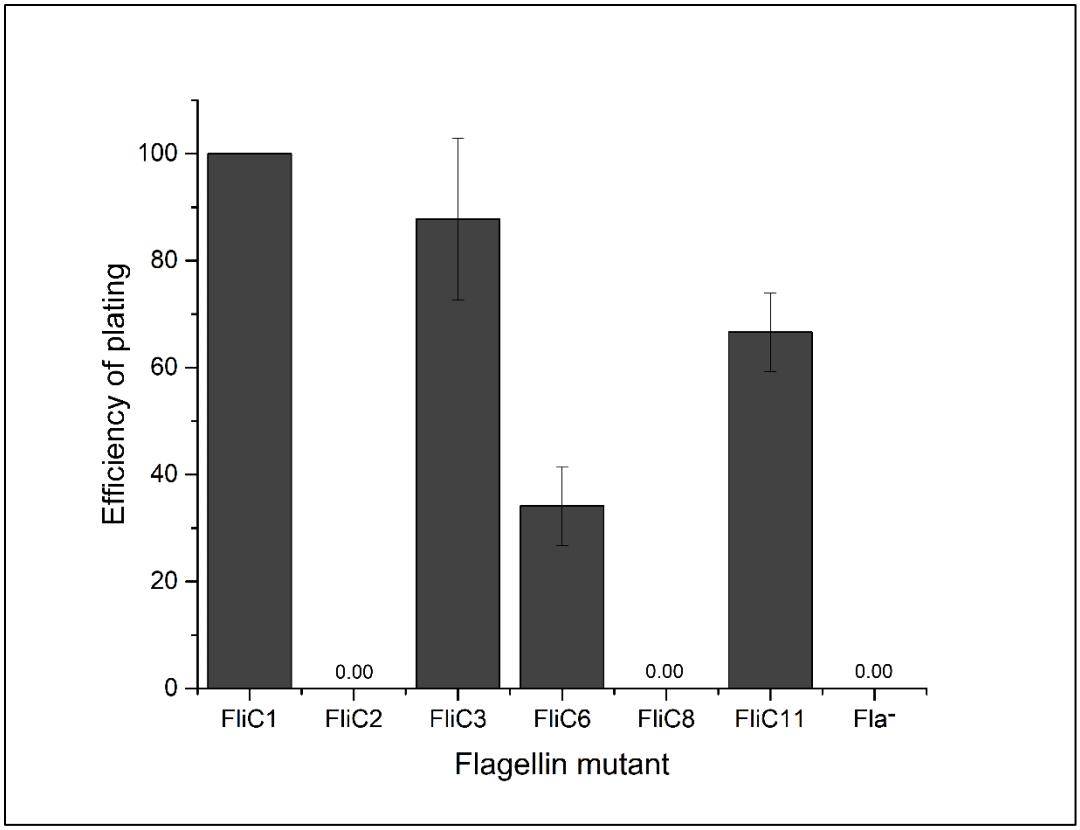


Figure 3.3. Efficiency of plating (EOP) data for FliC mutants. All EOP values are given as percentage of wild type (FliC1) and consist of three replicates. Error bars are given as standard deviation. Mutants which exhibited zero plaque formation are denoted with 0.00. The reduction in EOP seen with mutant FliC3 is not statistically significant when compared to FliC1. The EOP values of FliC6 and FliC11 are statistically significant from FliC1 and from each other ($P<0.05$), calculated via Student's T-Test.

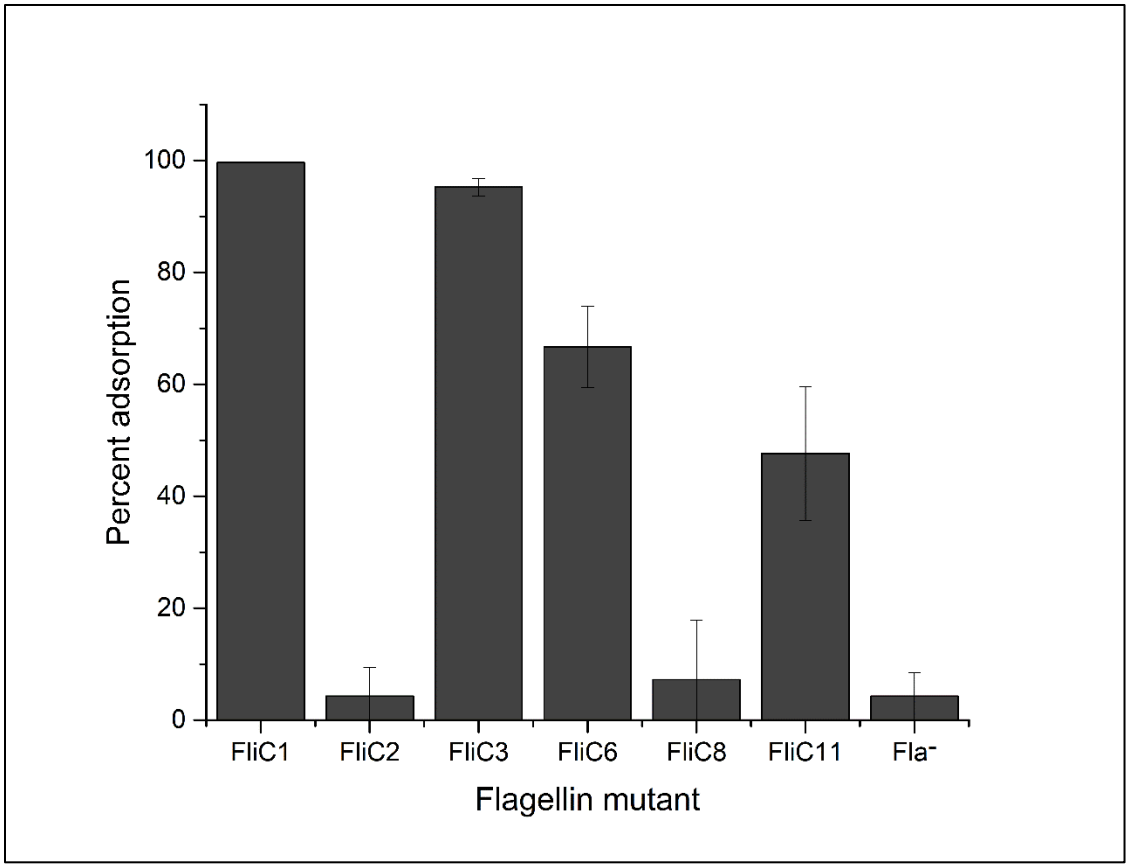


Figure 3.4. Percentage of phage particles adsorbed to cells after an incubation time of ten minutes. All adsorption values are significantly reduced as compared to FliC1 ($P<0.05$), calculated using Student's T-Test. Adsorption values for FliC2 and FliC8 are not significantly different compared to the Fla- negative control. The difference between FliC6 and FliC11 is not statistically significant. All values consist of three replicates and error bars are provided denoting standard deviations.

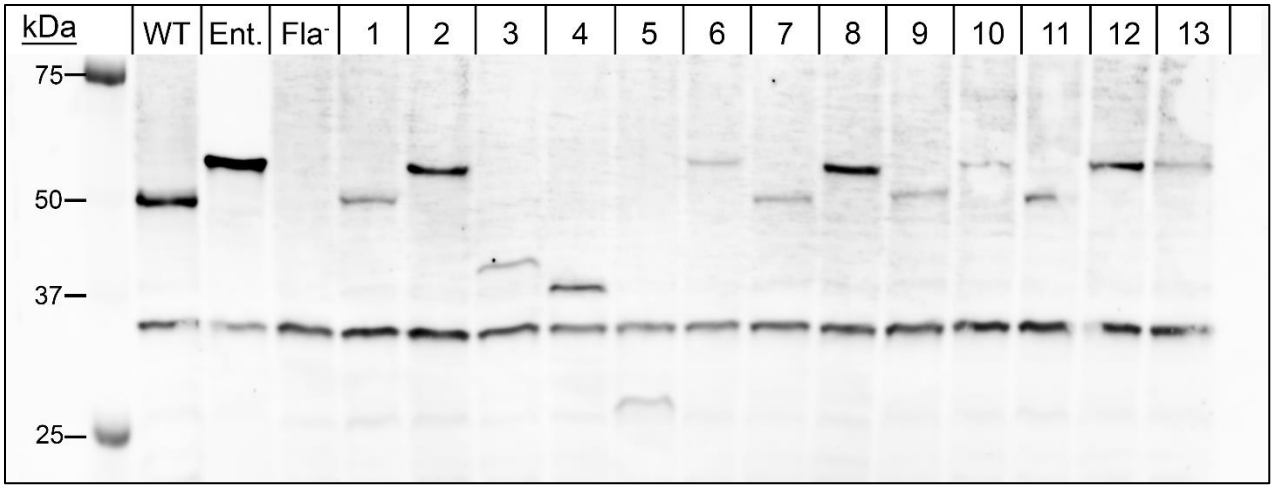


Figure 3.5. Immunoblot of whole cell lysates from pFliC mutants grown to an $OD_{600}$ of 2.0. Flagellin is detected by BD Difco *Salmonella* anti-H a-z antiserum. Ser. Typhimurium 14028s $FliC_{ON}$ Δ*fliB* (chromosomal mutant FliC1) is denoted as "WT." Wild type ser. Enteritidis P125109 is denoted as "Ent." Ser. Typhimurium 14028s Δ*fliC*Δ*fljBA* is denoted as "$Fla^-$." Numbers 1 through 13 refer to the corresponding pFliC plasmid mutants, as described in Fig. 3.1.

Chapter IV

# Characterization of the CHI_31 gene product: The χ phage tail fiber protein and its interactions with the flagellum

Nathaniel C. Esteves[1], W. Keith Ray[2], Richard F. Helm[2], Birgit E. Scharf[1]

1. Department of Biological Sciences; Virginia Tech
2. Department of Biochemistry; Virginia Tech

ABSTRACT

Despite its relatively long history of study, the majority of the genes in the χ genome are uncharacterized. Even those that have annotations are annotated due to sequence homology to other phages, rather than precise characterization of the encoded proteins. Within the χ genome, the gene CHI_31 is annotated as encoding a "tail fiber protein." The tail fiber is known to interact with the flagellum, as this interaction can be seen with electron microscopy. However, the fiber has not been definitively proven to consist of the CHI_31 gene product (gp31). To characterize this protein, we conducted crosslinking and mass spectrometry experiments. We used both purified χ phage mature virions and recombinant gp31 for our studies, and chemically crosslinked them to *Salmonella* flagellin FliC. The gp31 protein was purified using two distinct techniques: IMPACT and Ni-NTA purification. Coupled with the information from Chapter III, we have shown that gp31 interacts directly with flagellin FliC from *Salmonella enterica*. More specifically, our data indicate that amino acid residues within the C-terminal domain D2 of FliC interact directly with gp31, and that no other χ proteins were found to interact with the flagellum. Overall, our results strongly support our previous findings of the importance of FliC D2 domains for phage binding and confirm the annotation of the χ gene CHI_31.

INTRODUCTION

All phages use one or more receptor binding protein(s) (RBP) to interact with their receptors on the bacterial cell [1, 2]. Flagellotropic phages are no exception [3]. The RBP of χ has been known with confidence to be its single narrow tail fiber since the 1960s [4, 5], when this fiber was first visualized interacting with the flagellum via electron microscopy (EM). However, the gene(s) encoding this fiber remained elusive until a full genome sequence of χ became available

several decades later [6]. The gene CHI_31 was determined to putatively encode the tail fiber protein (gp31). Experimental proof of this, however, has not been acquired. A logical experiment would be to delete the CHI_31 gene and see if the phage particles no longer produced tail fibers. This experiment would be quite difficult as targeted mutagenesis in χ has not been attempted successfully to our knowledge. Mutagenesis in lytic phages is generally difficult, as the genome never integrates into the host chromosome. A CRISPR-Cas system or synthetic isothermal assembly of the complete phage genome [7, 8] would likely need to be used [9, 10]. Additionally, if the hypothesis is correct, a ΔCHI_31 mutant would lack an RBP and thus almost certainly be non-infectious, rendering it nearly impossible to propagate and produce enough of this phage to visualize the loss of the tail fiber using EM. Due to these technical difficulties, different approaches are required. Mass spectrometry (MS) can be used to identify interactions between proteins [11]. Since χ must slide along the flagellum to reach the cell surface [12], the interaction is expected to be transient. To ameliorate similar concerns about transient or weak protein-protein interactions, chemical crosslinking (CL) is often employed [11, 13, 14]. This technique uses a chemical compound capable of forming covalent bonds between interacting proteins, rendering their interaction permanent. Common crosslinkers include the dialdehyde glutaraldehyde (GA), and the succinimide diester disuccinimidyl suberate (DSS), both of which crosslink primary amine groups in certain amino acids, typically lysine and sometimes arginine residues [13, 15, 16]. In this study, we used CL-MS to identify interaction partners between flagellin FliC of *S. enterica* 14028s and χ gp31.

MATERIALS & METHODS

**Generation of a monophasic, flagellin-methylation-deficient 14028s mutant strain**

Lambda-red mutagenesis [17, 18] was used to construct a strain lacking the phase 2 flagellin gene *fljB*, the phase 1 flagellin repressor gene *fljA*, and the flagellin lysine methylase gene *fliB*. The *fljB* and *fljA* genes were inactivated by insertion of a single *tetRA* cassette. The methylase gene *fliB* was deleted scarlessly using two-step lambda-red mutagenesis and I-SceI counterselection with pWRG730 as described previously [19].

**Purification of bacterial flagellar filaments**

Bacterial flagella were mechanically sheared from motile *S. enterica* cells and purified by ultracentrifugation. First, *S. enterica* 14028s cells were grown to an $OD_{600}$ of approximately 2.0 in LB liquid medium. Motility was verified by phase-contrast microscopy. Next, 200 ml of culture was centrifuged at 8,000 x g for 8 minutes and washed twice with motility buffer (67 mM NaCl, 0.1 mM EDTA, 10 mM sodium phosphate buffer, pH 7.0,) and resuspended in 100 ml of motility buffer. Motility was verified again by phase contrast microscopy. The cell suspension was blended at maximum speed for 30 seconds in a blender (Oster 16-Speed). The cells were examined microscopically to verify loss of motility. Cells were removed by centrifugation at 8,000 x g for 8 minutes and again at 15,000 x g for 15 minutes, saving the supernatant each time. The clear supernatant was transferred to ultracentrifuge tubes and centrifuged at 87,000 x g for 2 hours at 4 °C in a fixed-angle ultracentrifuge rotor (Beckman-Coulter Type 70 Ti). The pellets containing flagella were washed once with motility buffer, the centrifugation was repeated, and filaments were resuspended in a total of approximately 1 ml of motility buffer. The purity of the filaments was estimated by gel electrophoresis of samples on denaturing 10% polyacrylamide

gels followed by Coomassie brilliant blue staining (data not shown). Heat treatment at 65°C for 1 hour was used to separate filaments into monomeric flagellin as indicated.

**Bacteriophage χ propagation and isolation**

Bacteriophage χ was propagated on *S. enterica* 14028s and purified using an overlay plate method and density gradient ultracentrifugation as described previously [20].

**Purification of the CHI_31 gene product and chemical crosslinking**

To expand our knowledge about the χ phage RBP, we recombinantly expressed and purified the CHI_31 gene product gp31 using intein-mediated purification with an affinity chitin-binding tag (IMPACT™) purification, a technique with the advantage of leaving no affinity tag after purification [21]. This is particularly useful for uncharacterized proteins, where the possible effects of a residual affinity tag are unknown. A chitin-binding domain (CBD) tag was fused to the protein of interest by an intein domain. The pTYB series of plasmids (New England Biolabs) were used as expression vectors for this process, as these plasmids contain the DNA encoding the CBD and intein fused to either the N-terminal (pTYB11) or C-terminal (pTYB1) end of the recombinant protein [21]. First, the CHI_31 gene was cloned into both pTYB plasmids via PCR and standard restriction enzyme cloning, yielding pBS0692 and pBS0693 for pTYB1 and pTYB11, respectively. *E. coli* ER2566 was transformed with pBS0692 or pBS0693. This expression strain carrying either plasmid was grown in 4 liters of LB medium with 100 µg/ml ampicillin (LB amp) at 37°C with 220 RPM shaking until an optical density of 0.8 was reached. IPTG was added to a final concentration of 400 µM, and cultures were left to induce overnight (approximately 16 hours) at 16°C with shaking. The following morning, cells were harvested by

centrifugation at 15,000 x g for 10 minutes at 4 °C, suspended in 1/50 volume IMPACT buffer (0.5 M NaCl, 1 mM EDTA, 20 mM Tris-HCl, pH 8.0) with 10% glycerol and 1 mM PMSF, and mechanically lysed using an Avestin Emulsiflex™ emulsifier. Insoluble debris and proteins were pelleted by centrifugation at 57,000 x g for 90 minutes at 4°C, and the resulting lysate supernatant was filtered through a 0.2 µm filter. The filtered lysate supernatant was then passed through a 25-ml gravity-flow column containing chitin-agarose resin at 4°C. The agarose was washed with 10 column volumes of IMPACT buffer with glycerol and PMSF, followed by on-column cleavage for 40 hours at 4°C with IMPACT buffer with glycerol and 50 mM dithiothreitol (DTT) to cleave the protein from the intein-CBD tag. Protein was eluted and fractions were analyzed by SDS-PAGE and Coomassie blue staining. The cleaved protein was then purified further by size-exclusion chromatography (SEC) at 4°C using a HiPrep™ Sephacryl S-300 HR SEC column attached to an ÄKTA Prime FPLC with SEC buffer (150 mM NaCl, 0.5 mM EDTA, 50 mM Tris-HCl pH 7.4, 10% glycerol), at a flow rate of 1 ml/min. SEC fractions were analyzed by SDS-PAGE and fractions containing pure protein were pooled and concentrated using an Amicon® Stirred Cell concentrator with a 10-kDa filter membrane.

We next purified gp31 using Ni-NTA affinity chromatography. Plasmid pQE30 (Qiagen) was used as the expression vector, as this plasmid provides an N-terminal 6xHis tag for affinity purification. The CHI_31 gene was cloned into this vector producing plasmid pBS0729, and *E. coli* M15/pREP4 was transformed with this plasmid construct. This expression strain was grown at 37°C with 220 RPM shaking in 4 liters of LB amp supplemented with 25 µg/ml kanamycin to retain pREP4. At an optical density of 0.8, 400 µM IPTG was added to induce expression, and cultures were incubated at 25°C for 4 hours before harvesting. Cell pellets were suspended in Ni-NTA binding buffer (0.5 M NaCl, 40 mM imidazole, 20 mM sodium phosphate buffer, pH 7.4)

and lysed by emulsification. For affinity purification, a HisTrap™ 5-ml Ni-NTA column attached to an ÄKTA Go FPLC was used at a flow rate of 5 ml/min at 4°C, and protein was eluted using Ni-NTA buffer supplemented with 0.5 M imidazole. The protein was purified again by SEC, analyzed by SDS-PAGE, and concentrated before use.

For CL, purified χ phage or χ gp31 was combined with purified flagellar filaments. Amounts of each sample (1:1 ratio by protein concentration) to add were approximated by band intensity on an SDS-PAGE gel and by measuring protein concentration via Bradford assay as described previously [22]. Control samples containing only χ, gp31, or flagellin were prepared in parallel. To one set of samples, crosslinker was added. For CL of χ virions to sheared flagella, two crosslinkers were used: GA at a final concentration of 1%, and DSS at a concentration of 1 mM. For CL of purified gp31 to sheared flagella, only 1 mM DSS was used. After addition of crosslinker, samples were incubated at 37°C for 1 hour. To quench reactions, Tris-HCl buffer (pH 7) was added to a final concentration of 0.1 M and samples were frozen at -20°C.

**Purification of recombinant flagellin FliC ΔD0 and crosslinking with gp31**

A mutant *S. enterica* 14028s FliC protein lacking D0 domains, specifically residues 47-465, was purified by Nickel-NTA purification. The gene encoding FliC ΔD0 was cloned into pQE60, yielding plasmid pBS0746; *E. coli* M15/pREP4 was transformed with this construct. FliC ΔD0 was then purified from lysed M15/pREP4 expression culture using a Nickel-NTA Spin Kit (Qiagen) following the kit protocol for protein purification under native conditions. The protein sample was dialyzed against SEC buffer for 24 hours using Thermo Scientific 0.1-0.5 ml Slide-A-Lyzer 10,000 MWCO dialysis cassettes. Concentration was measured by Bradford assay. CL experiments described above were repeated with FliC ΔD0 and gp31. Proteins were crosslinked

using 1 mM DSS and a 1:1 ratio of the two proteins as estimated via band intensity on an SDS-PAGE gel.

**Polyacrylamide gel electrophoresis**

Proteins and cell fractions were analyzed by sodium dodecyl sulfate polyacrylamide gel electrophoresis (SDS-PAGE). First, 15 µl of each sample or cell pellet were mixed with 15 µl of 2x Laemmli loading buffer (65.8 mM Tris pH 6.8, 2.1% SDS, 26.3% glycerol, 0.01% bromophenol blue, 5% β-mercaptoethanol) and boiled for 10 minutes before loading on SDS-PAGE gels. Precision Plus Protein dual-color molecular weight marker (Bio-Rad) was loaded to determine protein size. Denaturing 15% polyacrylamide SDS-PAGE gels were prepared manually, while gradient gels used in this study were Bio-Rad Criterion TGX precast 4-20% SDS-PAGE gels.

Native-PAGE gels were prepared manually and contained 10% polyacrylamide and no SDS. Samples for native-PAGE were not boiled, and a modified 2x Laemmli loading buffer lacking SDS and β-mercaptoethanol was used.

**Phage competition assay with gp31 and χ**

To determine whether gp31 competes with χ for flagellar binding, a competition assay was used, modified from a procedure described previously [23]. *S. enterica* 14028s was grown in LB medium with 220 RPM shaking at 37°C until an $OD_{600}$ of 1.0 was reached. Motility was verified by phase-contrast microscopy. Motile bacterial culture in LB was mixed with varying concentrations of Ni-NTA purified gp31 protein and incubated at room temperature for 10 minutes to allow binding. Next, 4 ml molten 0.5% agar LB medium was mixed with 200 µl of

the bacteria-gp31 mixture and poured onto an LB agar plate. After the agar solidified, 10 µl of χ phage dilutions in 0.85% NaCl were spotted on the surface of the plate. Plates were incubated at 37°C overnight and lysis spots were examined. Reduced lysis indicates competition occurred.

**MS sample preparation**

Optima™ LC/MS grade solvents and Pierce™ trypsin protease and Glu-C protease (sequencing grade) were from Thermo Fisher Scientific (Waltham, MA). Dithiothreitol (DTT), iodoacetamide (IAA) and formic acid were from MilliporeSigma (St. Louis, MO).

Samples were treated with DTT (4.5 mM) to reduce Cys residues then alkylated with IAA (10 mM). Unreacted IAA was quenched with additional DTT (10 mM). Samples were then digested with either sequencing grade trypsin or Glu-C. Peptides were desalted using OMIX C18 pipette tips (Agilent, Santa Clara, CA) using the manufacturer's recommended protocol then acetonitrile was removed by vacuum. Peptides were dissolved in 50 solvent A (2:98 LC/MS grade acetonitrile: LC/MS grade water supplemented with 0.1% (v/v) formic acid) and analyzed by analyzed using LC-MS/MS.

Samples were first loaded onto a precolumn (Acclaim PepMap 100 (Thermo Scientific, Waltham, MA), 100 µm x 2 cm) after which flow was diverted to an analytical column (50 cm µPAC (PharmaFluidics, Woburn, MA). The UPLC/autosampler utilized was an Easy-nLC 1200 (Thermo Scientific, Waltham, MA). Flow rate was maintained at 250 nl/min and peptides were eluted utilizing a 2 to 45% gradient of solvent B (80:20 LC/MS grade acetonitrile: LC/MS grade water supplemented with 0.1% (v/v) formic acid) in solvent A over 88 minutes. The mass spectrometer utilized was an Orbitrap Fusion Lumos Tribid™ from Thermo Scientific (Waltham, MA). Spray voltage on the µPAC compatible Easy-Spray emitter (PharmaFluidics, Woburn,

MA) was 1300 volts, the ion transfer tube was maintained at 275°C, the RF lens was set to 30% and the default charge state was set to 3.

MS data for the m/z range of 400-1500 was collected using the orbitrap at 120000 resolution in positive profile mode with an AGC target of $4.0x10^5$ and a maximum injection time of 50 ms. Peaks were filtered for MS/MS analysis based on having isotopic peak distribution expected of a peptide with an intensity above $2.0x10^4$ and a charge state of 2-5. Peaks were excluded dynamically for 15 seconds after 1 scan with the MS/MS set to be collected at 45% of a chromatographic peak width with an expected peak width (FWHM) of 15 seconds. MS/MS data starting at m/z of 150 was collected using the orbitrap at 15000 resolution in positive centroid mode with an AGC target of $1.0x10^5$ and a maximum injection time of 200 ms. Activation type was HCD stepped from 27 to 33.

**MS data analysis**

Data were analyzed utilizing Proteome Discoverer 2.5 (Thermo Scientific, Waltham, MA) combining a Sequest HT and Mascot 2.8 (Matrix Science, Boston, MA) search into one result summary for each sample. Both searches utilized the UniProt reference proteome from *Salmonella typhimurium* with *Chivirus chi* proteins from UniProt added and a common protein contaminant database provided with the Proteome Discoverer (PD) software package. Each search assumed either trypsin- or Glu-C-specific peptides with the possibility of 2 missed cleavages, a precursor mass tolerance of 10 ppm and a fragment mass tolerance of 0.1 Da. Searches included the following dynamic modifications: oxidation of Met, acetylation of the protein N-terminus, cyclization of a peptide N-terminal Gln to pyro-Glu and deamidation of Asn/Gln residues. Separate error-tolerant searches were conducted using Mascot 2.8 to identify

unexpected mass shifts as well as crosslinked peptides or peptides modified in some way by the treatment with DSS.

The region of the flagellin FliC protein most likely involved in interaction with gp31 was determined by the relative decrease in intensity of particular peptides after treatment with DSS using samples not treated with DSS as controls.

## RESULTS

### Purified flagellar filaments interact with gp31 on mature χ virions

To determine the mechanism of χ phage interactions with the flagellar filament, we began by mechanically shearing and purifying flagellar filaments and isolating them from the cell body. These purified filaments were mixed with viable χ phage and chemical crosslinkers GA (1%) or DSS (1 mM). The samples were analyzed using MS after enzymatic digestion. This technique provided direct evidence of the interaction between gp31 and the flagellar filament, as peptides within gp31 were found to be crosslinked by GA to peptides within domain CTD2 of flagellin FliC (Fig. 4.1). More specifically, peptides within residues 281-390 of FliC and 83-109 of gp31 were found to be depleted, indicating an interaction. However, these residues correspond to tryptic peptides; due to the relative infrequency of trypsin recognition sites [24], the peptides likely overestimate the residues participating in interactions.

### Recombinant production of gp31 in *E. coli* and purification using two techniques

After confirming the interaction between χ and isolated flagella using CL-MS, we next recombinantly expressed and purified χ gp31 using two different affinity chromatography methods: IMPACT™ as C-terminal fusion and Ni-NTA as N-terminal 6xHis fusion, both

coupled with SEC. An SDS-PAGE gel of SEC fractions (Fig. 4.2A) showed weak bands at the expected apparent molecular weight of 27 kDa. Numerous other contaminating bands were also visible. These additional proteins were present in our first crosslinking experiment (Fig. 4.3). MS analysis indicated that the sample was impure and contained *E. coli* chaperone proteins, a common issue with purification of recombinant heterologous proteins [25]. This impurity prevented further MS analysis or CL with the IMPACT-purified gp31. Nickel-NTA purification resulted in a higher protein yield with fewer contaminating proteins. The SDS-PAGE gel of SEC fractions from Ni-NTA purified gp31 (Fig. 4.2B) showed intense bands at 27 kDa, with comparatively fewer and fainter bands indicating protein contaminants present at low concentrations. MS confirmed the protein sample was sufficiently pure for subsequent analysis.

**Crosslinking of flagella and flagellin to purified gp31**

The Ni-NTA purified gp31 was sufficiently pure for CL-MS experiments, the results of which are still pending. However, Coomassie-stained SDS-PAGE gels of DSS-crosslinked samples (Fig. 4.4A) showed bands of higher molecular weights than either of the individual protein components, flagellin and gp31. This potentially indicates proteins were successfully crosslinked to each other. We attempted to use heat treatment on purified flagellar filaments to break down filaments into monomers of flagellin. A native-PAGE gel indicated that filaments were at least partially broken down (Fig. 4.4B). To ensure we could test interactions with monomeric flagellin, we repeated crosslinking with the same Ni-NTA-purified gp31 and a recombinant mutant flagellin FliC lacking the core D0 domains, preventing polymerization. This FliC ΔD0 was also purified via Ni-NTA. Analysis of fractions indicated a large amount of relatively pure protein was present (Fig. 4.5), and a final concentration of 580 µg/ml was reached. After

crosslinking with gp31 using DSS, numerous higher molecular weight bands were visible on an SDS-PAGE gel, potentially indicating the formation of crosslinks between gp31 and FliC ΔD0 (Fig. 4.6).

**Phage competition assay with gp31**

We conducted a phage competition assay by adding putative RBP to a culture of host bacteria, followed by addition of the phage itself. In theory, the RBP will saturate the receptor and prevent the binding of the phage and subsequent infection, which can be measured by a spot or plaque assay, or by lysis in liquid cultures. We used a spot assay method with increasing concentrations of protein to test for competition. Ultimately, no competition was seen at any concentration of gp31 protein, up to a maximum concentration of 1 mg/ml (Fig. 4.7).

DISCUSSION

The only χ protein found crosslinked when whole phage particles were incubated with sheared *S. enterica* flagella was gp31, leading to our hypothesis that this protein is the χ RBP. Since the 1960s, χ particles have been directly visualized attached to flagella by their tail fibers using EM [4]. This indicates that the tail fiber is almost certainly the RBP. We were able to chemically crosslink χ to isolated flagella, which are incapable of rotation, indicating that χ can bind, at least weakly, to paralyzed flagella. We hypothesize that χ phage binds to stationary flagella, but that translocation to the cell surface cannot occur without rotation, consistent with the nut-and-bolt model [12]. The tryptic peptides found to be depleted (and therefore likely are interaction partners) match well with previous data indicating the importance of flagellin D2 domains for interactions with χ phage [19].

Given the CHI_31 annotation coupled with our data, the identity of gp31 as the tail fiber protein and RBP is nearly certain. Successful purification of gp31 presents, to our knowledge, the first instance of a purified recombinant protein from bacteriophage χ. SDS-PAGE gels of chemically crosslinked samples indicated that interactions between flagella and gp31 may have occurred, but are inconclusive. Future MS identification of similar amino acid residues to the previous experiment with intact χ virions would definitively identify gp31 as the RBP.

The lack of competition during the competition assays is not mutually exclusive with our conclusion of gp31 being the RBP. There are many reasonable explanations for the lack of competition. In the mature χ virion, the tail fiber is almost certainly a polymer of the tail fiber protein. Its length can vary between 200 and 250 nm [4, 5], indicating that it is unlikely to be a well-defined oligomer. When the protein is expressed recombinantly, it may remain in a monomeric state or not polymerize properly. It is possible that monomers of gp31 do not attach to flagella. Alternatively, if the RBP-flagellum interaction is weak, it may be easily displaced and thus insufficient to prevent binding of χ phage particles. Lastly, due to the length of the flagellum, it is possible that the amount of gp31 protein that would need to be added to saturate the receptor to the point of causing measurable competition would be unrealistically high.

More information about the function of gp31 would be beneficial to the field of flagellotropic bacteriophages. Other proteases such as chymotrypsin can be used to further narrow down the amino acid residues participating in interactions using MS. Cryo-EM or X-ray crystallography should be able to characterize the structure of gp31, as we have shown that purification of gp31 at a high concentration is feasible. Cryo-EM could also be used to further analyze and potentially visualize the interaction between χ and the flagellum. If gp31 polymerization is essential for interactions with the flagellum, sonication could be used to fractionate χ virions [26], which

would then be separated using density gradient ultracentrifugation. The fraction containing intact tail fibers could then be purified and analyzed. Alternatively, if a χ-encoded chaperone or tape measure protein is crucial for correct tail fiber assembly, it may be possible to co-express this with gp31 to allow it to polymerize.

To further understand this complex interaction, targeted or random mutagenesis of the CHI_31 gene would provide invaluable information. Given what is known about the host range of χ and the binding interaction to the flagellum [5, 12, 19], it is likely that host range mutants would have mutations within the gene encoding the RBP. A chemical mutagen should be capable of introducing random mutations into the χ genome [27, 28]. Combining this with a directed evolution approach involving passaging χ on a non-host would introduce selective pressure toward the development of host range mutants [29]. Mutations would be identified via whole genome sequencing. Finding mutations within the region of gp31 that putatively interacts with FliC would support our CL-MS data. Overall, we have strong support of our previous findings regarding the importance of the FliC D2 domains for host specificity [19] via recombinant protein purification and CL-MS. Significantly more future experiments are necessary, but we have strong evidence that gp31 is the χ RBP and interacts directly with *S*. Typhimurium FliC.

REFERENCES


1. Rakhuba, D.V.; Kolomiets, E.I.; Dey, E.S.; and Novik, G.I., Bacteriophage Receptors, Mechanisms of Phage Adsorption and Penetration into Host Cell. *Pol J Microbiol*, **2010**. 59(3): p. 145-55.
2. Simpson, D.J.; Sacher, J.C.; and Szymanski, C.M., Development of an Assay for the Identification of Receptor Binding Proteins from Bacteriophages. *Viruses*, **2016**. 8(1): p. 17.
3. Esteves, N.C. and Scharf, B.E., Flagellotropic Bacteriophages: Opportunities and Challenges for Antimicrobial Applications. *Int J Mol Sci*, **2022**. 23(13).

4. Schade, S.Z.; Adler, J.; and Ris, H., How Bacteriophage X Attacks Motile Bacteria. *J Virol*, **1967**. 1(3): p. 599.

5. MEYNELL, E.W., A Phage, Øχ, Which Attacks Motile Bacteria. *Microbiology*, **1961**. 25(2): p. 253-290.

6. Hendrix, R.W.; Ko, C.-C.; Jacobs-Sera, D.; Hatfull, G.F.; Erhardt, M.; Hughes, K.T.; and Casjens, S.R., Genome Sequence of *Salmonella* Phage X. *Genome Announc*, **2015**. 3(1): p. e01229-14.

7. Pulkkinen, E.M.; Hinkley, T.C.; and Nugen, S.R., Utilizing in Vitro DNA Assembly to Engineer a Synthetic T7 Nanoluc Reporter Phage for Escherichia Coli Detection. *Integr Biol (Camb)*, **2019**. 11(3): p. 63-68.

8. Gibson, D.G.; Young, L.; Chuang, R.-Y.; Venter, J.C.; Hutchison, C.A.; and Smith, H.O., Enzymatic Assembly of DNA Molecules up to Several Hundred Kilobases. *Nat Methods*, **2009**. 6(5): p. 343-345.

9. Ramirez-Chamorro, L.; Boulanger, P.; and Rossier, O., Strategies for Bacteriophage T5 Mutagenesis: Expanding the Toolbox for Phage Genome Engineering. *Front Microbiol*, **2021**. 12: p. 667332.

10. Lemay, M.L.; Renaud, A.C.; Rousseau, G.M.; and Moineau, S., Targeted Genome Editing of Virulent Phages Using Crispr-Cas9. *Bio Protoc*, **2018**. 8(1): p. e2674.

11. Piersimoni, L.; Kastritis, P.L.; Arlt, C.; and Sinz, A., Cross-Linking Mass Spectrometry for Investigating Protein Conformations and Protein–Protein Interactions─a Method for All Seasons. *Chemical Reviews*, **2022**. 122(8): p. 7500-7531.

12. Samuel, A.D.; Pitta, T.P.; Ryu, W.S.; Danese, P.N.; Leung, E.C.; and Berg, H.C., Flagellar Determinants of Bacterial Sensitivity to Chi-Phage. *Proc Natl Acad Sci U S A*, **1999**. 96(17): p. 9863-9866.

13. López-Gallego, F.; Guisán, J.M.; and Betancor, L., Glutaraldehyde-Mediated Protein Immobilization. *Methods Mol Biol*, **2013**. 1051: p. 33-41.

14. O'Reilly, F.J. and Rappsilber, J., Cross-Linking Mass Spectrometry: Methods and Applications in Structural, Molecular and Systems Biology. *Nature Structural & Molecular Biology*, **2018**. 25(11): p. 1000-1008.

15. Trabjerg, E.; Keller, A.; and Leitner, A., Ph Dependence of Succinimide-Ester-Based Protein Cross-Linking for Structural Mass Spectrometry Applications. *ACS Meas Sci Au*, **2022**. 2(2): p. 132-138.

16. Salem, M.; Mauguen, Y.; and Prangé, T., Revisiting Glutaraldehyde Cross-Linking: The Case of the Arg-Lys Intermolecular Doublet. *Acta Crystallogr Sect F Struct Biol Cryst Commun*, **2010**. 66(Pt 3): p. 225-8.

17. Hoffmann, S.; Schmidt, C.; Walter, S.; Bender, J.K.; and Gerlach, R.G., Scarless Deletion of up to Seven Methyl-Accepting Chemotaxis Genes with an Optimized Method

Highlights Key Function of Chem in *Salmonella* Typhimurium. *PLoS One*, **2017**. 12(2): p. e0172630.

18. Datsenko, K.A. and Wanner, B.L., One-Step Inactivation of Chromosomal Genes in *Escherichia Coli* K-12 Using Pcr Products. *Proc Natl Acad Sci U S A*, **2000**. 97(12): p. 6640-5.

19. Esteves, N.C.; Bigham, D.N.; and Scharf, B.E., Phages on Filaments: A Genetic Screen Elucidates the Complex Interactions between *Salmonella Enterica* Flagellin and Bacteriophage Chi. *PLoS Pathog*, **2023**. 19(8): p. e1011537.

20. Esteves, N.C.; Porwollik, S.; McClelland, M.; and Scharf, B.E., The Multi-Drug Efflux System Acrabz-Tolc Is Essential for Infection of *Salmonella* Typhimurium by the Flagellum-Dependent Bacteriophage Chi. *J Virol*, **2021**. 95(11).

21. Chong, S.; Mersha, F.B.; Comb, D.G.; Scott, M.E.; Landry, D.; Vence, L.M.; Perler, F.B.; Benner, J.; Kucera, R.B.; Hirvonen, C.A., et al., Single-Column Purification of Free Recombinant Proteins Using a Self-Cleavable Affinity Tag Derived from a Protein Splicing Element. *Gene*, **1997**. 192(2): p. 271-81.

22. Bradford, M.M., A Rapid and Sensitive Method for the Quantitation of Microgram Quantities of Protein Utilizing the Principle of Protein-Dye Binding. *Anal Biochem*, **1976**. 72: p. 248-54.

23. Buth, S.A.; Shneider, M.M.; Scholl, D.; and Leiman, P.G., Structure and Analysis of R1 and R2 Pyocin Receptor-Binding Fibers. *Viruses*, **2018**. 10(8).

24. Rawlings, N.D. and Barrett, A.J., Families of Serine Peptidases. *Methods Enzymol*, **1994**. 244: p. 19-61.

25. Morales, E.S.; Parcerisa, I.L.; and Ceccarelli, E.A., A Novel Method for Removing Contaminant Hsp70 Molecular Chaperones from Recombinant Proteins. *Protein Sci*, **2019**. 28(4): p. 800-807.

26. Papadopoulos, S. and Smith, P.R., The Structure of the Tail of the Bacteriophage Φcbk. *Journal of Ultrastructure Research*, **1982**. 80(1): p. 62-70.

27. Pietrzykowska, I.; Krych, M.; and Shugar, D., Mutagenesis Induced by 5-Bromouracil and Methyl Methane Sulfonate: Role of DNA Polymerase I. *Acta Biochim Pol*, **1984**. 31(1): p. 65-75.

28. Dodson, L.A. and Masker, W.E., Survival and Mutagenesis of Bacteriophage T7 Damaged by Methyl Methanesulfonate and Ethyl Methanesulfonate. *Mutat Res*, **1986**. 162(2): p. 137-44.

29. Bull, J.J.; Wichman, H.A.; and Krone, S.M., Modeling the Directed Evolution of Broad Host Range Phages. *Antibiotics (Basel)*, **2022**. 11(12).

FIGURES

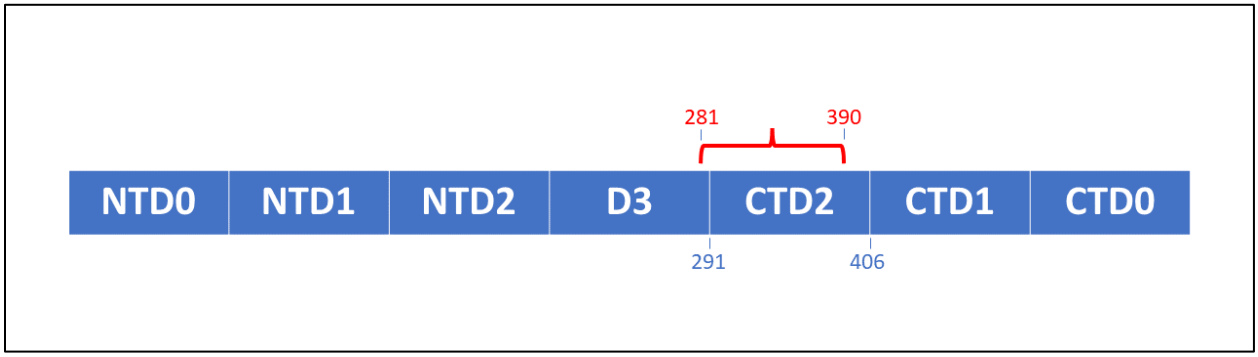


Figure 4.1. (Red) Amino acid residues in *S. enterica* 14028s FliC putatively interacting with χ gp31. Residue numbers correspond to tryptic peptides and thus likely overestimate the range of interaction partners. (Blue) Residue numbers at the beginning and end of 14028s FliC CTD2.

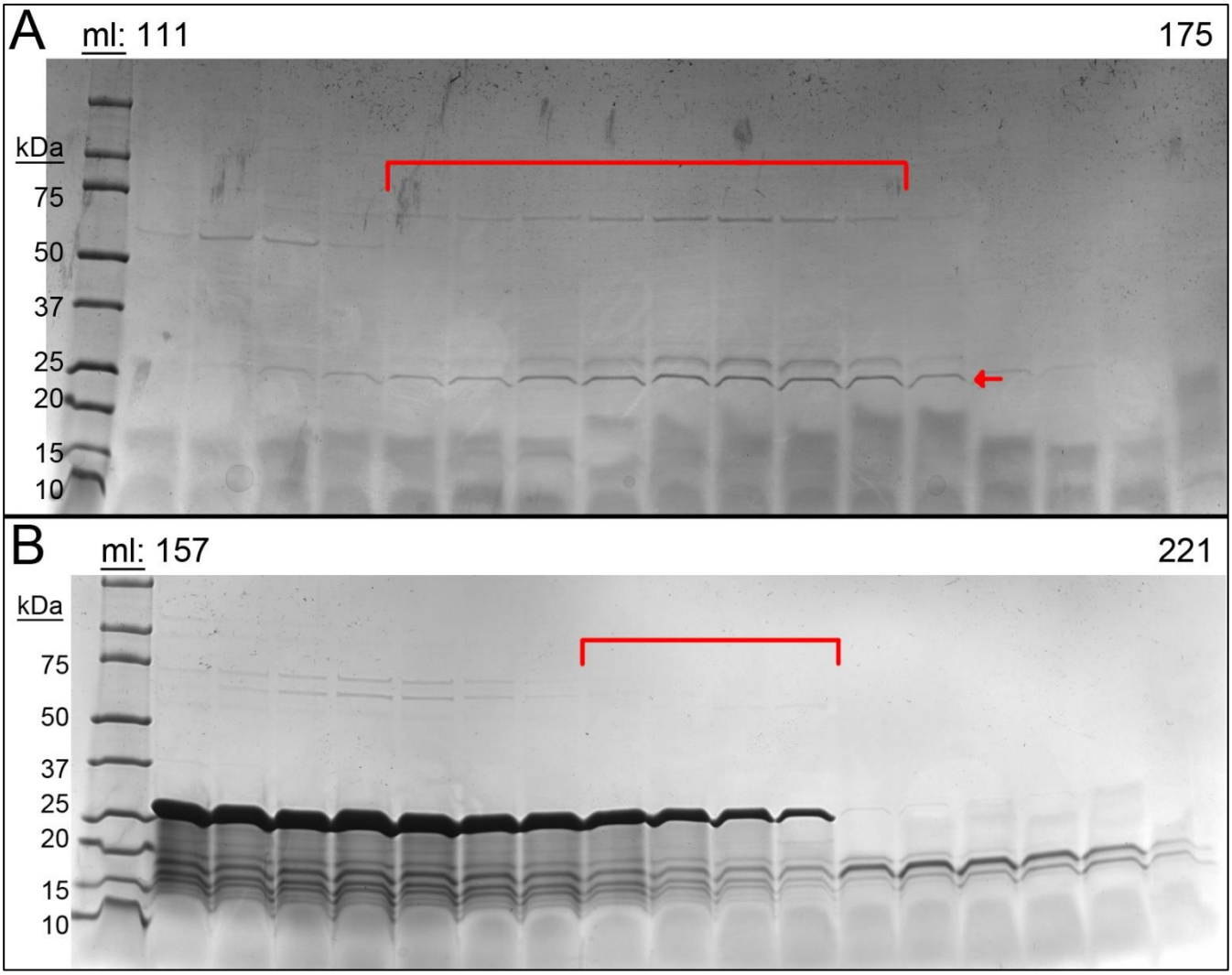


Figure 4.2. [A] Coomassie blue-stained 4-20% SDS PAGE gel of size exclusion chromatography (SEC) fractions of IMPACT purified gp31. Lanes represent consecutive 4-ml fractions from a HiPrep™ Sephacryl S-300 HR SEC column attached to an AKTA Prime FPLC. First and last lanes are labelled with the volume at which the corresponding fraction flowed through the column. The red bracket indicates the fractions that were pooled and used for subsequent experiments. The red arrow shows the expected molecular weight for gp31. Samples were loaded next to a Precision Plus Protein Standard. [B] Coomassie blue-stained 4-20% SDS PAGE gel of SEC fractions of Ni-NTA purified gp31. Lanes represent consecutive 4-ml fractions from a HiPrep™ Sephacryl S-300 HR SEC column attached to an AKTA Go FPLC. First and last lanes are labelled with the volume at which the corresponding fraction flowed through the column. The red bracket indicates the fractions that were pooled and used for subsequent experiments. Samples were loaded next to a Precision Plus Protein Standard.

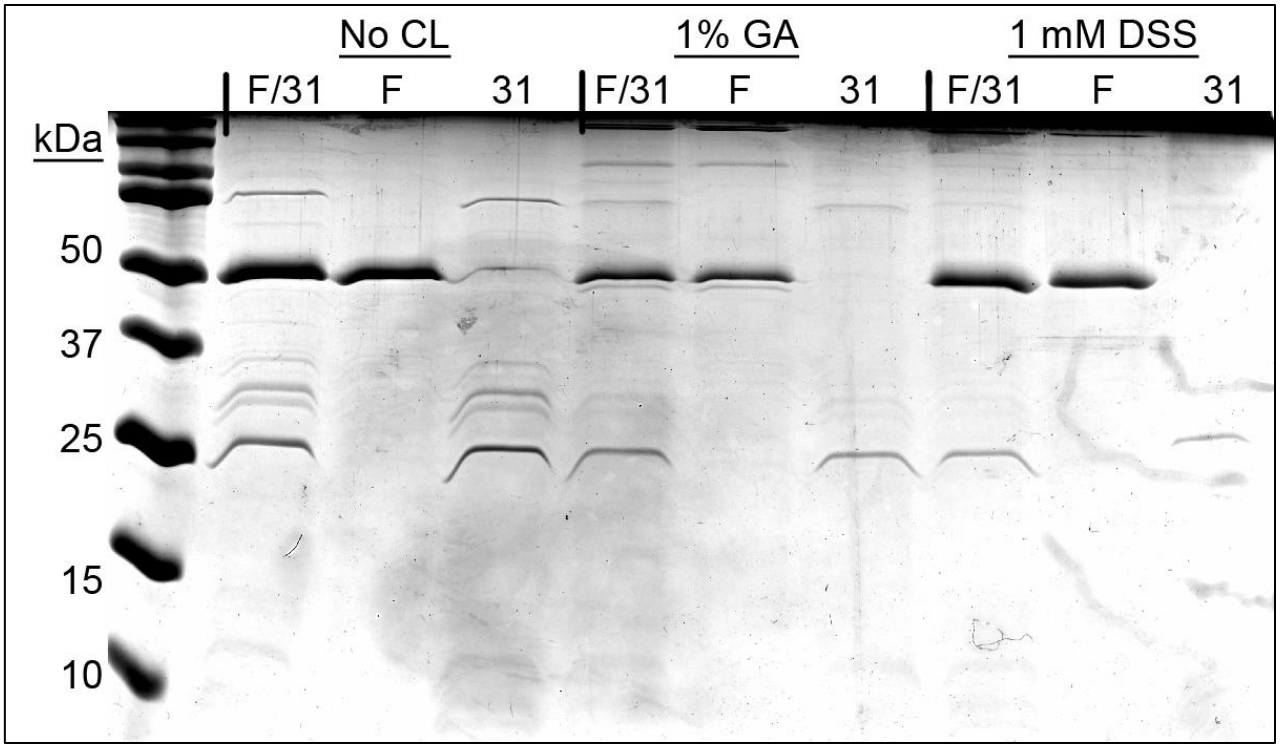


Figure 4.3. Coomassie blue-stained 15% SDS-PAGE gel of chemical crosslinking samples of IMPACT purified gp31 (31) and sheared flagellar filaments (F). Samples were either not treated (No CL), treated with 1% glutaraldehyde (GA), or treated with 1 mM disuccinimidyl suberate (DSS). Samples were loaded next to a Precision Plus Protein Standard.

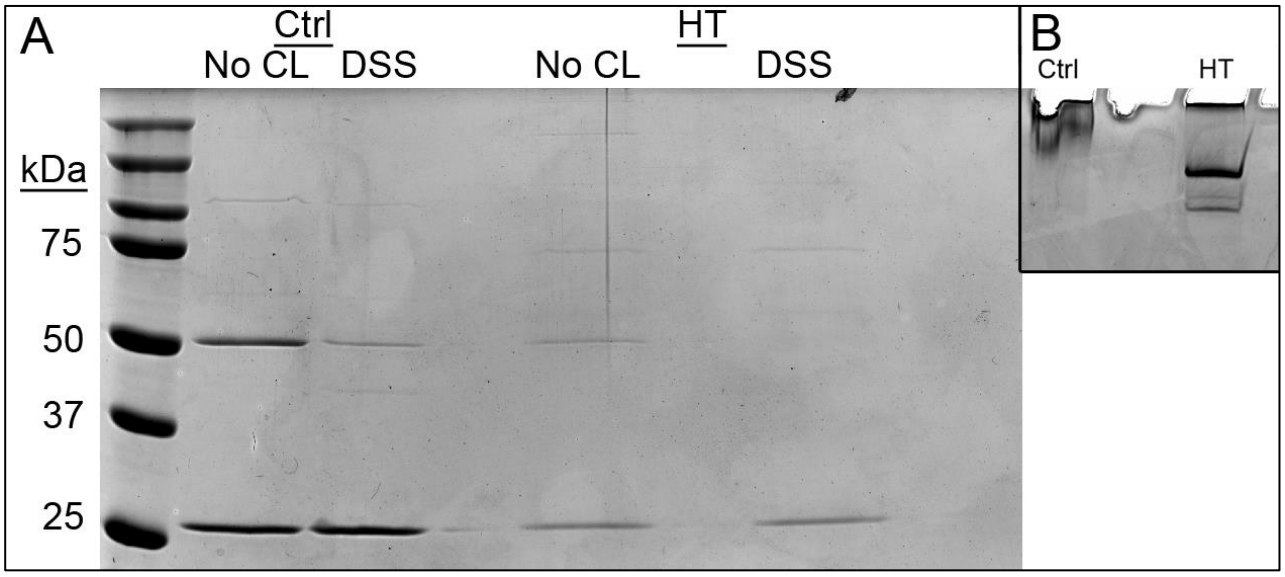


Figure 4.4. [A] Coomassie blue-stained 15% SDS-PAGE gel of chemical crosslinking samples of Ni-NTA-purified gp31 and sheared flagellar filaments (Ctrl), or flagellar filaments heat treated to convert them into flagellin monomers (HT). Samples were either not treated (No CL) or treated with 1 mM disuccinimidyl suberate (DSS). Samples were loaded next to a Precision Plus Protein Standard. [B] Coomassie blue-stained 10% non-denaturing native-PAGE gel of flagellar filaments (Ctrl) or heat-treated flagellar filaments (HT) to estimate oligomeric state.

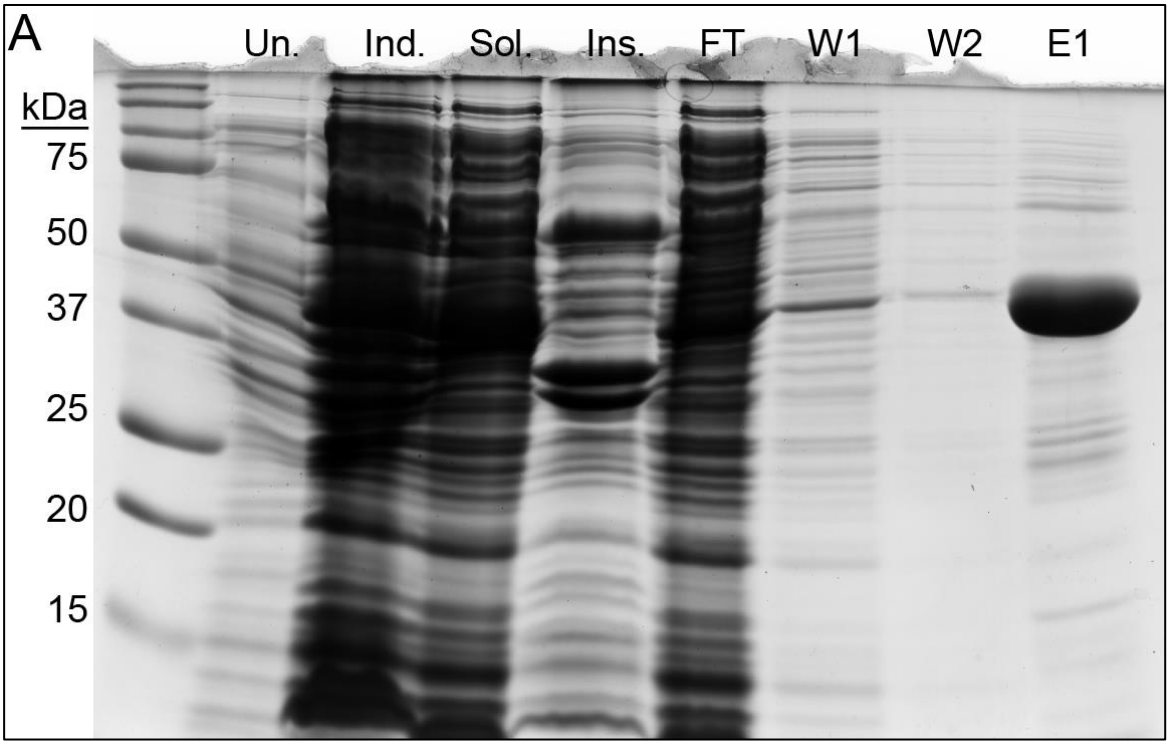


Figure 4.5. [A] Coomassie blue-stained 15% SDS-PAGE gel of fractions from Ni-NTA purification of FliC ΔD0 using a Qiagen Ni-NTA spin column purification kit. From left to right: uninduced cell lysate (Un.), induced cell lysate (Ind.), soluble fraction (Sol.), insoluble fraction (Ins.), column flowthrough (FT), washes (W), elution (E1). Samples were loaded next to a Precision Plus Protein Standard.

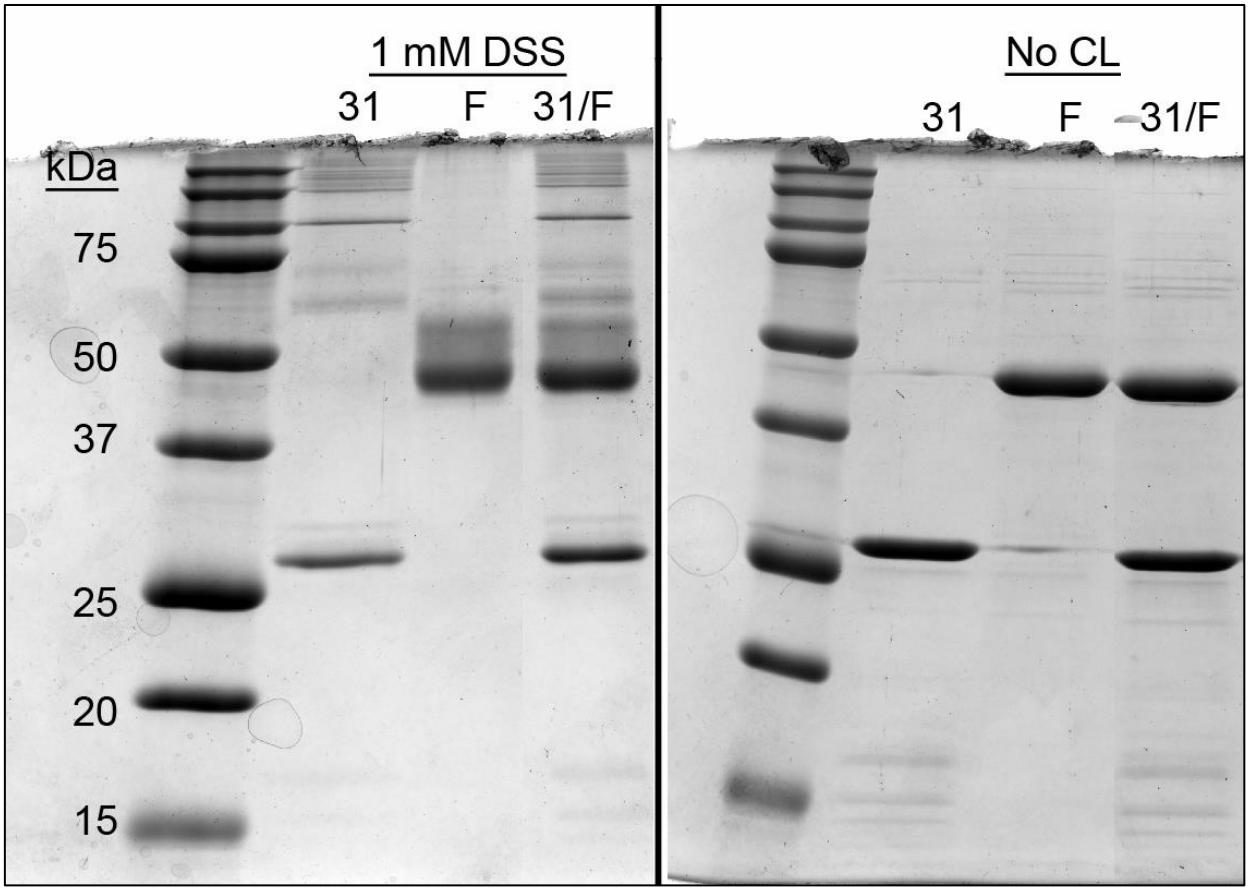


Figure 4.6. Coomassie blue-stained 15% SDS-PAGE gels of recombinant χ gp31 (31), recombinant FliC ΔD0 (F), and the two proteins combined (31/F). Two separate gels were prepared for samples with and without 1 mM DSS crosslinker added. Numerous bands appeared above 50 kDa after 1 hour of DSS crosslinking. Samples were loaded next to a Precision Plus Protein Standard.

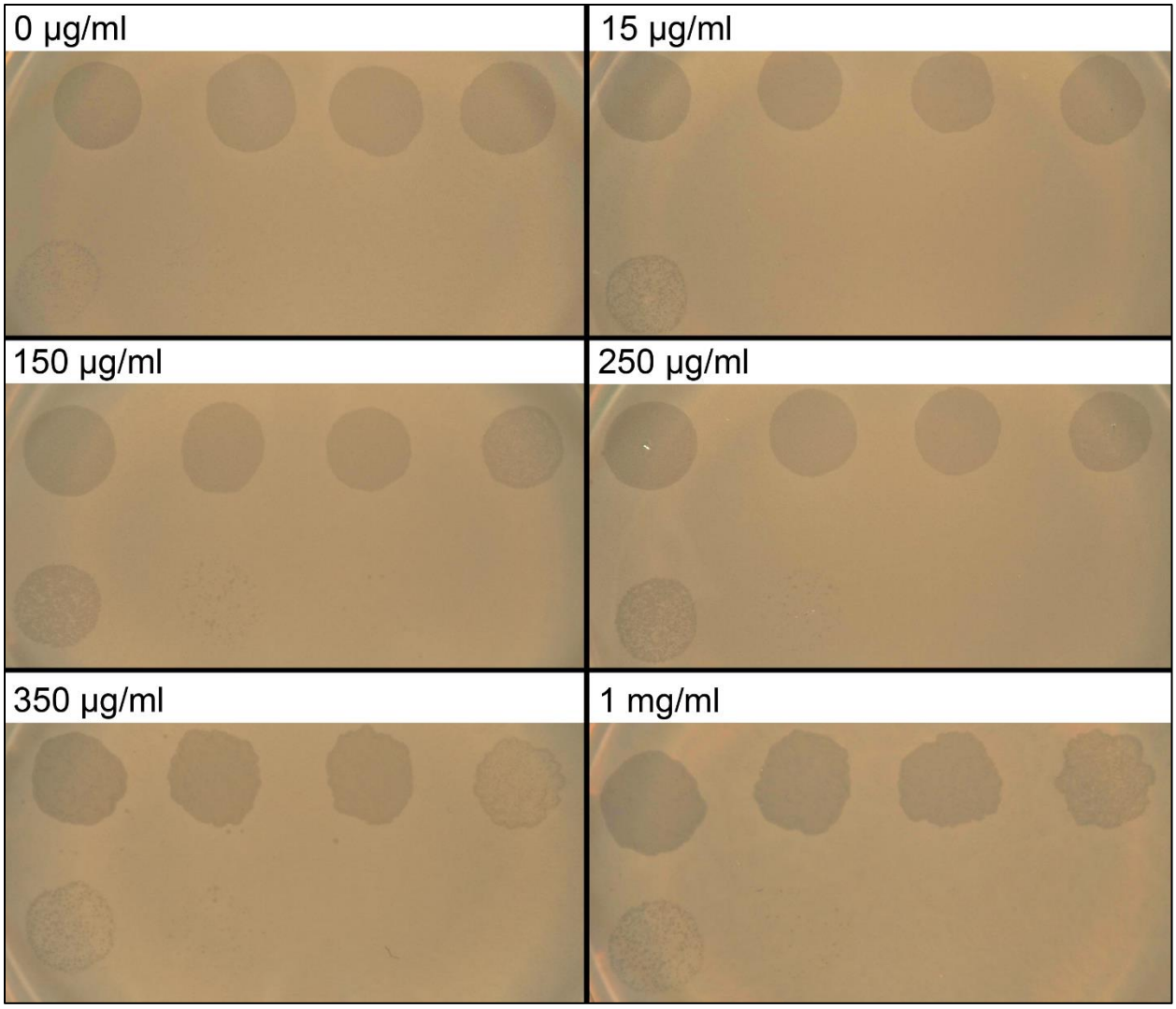


Fig 4.7. Phage competition assay with gp31 and χ. Protein was combined with motile *S. enterica* 14028s cells and molten agar and poured onto an LB plate. Bacteriophage χ dilutions were prepared and 10 µl of dilutions $10^{-1}$-$10^{-8}$ were spotted on the surface of the plate. Reduced phage lysis would indicate that competition had occurred. Concentrations represent the final concentration of gp31 in the cells-protein mixture prior to pouring.

Chapter V

# *Serratia marcescens* ATCC 274 increases production of the red pigment prodigiosin in response to Chi phage infection

Nathaniel C. Esteves and Birgit E. Scharf

Virginia Polytechnic Institute and State University, Blacksburg, VA 24061

Running title: *Serratia* pigmentation increases in response to Chi phage

ABSTRACT

*Serratia marcescens* is an opportunistic human pathogen with the characteristic ability to produce a vibrant red pigment called prodigiosin. Prodigiosin has implications in virulence of *S. marcescens*, and the molecule itself has promising clinical applications. We have discovered that addition of the virulent flagellotropic bacteriophage χ (Chi) to a culture of *S. marcescens* stimulates a greater than fivefold overproduction of prodigiosin. Active phage infection is required for the effect, as a χ-resistant strain lacking flagella does not respond to phage presence. Via a β-galactosidase reporter fusion assay and targeted mutagenesis, we have determined that the addition of a χ-induced *S. marcescens* cell lysate to an uninfected culture causes a threefold increase in transcription of the 21-kb *pig* operon, which contains genes essential for pigment biosynthesis. Replacement of the native *pig* promoter with a constitutive promoter abolished the pigmentation increase, indicating that regulatory elements present in the *pig* promoter likely mediate the phenomenon. We hypothesize that *S. marcescens* detects the threat of phage-mediated cell death and reacts by producing prodigiosin as a stress response. Our findings are of clinical significance for two main reasons: (i) elucidating the complex interactions between a phage and its host is crucial for development of therapeutic phage treatments, and (ii) significant overproduction of prodigiosin in response to phage could be exploited for biosynthesis of the compound for subsequent use as a pharmaceutical.

IMPORTANCE

The pathogenic bacterium *Serratia marcescens* is well known for its vibrant red pigment, prodigiosin, which plays a role in pathogenesis and is being investigated for clinical use. We found that *S. marcescens* is capable of detecting infection or cell death caused by bacteriophage χ, a virus that is of interest for clinical applications. In this study, we have uncovered information

about bacteriophage-host interactions, which is necessary for effective usage of bacteriophages as antibacterial agents. Due to the frequent multidrug resistance of *S. marcescens* and its ability to form robust biofilms, phage therapy may be a particularly effective technique against this organism.

KEYWORDS: Flagella, Gene Expression, Genetic Transcription, Phage Therapy

## INTRODUCTION

*Serratia marcescens* is a Gram-negative opportunistic human pathogen of the family *Yersiniaceae* known for biofilm formation (1), robust swimming and swarming motility (2, 3), frequent multi-drug resistance (MDR) (4), and vibrant red pigment, prodigiosin (5, 6). *S. marcescens* is a common cause of nosocomial infections, particularly among immunocompromised individuals (6). Its robust biofilms and antimicrobial resistance make these infections difficult to eradicate with traditional antibiotics. One promising approach to treating MDR bacterial infections is bacteriophage (phage) therapy (7-9). This technique makes use of phages, the viruses of bacteria, as antibacterial agents. In addition to circumventing MDR, bacteriophages have been shown to be highly effective against disrupting biofilms, including in a clinical setting (10-14). Bacteriophage χ is a flagellotropic (flagellum-dependent) *siphoviridae* phage, meaning the infection process begins with attachment to its host's flagellar filament (15-17). Infection is then postulated to follow the "nut and bolt" model, where rotation of the flagellum brings the phage to the cell surface (18). As a virulent phage, χ cannot lysogenize (19). Approximately 200 virions are released after the cell is lysed following a 52–60-minute latent period (19, 20). Due to the flagellum's nature as a virulence factor (21, 22), χ and other flagellotropic phages may be of particular interest for therapeutic applications (16). These viruses impose an evolutionary tradeoff that may prove exploitable: a pathogenic bacterium

repressing motility to avoid infection by χ would likely be simultaneously attenuating its own virulence.

**Prodigiosin and pigmentation genes**

The *S. marcescens* pigment prodigiosin is of clinical significance for several reasons. In addition to its involvement in *Serratia* competition against other bacterial species (23), the compound itself and other similar molecules have been shown to have antimicrobial, anticancer, and immunomodulatory effects in mammals and is currently under investigation for use as a therapeutic agent (5, 24-26). Regulation of pigment production is complex, and dozens of regulatory mechanisms control its production (26, 27). The primary target of transcriptional regulation of pigment production in *S. marcescens* is the *pig* operon *pigABCDEFGHIJKLMN*, with the additional gene *pigO* being present in certain strains of *Serratia* spp. but absent in *S. marcescens* ATCC 274 (26, 28). These 14 or 15 genes are co-transcribed as a single polycistronic mRNA of approximately 21 kilobases (28) under the control of the $P_{pig}$ promoter, which contains several known and predicted regulatory elements (26, 27). The resulting encoded proteins play various roles in the biosynthesis of prodigiosin through two biosynthetic pathways producing two essential precursor molecules. The monopyrrole 2-methyl-3-n-amyl-pyrrole is synthesized starting with the monounsaturated fatty aldehyde trans-2-octenal, while the dipyrrole 4-methoxy-2,2'-bipyrrole-5-carbaldehyde is synthesized beginning with the amino acid L-proline (26, 29). These two molecules are joined by a condensation reaction to form the tripyrrole prodigiosin (26, 29). Other molecules including malonyl-CoA and pyruvate serve as essential precursors (26, 29). PigP, its gene located elsewhere on the chromosome, seemingly serves as a master regulator of pigmentation in certain *Serratia* strains, such as *Serratia* sp.

ATCC 39006 (30, 31). A functional homolog of PigP is also present in some strains of *S. marcescens* (32). Certain regulatory elements may act on the promoter of *pigP* rather than the *pigA-pigN* promoter (32). While a multi-sequence alignment of ATCC 274 with *Serratia* sp. ATCC 39006 indicated a *pigP* homolog is present in the ATCC 274 genome (33), the gene is not annotated as such and has not been proven to serve as the pigmentation master regulator in this strain.

**Quorum sensing mechanisms and external factors influencing pigment production**

Factors such as temperature (34), phosphate availability (28, 35), oxidative stress (36), envelope stress, denatured proteins (37), cAMP (32), and cell density are known to influence the quantity of prodigiosin produced in *Serratia* spp. (27). Across *Serratia* species, several quorum sensing (QS) systems influence prodigiosin production, including LuxIR homologs producing and responding to acyl-homoserine lactone (AHL) autoinducers (26), and LuxS homologs, which rely on the QS molecule autoinducer-2 (AI-2) (26), a unique boron-containing compound (38). There is a remarkable level of diversity among *Serratia* spp. strains regarding which QS systems are present (26), structure and sequence of the $P_{pig}$ promoter and operon (26, 28), and the presence or absence of *pigP*. A LuxS homolog is the only characterized QS system influencing pigmentation in *S. marcescens* ATCC 274 (39), which lacks the LuxIR homolog SmaIR present in other *Serratia* strains (26). It is unlikely that any other QS systems are present in ATCC 274, as the genome lacks *luxI* homologs (33). In addition to QS systems, many conserved regulators such as Fnr (40), CpxRA (37, 41), OhrR (36), OmpR (42), and PhoBR (35) influence pigmentation. Dozens of possible regulatory elements have been predicted in the $P_{pig}$ promoter or

*pig* operon by sequence analysis, and the corresponding regulators may influence pigmentation as well (27).

In this study, we determined that the addition of bacteriophage χ or a χ phage lysate to a liquid culture of *S. marcescens* ATCC 274 stimulates a significant increase in prodigiosin production. This effect is due, at least in part, to increased transcription of the *pig* operon. While the regulator(s) responsible for this effect remain elusive, it is very likely that they act directly on the $P_{pig}$ promoter, as modification of this promoter abolished the increased pigmentation phenomenon.

## RESULTS

### The magnitude of pigment production after χ addition is increased at stationary phase

In this study, we measured the effect on pigmentation of *S. marcescens* ATCC 274 when χ was added at 0.1 multiplicity of infection (MOI) during exponential phase ($OD_{600}$ = 0.5) or stationary phase ($OD_{600}$ = 2.0). We observed a remarkable difference between these conditions both visually and quantitatively (Fig. 5.1). When χ was added during exponential phase growth at the pigment-permissive temperature of 25°C, a 1.7-fold increase in pigment concentration occurred, as measured by spectrophotometer absorbance at 535 nm ($A_{535}$) 18 hours after phage was added. In contrast, addition of phage during stationary phase resulted in a 5.5-fold increase in pigment concentration in liquid cultures after 18 hours of incubation at 25°C. This remarkable difference in pigmentation intensity between the two growth conditions is due to both a sizeable reduction in pigmentation of the control culture and a modest but significant increase in pigmentation of the culture that received phage (Fig. 5.1). Productive phage infection is required for this effect, as a χ-resistant strain lacking flagellin (Δ*fliC*) exhibited pigment production comparable to WT

in the absence of phage (average $A_{535}$ = 0.761 vs 0.795 for WT after 18 hours of incubation) but did not respond to the addition of χ (Fig. 5.2).

**Replacement of the $P_{pig}$ promoter with a constitutive promoter abolishes the effect**

To investigate the genetic mechanism of this phenomenon, we replaced the native $P_{pig}$ promoter with the strong constitutive promoter J23119 (iGEM Part:BBa_J23119), generating a mutant strain we have named *pig*$^{q}$. This promoter has an *E. coli* sigma-70 consensus sequence and therefore shows a very high transcription level in *E. coli* (43), but has not, to our knowledge, been used previously in *S. marcescens*. When we replaced the entirety of the native *pig* operon 5'-UTR with J23119 and a strong ribosome binding site, we noted a greater overall level of pigmentation (an average $A_{535}$ of 2.09 for *pig*$^{q}$ versus 0.795 for WT after 18 hours of incubation). However, *pig*$^{q}$ cultures showed no statistically significant change in $A_{535}$ values regardless of growth phase in response to χ (Fig. 5.2). Phage infection does occur with this strain: the *pig*$^{q}$ mutant exhibited a comparable level of χ susceptibility compared to WT, as demonstrated by a semi-quantitative χ spot assay (Fig. 5.3).

**The pigmentation increase is statistically significant 3 hours after the addition of phage**

To determine how quickly the pigmentation change becomes significant, we spectrophotometrically measured pigmentation at 1-hour timepoints after addition of 0.1 MOI χ phage at stationary phase ($OD_{600}$ = 2.0). The difference in pigmentation between the two cultures became significant ($P < 0.05$) 3 hours after addition of phage (Fig. 5.4). $A_{535}$ continued to rise in both cultures, but the increase was much larger in the culture with added phage. The difference in $A_{535}$ remained statistically significant throughout the remainder of the experiment. Pigment

production began to plateau at around 10 hours, but pigmentation still continued to increase slightly for the next 2 hours.

**A χ phage lysate stimulates a pigmentation response in a χ-resistant strain**

To investigate whether *S. marcescens* cells were responding to a compound present in a χ phage *S. marcescens* cell lysate, we first generated a lysate by infecting *S. marcescens* Δ*pig* to prevent the presence of prodigiosin in the lysate itself. As removal of phage is not trivial without significantly altering the chemical composition of the lysate, we tested the lysate on a χ resistant strain, namely Δ*fliC*. We found that χ alone had no effect on pigmentation in Δ*fliC* (Fig. 5.2). Therefore, residual phage in the lysate did not contribute to our observations. Use of a flagellin mutant ensured that no new phage infection occurred, therefore any response observed was due to the presence of the lysate. We found that addition of this lysate to an exponential-phase culture resulted in a 1.6-fold increase in $A_{535}$ after 18 hours when compared to a control culture, which received fresh LB medium (Fig. 5.5). This effect is similar to the one obtained when χ phage was added to exponential phase cultures (Fig. 5.1B). Addition of supernatant from an uninfected *S. marcescens* culture caused a statistically significant 1.2-fold increase, indicating that the effect seen with the χ lysate was to a small degree due to compounds also present in an uninfected culture supernatant. A similar effect was seen when the χ lysate was added to stationary phase cultures as it prompted a 1.5-fold increase in $A_{535}$. Moreover, addition of a culture supernatant caused no statistically significant effect at stationary phase (Fig. 5.5). We noted significantly lower overall pigmentation in all cultures at stationary phase compared to exponential-phase cultures. This is different from our findings when χ phage was added, where the effect was much more pronounced in stationary phase cultures (Fig. 5.1). To confirm whether

the increase in pigmentation was specific to the addition of χ lysates, we tested the effect of the supernatant from an *S. marcescens* culture that was mechanically lysed by emulsification, and found that the $A_{535}$ change was the same as previously determined for a non-lysed culture supernatant (data not shown). Overall, the addition of a χ phage lysate prompted a response similar to the addition of the phage itself.

**Pigment overproduction correlates with increased *pigA-pigN* operon transcription**

To gauge *pig* operon transcription in the presence of a χ phage *S. marcescens* cell lysate, we conducted a transcriptional reporter assay by replacing the first gene in the *pig* operon, *pigA*, with the *lacZ* gene from *E. coli* and performing b-galactosidase assays. Immediately and one hour after addition of the lysate, β-galactosidase activity, and thus *pigA-pigN* transcription, was unaffected regardless whether a χ lysate supernatant, uninfected *S. marcescens* cell supernatant, or fresh LB medium was added (Fig. 5.6). However, two hours after the addition of the lysate, β-galactosidase activity rose in the sample that received the χ lysate, reaching 3.3- and 2.6-fold higher values than the cultures that received fresh LB and uninfected culture supernatant, respectively. These trends continued for the next two hours, with the culture that received χ lysate displaying β-galactosidase activities 1.8- and 2.0-fold higher than the culture with fresh LB added, respectively. The samples that received an uninfected supernatant showed an intermediate phenotype of 1.3-fold higher than the LB control at both the 3- and 4-hour timepoints. Overall, the time frame of increase in the *pig* operon transcription aligns with the observations from the pigmentation time-course experiment.

DISCUSSION

In this study, we found that the presence of the flagellotropic bacteriophage χ or a cell lysate generated by infecting *S. marcescens* with χ stimulates a significant increase in the production of the red pigment prodigiosin. Prodigiosin is known to be produced as a response to stressful stimuli (26). There are overlapping regulatory mechanisms between pigmentation and motility (32), and an association between flagellar variation and prodigiosin production (44). The presence of a flagellum-dependent phage like χ would impart significant selective pressure against motility. Altered motility regulation may inadvertently increase *pig* operon expression as a pleiotropic effect.

**Reasons for differences in pigmentation intensity between exponential and stationary phase**

We found that the pigmentation effect was manyfold higher when χ was added to cultures in early stationary phase, rather than exponential phase. This result was not anticipated, as cells display higher motility in exponential phase and motility is a requirement for χ infection. The control cultures that did not receive phage were significantly less pigmented when grown overnight at 37°C, diluted to an $OD_{600}$ of 2.0, and transferred to the pigmentation-permissive temperature of 25°C. This is due to the fact that these cultures were incubated at the pigment-permissive temperature for a shorter amount of time. Interestingly, cultures that received phage showed an inverse effect, being more pigmented when χ was added at an $OD_{600}$ of 2.0 and transferred to 25°C, even though these cultures were also incubated at the pigment-permissive temperature for a shorter time than the exponential phase cultures. This indicates that the increased pigmentation response in stationary phase cultures is large enough to overcome the effects of shorter incubation at 25°C. Both decreased pigmentation in the control cultures and

increased pigmentation in the infected cultures contributed to the large difference in $A_{535}$ between the two growth conditions. Lower motility and higher cell density may result in a smaller proportion of cells being infected by χ at stationary phase. This would result in a greater proportion of viable cells, capable of responding to the cell lysis that occurs in their surroundings. This factor is eliminated when a lysate is added, as new phage infection does not occur, explaining why the difference in $A_{535}$ increase is reversed in the lysate experiment. Finally, differences in overall gene regulation between stationary and exponential phases may also play a role (45-47).

**Transcriptional regulators responsible for the phenomenon likely target the *pig* promoter directly**

In this study, we presented results of a reporter fusion assay and promoter replacement, both of which led to the conclusion that the regulator(s) responsible for the prodigiosin production increase act on the $P_{pig}$ promoter. While growth conditions and certain stressful stimuli are known to induce prodigiosin overproduction (48), the number of studies on biological interactions that induce a similar effect is limited. Chilczuk et al. discovered that certain compounds produced by a cyanobacterial species stimulate prodigiosin production by *Serratia* sp. ATCC 39006 (49). Interestingly, they found that this increase was largely due to changes in L-proline uptake and fatty acid biosynthesis rather than an effect on *pig* operon transcription or QS systems. This mechanism is very different from our findings in *S. marcescens* ATCC 274, demonstrating the complexity of prodigiosin biosynthesis and the diversity among *Serratia* species. While we have shown that the observed phenomenon is due, at least partially, to *pig* operon transcriptional regulation, it is certainly possible that χ may be influencing precursor availability as well. Connections between phage and QS have been described, and certain phage

genomes contain functional QS gene homologs (50). We constructed a Δ*luxS* mutant, which was incapable of performing AI-2 QS, the only known QS system in ATCC 274. This strain still responded to χ in a manner similar to WT. Thus, QS does not mediate the pigment response, unless an undiscovered QS system exists in ATCC 274. This is unlikely, as no *luxI* homologs are present in the genome. While we do not know the transcriptional regulators controlling the pigment overproduction during χ infection, we demonstrated that replacement of the $P_{pig}$ promoter abolishes the effect. The fact that addition of the supernatant of a mechanically lysed culture was statistically indistinguishable from that of a non-lysed culture further indicates that the pigmentation effect is specific to phage-mediated lysis.

**A χ-induced cell lysate mimics the effect of χ on pigmentation**

To further explore the effect of χ on host transcription, we exposed cultures to a χ-induced cell lysate. This approach was necessary, as very rapidly after phage DNA entry, host gene transcription is often severely reduced (51-54), limiting the effectiveness of gene transcription assays in phage-infected samples. In addition, the χ genome includes the genes CHI_9 and CHI_58, putatively encoding an endonuclease and exonuclease, respectively (55). It is possible that these nucleases digest the host genetic material, which would also halt host gene transcription. Since assays like RT-qPCR and transcriptional reporter gene fusions traditionally measure transcription levels as an average of a cell population, the reduction in overall gene transcription in infected cells would likely mask the increased *pig* operon transcription in uninfected cells. Through a β-galactosidase assay of cultures grown in the presence of χ, we found that within 1 hour of infection, overall transcription decreased to a level that outweighs any inducing effect on the *pig* operon (data not shown). To ameliorate these concerns, we used a

phage lysate instead of χ. The results from the lysate experiments aligned well with the pigment concentration ($A_{535}$) time-course experiment. We found that the difference in β-galactosidase activity becomes significant after two hours, and subsequently, the difference in pigmentation intensity becomes significant at three hours.

**Clinical and industrial implications of this work**

Prodigiosin plays a key role in the lifestyle of *Serratia* species. It is used by *Serratia* species to compete with other bacterial species (23), which may contribute to overall fitness and virulence of *S. marcescens* in certain environments (56). In contrast, it has been known for several decades that most clinical isolates of *Serratia* are non-pigmented (57, 58). The overall metabolic cost of synthesizing over a dozen different proteins and diverting precursors to produce the pigment appears to be high, as spontaneous pigmentation mutants arise regularly (59). Therefore, *Serratia* has to balance between the advantages prodigiosin provides and its energetic burden. Our results indicate that the interaction between χ phage and its host is highly complex, and that the bacterium is able to detect phage infection or lysis and to respond by altering transcriptional regulation. It is very likely that χ phage's other hosts are capable of detecting and responding to phage infection as well; *Salmonella enterica* and *Escherichia coli* simply lack a vibrant pigment, thus rendering the response less easily observable. Uncovering more information about phage-host interactions is key to developing phage therapy treatments against pathogenic bacteria.

In addition to the clear applications for phage therapy to treat *S. marcescens* infections, a separate consideration can be made for the implications of this work on the therapeutic applications of prodigiosin itself, as prodiginines have well-demonstrated antibacterial, anticancer, antimalarial, and immunomodulatory activities with strong evidence through in vitro

and in vivo studies (5, 23, 24, 60). We found that addition of a bacteriophage can increase pigment production by more than five times. Additionally, by replacing the promoter of the *pig* operon with a strong constitutive promoter, we generated a strain, *pig*$^{q}$, that significantly overproduces pigment without the need of an outside stimulus. Either addition of χ or the utilization of the *pig*$^{q}$ strain in an industrial setting could be exploited to vastly increase prodigiosin yields in *S. marcescens* cultures for subsequent purification and downstream clinical applications. This would be particularly useful if the effect of χ is found to be additive to other existing strategies for increasing prodigiosin production.

**Future study**

In the future, identification of the regulator(s) responsible for the pigment overproduction would be desirable. RNA-seq could be used to identify genes with increased or decreased expression in response to χ or a χ lysate. Transcription of the *pig* operon should be measured in response to χ. This is not a trivial experiment, but could be successful by sorting cells via flow cytometry using a fluorescently labelled χ phage to differentiate infected and uninfected cells (61). Alternatively, a single-cell RNA sequencing method could be employed, as this has recently become feasible in bacteria (62). Lastly, it needs to be determined whether this phenomenon is specific to χ or flagellotropic phages by exploring other *S. marcescens* phages.

EXPERIMENTAL PROCEDURES

**Construction of mutant strains**

To construct *S. marcescens* mutants including those with gene deletions, promoter replacements, and reporter fusions, we developed an optimized targeted allelic exchange approach with the

plasmid pKNG101 (63) and provide a detailed protocol below. First, the desired allele was amplified by PCR and cloned into pKNG101 following standard restriction enzyme cloning procedures. *Escherichia coli* DH5α-λpir was transformed with the resulting ligation mixture and plated on lysogeny broth LB (64) with 50 µg/ml streptomycin (LB str). Deletion constructs were introduced into *E. coli* SM10-λpir by transformation. The plasmid was then mobilized into *S. marcescens* ATCC 274 by biparental mating conjugation. Briefly, ATCC 274 and SM10-λpir containing the deletion plasmid were grown in LB at 37°C with shaking until an $OD_{600}$ of 0.5 was reached. The two cultures were then mixed at a ratio of 1:1 by optical density, and 100 µl of this mixture was spread onto an LB agar plate without antibiotics. After 24 hours of incubation at 37°C, the bacterial lawn was scraped into a tube containing 1 ml of LB, suspended by vortexing, and spread onto LB containing 50 µg/ml streptomycin and 10 µg/ml tetracycline (LB str/tet) to select against the *E. coli* SM10-λpir strain, taking advantage of the intrinsic tetracycline resistance of ATCC 274. After an overnight incubation step, colonies were streaked on LB str/tet, and a single colony from this plate was inoculated into 10 ml of LB without antibiotics, which was incubated with shaking for 24 hours at 37°C to allow a second homologous recombination event to occur. The culture was then centrifuged at 15,000 x g for 5 minutes and washed twice with M9 salts (47.7 mM $Na_2HPO_4$, 22 mM $KH_2PO_4$, 8.6 mM NaCl, 18.7 mM $NH_4Cl$, 2mM $MgSO_4$, 0.1 mM $CaCl_2$,). Dilutions were prepared in M9 salts and spread plated on M9F agar plates containing 10% w/v sucrose as the sole carbon source for SacB counterselection. M9F is a modified M9 minimal medium (65) containing 0.2 mM $FeSO_4$ for improved growth of *S. marcescens*. These plates were incubated at room temperature for three to four days. It is important to note that incubation at higher temperatures or the presence of carbon sources other than sucrose vastly reduced the quality of selection. Large colonies were patched

on LB str to verify loss of streptomycin resistance. Genomic DNA was purified by phenol-chloroform extraction, and deletion loci were amplified by PCR followed by confirmation via Sanger sequencing. Note that the DNA purification step is crucial, as *S. marcescens* produces a remarkably robust extracellular nuclease (66) that we found to be capable of retaining activity after colony PCR cycles and subsequently rapidly digesting PCR products. Proteinase K treatment during DNA purification effectively inactivated the nuclease.

**Spectrophotometric determination of prodigiosin concentration in cultures and imaging**

*S. marcescens* cultures were routinely grown overnight in LB at 37°C with 220 RPM shaking. At this temperature, no prodigiosin is produced in the wild-type strain (34). To test the effect of χ addition at exponential phase, overnight cultures were diluted 1:100 and grown at 25°C with 220 RPM shaking until an $OD_{600}$ of 0.5 was reached. Phage was then added at an MOI of 0.1, followed by 18 hours of incubation at 25°C with shaking. To test the effect of χ at stationary phase, overnight stationary phase cultures grown at 37°C were diluted to an $OD_{600}$ of 2.0, χ was immediately added at an MOI of 0.1, and cultures were transferred to a shaking incubator at 25°C and incubated for 18 hours. Relative prodigiosin concentration was determined by measuring absorbance at 535 nm after lysing cells using a modified acidified ethanol lysis method (67). Briefly, *S. marcescens* culture in LB was mixed with two volumes of acidified ethanol (100% ethanol with 40 mM HCl) and vortexed vigorously. Cell debris was pelleted in a centrifuge at 5,000 x g for 10 min. One milliliter of supernatant was pipetted into a quartz spectrophotometer cuvette and absorbance at 535 nm was measured. For pigmentation time-courses, 0.5 ml samples of *S. marcescens* cultures were taken at regular intervals and immediately lysed by the addition of 1 ml of acidified ethanol. All samples were assayed via

spectrophotometer. Although A535 values are often normalized to OD600 in other experiments described in the literature, we elected not to normalize, due to the fact that phage-lysed cells and cell debris contribute to OD600. If χ were to cause a large amount of cell death, OD600 would likely not decrease proportionally to the reduction in viable cell count. This would cause misrepresentation of results. This is supported by the observation that despite the fact that χ-mediated lysis occurs in liquid cultures, no reduction in OD600 occurs in χ-infected cultures compared to a control unless a very high MOI is used.

A Cytiva IQ800 instrument was used to capture color images of *S. marcescens* cultures. First, 10 ml of culture in LB was pipetted into each half of a split 10 cm circular petri dish. For 6-well rectangular plates, 5 ml of culture was pipetted into each well. Plates were placed into the imager without lids and imaged using epi-illumination with the white tray insert.

**Generation of a χ phage cell lysate lacking pigment**

To generate the lysate for use in further experiments, a 37°C overnight liquid culture of *S. marcescens* Δ*pig* was diluted 1:100 and grown in LB at 25°C with 220 RPM shaking until an $OD_{600}$ of 0.75 was reached. Motility was verified by phase contrast microscopy. Next, χ was added to the culture at an MOI of 0.1, and the culture was returned to the shaking incubator. A second culture was prepared in parallel and did not receive phage. After 3 hours, both cultures were centrifuged at 16,000 x g for 10 minutes, and supernatants were filtered through 0.2 µm syringe filters. Prior to centrifugation, a small amount of each culture was serially diluted in fresh LB and plated to determine viable cfu/ml, to allow for normalization of the amount of lysate and control supernatant to add in further experiments. The mechanical lysate was prepared similarly to the control supernatant, but cells were lysed using an EmulsiFlex C3 emulsifier

(Avestin) prior to centrifugation. After filtration, lysates were stored at 4°C, and retained their activity for at least four weeks (data not shown).

**Spot assays for determining phage susceptibility**

Spot assays were used to determine susceptibility to χ phage. Briefly, *S. marcescens* was grown in LB at 25°C to an $OD_{600}$ of approximately 1.0. Motility was verified by phase contrast microscopy for strains expected to be motile. Next, 100 µl of culture was mixed with 4 ml of LB with 0.5% agar molten at 50°C, and poured onto an LB agar plate. Fresh 1:10 serial dilutions of χ phage in 0.85% NaCl were prepared. After the top agar solidified, 10 µl of phage dilutions were spotted on the agar surface. Plates were incubated at 25°C overnight. Zones of lysis indicated phage infection and thus susceptibility. Plates were imaged using a Cytiva IQ800 instrument with trans-illumination.

**Beta-galactosidase (LacZ) transcriptional reporter fusion assay**

The mutagenesis technique described above was used to generate a mutant strain (*pig-lacZ*) where the *pigA* gene on the chromosome was replaced with the *lacZ* gene PCR-amplified from *E. coli* MG1655, leaving the $P_{pig}$ promoter and the remainder of the *pig* operon intact. To make this strain χ resistant, the flagellin gene *fliC* was deleted additionally. Cultures of *pig-lacZ* were grown overnight at 37°C in LB. The following day, cultures were diluted 1:100 into fresh LB and grown at 25°C to an $OD_{600}$ of 0.8. Phage lysate, control supernatant, or fresh LB was added to each set of cultures at a volume ratio of 1:1. Aliquots of each culture were harvested at 0, 1, 2, 3, and 4 hours after addition of lysates by centrifuging at 16,000 x g for 10 minutes and freezing

pellets at -20°C. A β-galactosidase assay was conducted following an established protocol previously described by Miller (65).

ACKNOWLEDGEMENTS

We thank Rasika Harshey for *S. marcescens* wild type ATCC 274, Clay Fuqua for *E. coli* SM10-λpir, the late Howard C. Berg for *E. coli* DH5α-λpir, and Sarah J. Coulthurst for plasmid pKNG101. We thank Danielle Bigham and Bryce Brunelli for their assistance with pigmentation time-course experiments and *S. marcescens* mutant construction, respectively. This work was funded by the National Science Foundation fund number IOS-2054392 and a Virginia Tech Center for Emerging, Zoonotic, and Arthropod-Borne Pathogens (CeZAP) mini-grant to N.C.E.

AUTHOR CONTRIBUTIONS

Conceptualization: N.C.E. and B.E.S.; Data Curation: N.C.E.; Formal Analysis: N.C.E. and B.E.S.; Funding Acquisition: N.C.E. and B.E.S.; Investigation: N.C.E.; Methodology: N.C.E. and B.E.S.; Project Administration: N.C.E. and B.E.S.; Resources: B.E.S.; Supervision: N.C.E. and B.E.S.; Validation: N.C.E.; Visualization: N.C.E. and B.E.S.; Writing – Original Draft Preparation: N.C.E. and B.E.S.; Writing – Review & Editing: N.C.E. and B.E.S.

REFERENCES


1. Ray C, Shenoy AT, Orihuela CJ, González-Juarbe N. 2017. Killing of *Serratia marcescens* biofilms with chloramphenicol. Ann Clin Microbiol Antimicrob 16:19.
2. Alberti L, Harshey RM. 1990. Differentiation of *Serratia marcescens* 274 into swimmer and swarmer cells. J Bacteriol 172:4322-8.
3. O'Rear J, Alberti L, Harshey RM. 1992. Mutations that impair swarming motility in *Serratia marcescens* 274 include but are not limited to those affecting chemotaxis or flagellar function. J Bacteriol 174:6125-37.
4. Zivkovic Zaric R, Zaric M, Sekulic M, Zornic N, Nesic J, Rosic V, Vulovic T, Spasic M, Vuleta M, Jovanovic J, Jovanovic D, Jakovljevic S, Canovic P. 2023. Antimicrobial Treatment of *Serratia marcescens* Invasive Infections: Systematic Review. Antibiotics (Basel) 12.
5. Stankovic N, Senerovic L, Ilic-Tomic T, Vasiljevic B, Nikodinovic-Runic J. 2014. Properties and applications of undecylprodigiosin and other bacterial prodigiosins. Appl Microbiol Biotechnol 98:3841-58.
6. Hejazi A, Falkiner FR. 1997. *Serratia marcescens*. J Med Microbiol 46:903-912.
7. Romero-Calle D, Guimaraes Benevides R, Goes-Neto A, Billington C. 2019. Bacteriophages as alternatives to antibiotics in clinical care. Antibiotics (Basel) 8.
8. Kortright KE, Chan BK, Koff JL, Turner PE. 2019. Phage Therapy: A Renewed Approach to Combat Antibiotic-Resistant Bacteria. Cell Host Microbe 25:219-232.
9. Golkar Z, Bagasra O, Pace DG. 2014. Bacteriophage therapy: a potential solution for the antibiotic resistance crisis. J Infect Dev Ctries 8:129-36.
10. Ferriol-González C, Domingo-Calap P. 2020. Phages for Biofilm Removal. Antibiotics (Basel) 9.
11. Cornelissen A, Ceyssens PJ, T'Syen J, Van Praet H, Noben JP, Shaburova OV, Krylov VN, Volckaert G, Lavigne R. 2011. The T7-related Pseudomonas putida phage φ15 displays virion-associated biofilm degradation properties. PLoS One 6:e18597.
12. Hanlon GW, Denyer SP, Olliff CJ, Ibrahim LJ. 2001. Reduction in exopolysaccharide viscosity as an aid to bacteriophage penetration through Pseudomonas aeruginosa biofilms. Appl Environ Microbiol 67:2746-53.
13. Maszewska A, Zygmunt M, Grzejdziak I, Różalski A. 2018. Use of polyvalent bacteriophages to combat biofilm of Proteus mirabilis causing catheter-associated urinary tract infections. J Appl Microbiol 125:1253-1265.
14. Tkhilaishvili T, Wang L, Tavanti A, Trampuz A, Di Luca M. 2020. Antibacterial Efficacy of Two Commercially Available Bacteriophage Formulations, Staphylococcal Bacteriophage and PYO Bacteriophage, Against Methicillin-Resistant Staphylococcus aureus: Prevention and Eradication of Biofilm Formation and Control of a Systemic Infection of Galleria mellonella Larvae. Front Microbiol 11:110.
15. Schade SZ, Adler J, Ris H. 1967. How bacteriophage χ attacks motile bacteria. J Virol 1:599.
16. Esteves NC, Scharf BE. 2022. Flagellotropic Bacteriophages: Opportunities and Challenges for Antimicrobial Applications. Int J Mol Sci 23.
17. Esteves NC, Bigham DN, Scharf BE. 2023. Phages on filaments: A genetic screen elucidates the complex interactions between *Salmonella enterica* flagellin and bacteriophage Chi. PLoS Pathog 19:e1011537.

18. Samuel AD, Pitta TP, Ryu WS, Danese PN, Leung EC, Berg HC. 1999. Flagellar determinants of bacterial sensitivity to chi-phage. Proc Natl Acad Sci U S A 96:9863-9866.
19. MEYNELL EW. 1961. A phage, øχ, which attacks motile bacteria. Microbiology 25:253-290.
20. Schade S, Adler J. 1967. Purification and chemistry of bacteriophage chi. J Virol 1:591-8.
21. Jonson AB, Normark S, Rhen M. 2005. Fimbriae, pili, flagella and bacterial virulence. Contrib Microbiol 12:67-89.
22. Duan Q, Zhou M, Zhu L, Zhu G. 2013. Flagella and bacterial pathogenicity. J Basic Microbiol 53:1-8.
23. Yip CH, Mahalingam S, Wan KL, Nathan S. 2021. Prodigiosin inhibits bacterial growth and virulence factors as a potential physiological response to interspecies competition. PLoS One 16:e0253445.
24. Nguyen SLT, Nguyen TC, Do TT, Vu TL, Nguyen TT, Do TT, Nguyen THT, Le TH, Trinh DK, Nguyen TAT. 2022. Study on the Anticancer Activity of Prodigiosin from Variants of *Serratia marcescens* QBN VTCC 910026. Biomed Res Int 2022:4053074.
25. Espona-Fiedler M, Soto-Cerrato V, Hosseini A, Lizcano JM, Guallar V, Quesada R, Gao T, Pérez-Tomás R. 2012. Identification of dual mTORC1 and mTORC2 inhibitors in melanoma cells: prodigiosin vs. obatoclax. Biochem Pharmacol 83:489-96.
26. Williamson NR, Fineran PC, Leeper FJ, Salmond GP. 2006. The biosynthesis and regulation of bacterial prodiginines. Nat Rev Microbiol 4:887-99.
27. Ravindran A, Sunderrajan S, Pennathur G. 2019. Phylogenetic Studies on the Prodigiosin Biosynthetic Operon. Curr Microbiol 76:597-606.
28. Harris AKP, Williamson NR, Slater H, Cox A, Abbasi S, Foulds I, Simonsen HT, Leeper FJ, Salmond GPC. 2004. The *Serratia* gene cluster encoding biosynthesis of the red antibiotic, prodigiosin, shows species- and strain-dependent genome context variation. Microbiology 150:3547-3560.
29. Williamson NR, Simonsen HT, Ahmed RAA, Goldet G, Slater H, Woodley L, Leeper FJ, Salmond GPC. 2005. Biosynthesis of the red antibiotic, prodigiosin, in *Serratia*: identification of a novel 2-methyl-3-n-amyl-pyrrole (MAP) assembly pathway, definition of the terminal condensing enzyme, and implications for undecylprodigiosin biosynthesis in *Streptomyces*. Mol Microbiol 56:971-989.
30. Gristwood T, McNeil MB, Clulow JS, Salmond GP, Fineran PC. 2011. PigS and PigP regulate prodigiosin biosynthesis in *Serratia* via differential control of divergent operons, which include predicted transporters of sulfur-containing molecules. J Bacteriol 193:1076-85.
31. Fineran PC, Slater H, Everson L, Hughes K, Salmond GP. 2005. Biosynthesis of tripyrrole and beta-lactam secondary metabolites in *Serratia*: integration of quorum sensing with multiple new regulatory components in the control of prodigiosin and carbapenem antibiotic production. Mol Microbiol 56:1495-517.
32. Shanks RM, Lahr RM, Stella NA, Arena KE, Brothers KM, Kwak DH, Liu X, Kalivoda EJ. 2013. A *Serratia marcescens* PigP homolog controls prodigiosin biosynthesis, swarming motility and hemolysis and is regulated by cAMP-CRP and HexS. PLoS One 8:e57634.
33. Yabe S, Fukushima J. 2020. Complete Genome Sequence of Temperature-Dependent Pigment-Producing *Serratia marcescens* ATCC 274. Microbiol Resour Announc 9.

34. Tanikawa T, Nakagawa Y, Matsuyama T. 2006. Transcriptional downregulator HexS controlling prodigiosin and serrawettin W1 biosynthesis in *Serratia marcescens*. Microbiol Immunol 50:587-96.
35. Gristwood T, Fineran PC, Everson L, Williamson NR, Salmond GP. 2009. The PhoBR two-component system regulates antibiotic biosynthesis in *Serratia* in response to phosphate. BMC Microbiol 9:112.
36. Sun D, Liu W, Zhou X, Ru Y, Liu J, Zhu J, Liu C. 2022. Organic Hydroperoxide Induces Prodigiosin Biosynthesis in *Serratia* sp. ATCC 39006 in an OhrR-Dependent Manner. Appl Environ Microbiol 88:e0204121.
37. Qiu S, Jia S, Zhang F, Liu X, Ran T, Wang W, Wang C, Xu D. 2021. Two component system CpxR/A regulates the prodigiosin biosynthesis by negative control in *Serratia marcescens* FS14. Biochem Biophys Res Commun 579:136-140.
38. Chen X, Schauder S, Potier N, Van Dorsselaer A, Pelczer I, Bassler BL, Hughson FM. 2002. Structural identification of a bacterial quorum-sensing signal containing boron. Nature 415:545-9.
39. Coulthurst SJ, Kurz CL, Salmond GPC. 2004. luxS mutants of Serratia defective in autoinducer-2-dependent 'quorum sensing' show strain-dependent impacts on virulence and production of carbapenem and prodigiosin. Microbiology (Reading) 150:1901-1910.
40. Sun D, Zhou X, Liu C, Zhu J, Ru Y, Liu W, Liu J. 2021. Fnr Negatively Regulates Prodigiosin Synthesis in *Serratia* sp. ATCC 39006 During Aerobic Fermentation. Front Microbiol 12:734854.
41. Sun Y, Wang L, Pan X, Osire T, Fang H, Zhang H, Yang ST, Yang T, Rao Z. 2020. Improved Prodigiosin Production by Relieving CpxR Temperature-Sensitive Inhibition. Front Bioeng Biotechnol 8:344.
42. Jia X, Zhao K, Liu F, Lin J, Lin C, Chen J. 2022. Transcriptional factor OmpR positively regulates prodigiosin biosynthesis in *Serratia marcescens* FZSF02 by binding with the promoter of the prodigiosin cluster. Front Microbiol 13:1041146.
43. Chen R, Zhu Y, Wang H, Liu Y, Meng J, Chen Y, Mu W. 2023. Engineering *Escherichia coli* MG1655 for Highly Efficient Biosynthesis of 2'-Fucosyllactose by De Novo GDP-Fucose Pathway. J Agric Food Chem 71:14678-14686.
44. Paruchuri DK, Harshey RM. 1987. Flagellar variation in *Serratia marcescens* is associated with color variation. J Bacteriol 169:61-5.
45. Chang DE, Smalley DJ, Conway T. 2002. Gene expression profiling of *Escherichia coli* growth transitions: an expanded stringent response model. Mol Microbiol 45:289-306.
46. Ishihama A. 1997. Adaptation of gene expression in stationary phase bacteria. Current Opinion in Genetics & Development 7:582-588.
47. Navarro Llorens JM, Tormo A, Martínez-García E. 2010. Stationary phase in Gram-negative bacteria. FEMS Microbiology Reviews 34:476-495.
48. Lin S-R, Chen Y-H, Tseng F-J, Weng C-F. 2020. The production and bioactivity of prodigiosin: quo vadis? Drug Discov Today 25:828-836.
49. Chilczuk T, Monson R, Schmieder P, Christov V, Enke H, Salmond G, Niedermeyer THJ. 2020. Ambigols from the Cyanobacterium *Fischerella ambigua* Increase Prodigiosin Production in *Serratia* spp. ACS Chem Biol 15:2929-2936.
50. Silpe JE, Bassler BL. 2019. A Host-Produced Quorum-Sensing Autoinducer Controls a Phage Lysis-Lysogeny Decision. Cell 176:268-280.e13.

51. Kashlev M, Nudler E, Goldfarb A, White T, Kutter E. 1993. Bacteriophage T4 Alc protein: a transcription termination factor sensing local modification of DNA. Cell 75:147-54.
52. Yang H, Ma Y, Wang Y, Yang H, Shen W, Chen X. 2014. Transcription regulation mechanisms of bacteriophages: recent advances and future prospects. Bioengineered 5:300-4.
53. Nechaev S, Severinov K. 2003. Bacteriophage-induced modifications of host RNA polymerase. Annu Rev Microbiol 57:301-22.
54. Pani B, Banerjee S, Chalissery J, Muralimohan A, Loganathan RM, Suganthan RB, Sen R. 2006. Mechanism of inhibition of Rho-dependent transcription termination by bacteriophage P4 protein Psu. J Biol Chem 281:26491-500.
55. Hendrix RW, Ko C-C, Jacobs-Sera D, Hatfull GF, Erhardt M, Hughes KT, Casjens SR. 2015. Genome sequence of *Salmonella* phage χ. Genome Announc 3:e01229-14.
56. Haddix PL, Shanks RMQ. 2018. Prodigiosin pigment of *Serratia marcescens* is associated with increased biomass production. Arch Microbiol 200:989-999.
57. Wilfert JN, Barrett FF, Ewing WH, Finland M, Kass EH. 1970. *Serratia marcescens*: biochemical, serological, and epidemiological characteristics and antibiotic susceptibility of strains isolated at Boston City Hospital. Appl Microbiol 19:345-52.
58. Carbonell GV, Della Colleta HH, Yano T, Darini AL, Levy CE, Fonseca BA. 2000. Clinical relevance and virulence factors of pigmented *Serratia marcescens*. FEMS Immunol Med Microbiol 28:143-9.
59. Xiang T, Zhou W, Xu C, Xu J, Liu R, Wang N, Xu L, Zhao Y, Luo M, Mo X, Mao Z, Wan Y. 2021. Transcriptomic Analysis Reveals Competitive Growth Advantage of Non-pigmented *Serratia marcescens* Mutants. Front Microbiol 12:793202.
60. Papireddy K, Smilkstein M, Kelly JX, Shweta, Salem SM, Alhamadsheh M, Haynes SW, Challis GL, Reynolds KA. 2011. Antimalarial activity of natural and synthetic prodiginines. J Med Chem 54:5296-306.
61. Low HZ, Böhnlein C, Sprotte S, Wagner N, Fiedler G, Kabisch J, Franz C. 2020. Fast and Easy Phage-Tagging and Live/Dead Analysis for the Rapid Monitoring of Bacteriophage Infection. Front Microbiol 11:602444.
62. McNulty R, Sritharan D, Pahng SH, Meisch JP, Liu S, Brennan MA, Saxer G, Hormoz S, Rosenthal AZ. 2023. Probe-based bacterial single-cell RNA sequencing predicts toxin regulation. Nat Microbiol 8:934-945.
63. Kaniga K, Delor I, Cornelis GR. 1991. A wide-host-range suicide vector for improving reverse genetics in gram-negative bacteria: inactivation of the *blaA* gene of *Yersinia enterocolitica*. Gene 109:137-41.
64. Bertani G. 1951. Studies on lysogenesis. I. The mode of phage liberation by lysogenic *Escherichia coli*. J Bacteriol 62:293-300.
65. Miller JH. 1972. Experiments in molecular genetics. Cold Spring Harbor Laboratory Press, Cold Spring Harbor, N.Y.
66. Biedermann K, Jepsen PK, Riise E, Svendsen I. 1989. Purification and characterization of a *Serratia marcescens* nuclease produced by *Escherichia coli*. Carlsberg Research Communications 54:17-27.
67. Slater H, Crow M, Everson L, Salmond GPC. 2003. Phosphate availability regulates biosynthesis of two antibiotics, prodigiosin and carbapenem, in Serratia via both quorum-sensing-dependent and -independent pathways. Molecular Microbiology 47:303-320.

TABLES

Table 5.1. Strains, plasmids, and phage used in this study.

| **Strain, plasmid, or phage** | **Parental strain/Backbone** | **Relevant characteristics** | **Source** |
|---|---|---|---|
| *Serratia marcescens* ATCC 274 (WT) | ATCC 274 | Wild type | Rasika Harshey |
| Δ*fliC* | ATCC 274 | Δ*fliC* (*flaF*) | This study |
| Δ*pig* | ATCC 274 | Δ*pigABCDEFGHIJKLMN* | This study |
| *pig-lacZ* | ATCC 274 | Δ*fliC*; *pigA*::*lacZ* | This study |
| *pig*$^{q}$ | ATCC 274 | $P_{pig}$ replaced with J23119 | This study |
| pKNG101 | - | MCS, *strAB*, *sacB*, *mobRK2*, *oriV* R6Kγ, *traJK* | Sarah J Coulthurst |
| pBS1315 | pUC18 | Cloning vector with J23119 promoter | This study |
| pBS1355 | pKNG101 | *fliC* (*flaF*) deletion construct | This study |
| pBS1359 | pKNG101 | *pig*$^{q}$ mutant construct | This study |
| pBS1361 | pKNG101 | *pig* operon deletion construct | This study |
| pBS1362 | pKNG101 | *pig-lacZ* fusion mutant construct | This study |
| DH5α-λpir | *Escherichia coli* K-12 | $F^{-}$ φ80*lacZ*ΔM15 Δ(*lacZYA-argF*)U169 *recA*1 *endA*1 *hsdR*17($r_K^{-}$, $m_K^{+}$) *phoA supE*44 $\lambda^{-}$*thi*-1 *gyrA*96 *relA*1 *LAMpir* | Howard C. Berg |
| SM10-λpir | *Escherichia coli* K-12 | *thi thr leu tonA lacY supE recA*::RP4-2-Tc::Mu Km *LAMpir* | Clay Fuqua |
| χ (Chi) | - | Wild type | Saeed Tavazoie |

FIGURES

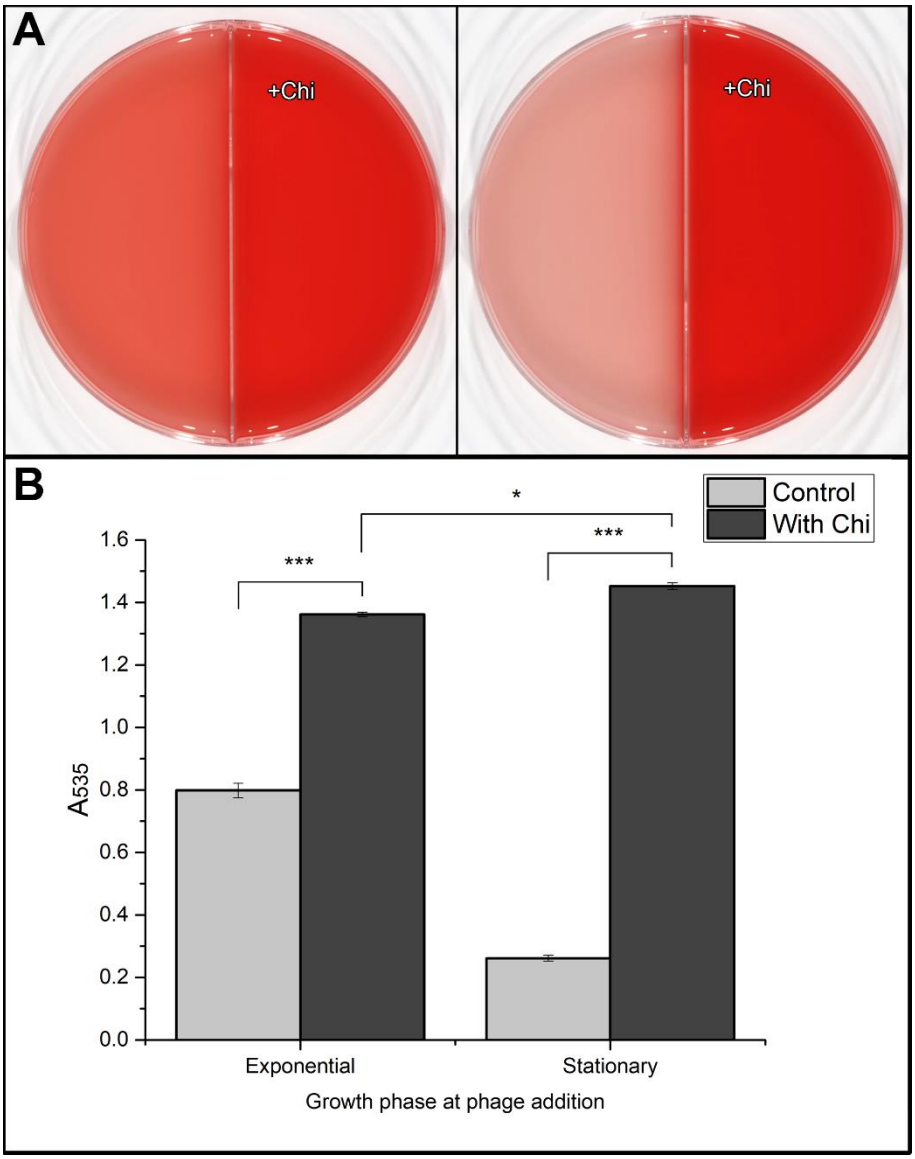


Fig 5.1. (A) Liquid cultures of *S. marcescens* wild type with and without the addition of 0.1 MOI χ phage. After 18 hours of incubation at 25°C with shaking, 10 ml of each culture was pipetted into one half of a split 10 cm petri dish. Plates were imaged with a Cytiva IQ800 instrument. Left, phage was added during exponential phase growth ($OD_{600}$ = 0.5); Right, phage was added during stationary phase growth ($OD_{600}$ = 2.0). (B) Pigmentation in *S. marcescens* wild type cultures as $A_{535}$ quantified via spectrophotometer 18 hours after addition of 0.1 MOI of χ phage to cultures in exponential phase ($OD_{600}$ = 0.5) or stationary phase ($OD_{600}$ = 2.0). Both sets are compared to a control sample without the addition of phage. Data points are mean values consisting of n=3 replicates. Error bars indicate standard deviation. Student's T-Test was used to determine statistical significance. P values are represented by asterisks: *P<0.05; **P<0.01; ***P<0.001.

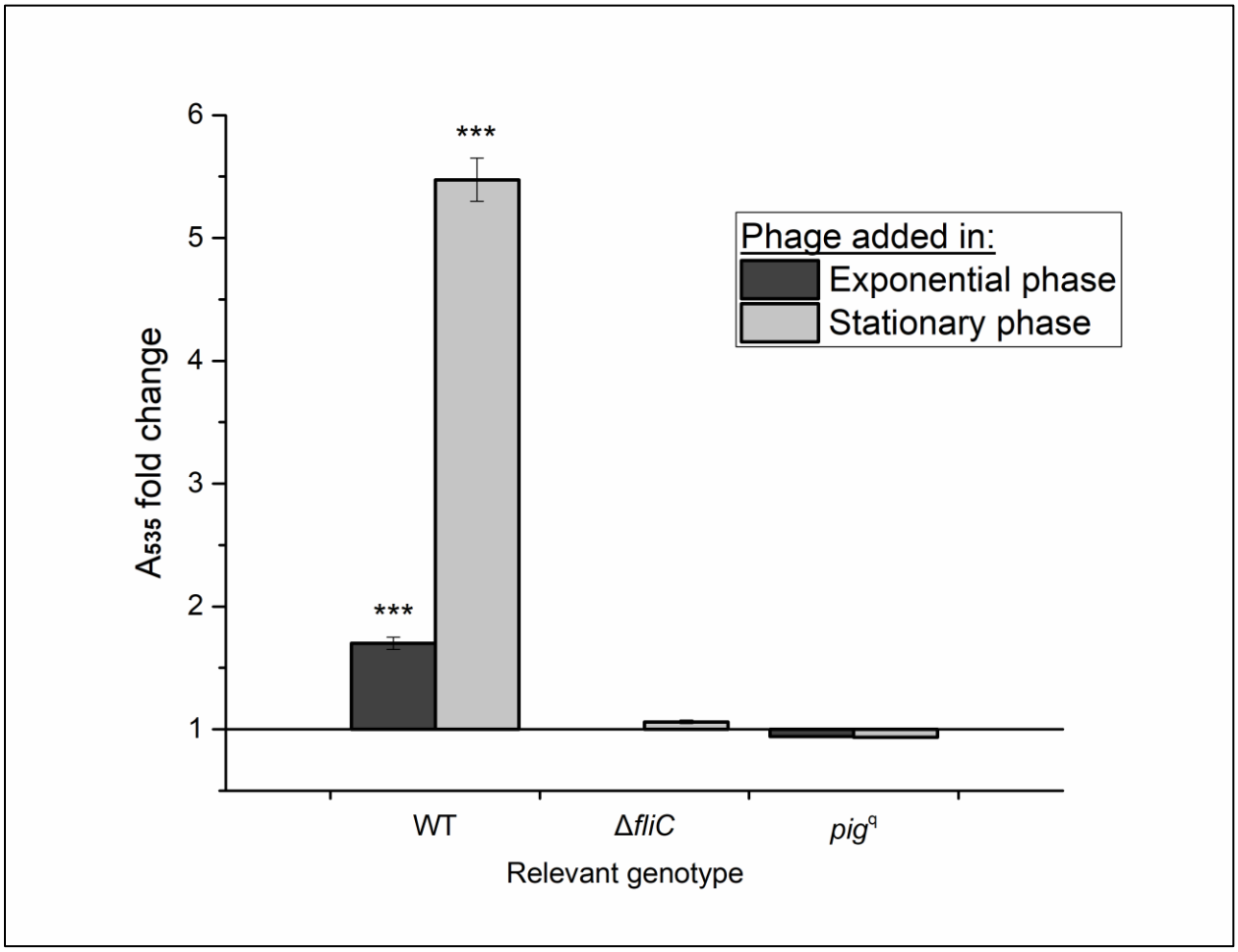


Fig 5.2. Prodigiosin concentration in *S. marcescens* wild-type or mutant cultures represented as fold change in $A_{535}$ between samples with and without the addition of 0.1 MOI of χ phage in exponential phase ($OD_{600}$ = 0.5) or stationary phase ($OD_{600}$ = 2.0). All samples were measured via spectrophotometer 18 hours after the addition of phage. Data points are mean values consisting of n=3 replicates. Error bars indicate standard deviation. Student's T-Test was used to determine statistical significance. Asterisks indicate that differences between the samples with and without phage are statistically significant. P values are represented as follows: *P<0.05; **P<0.01; ***P<0.001.

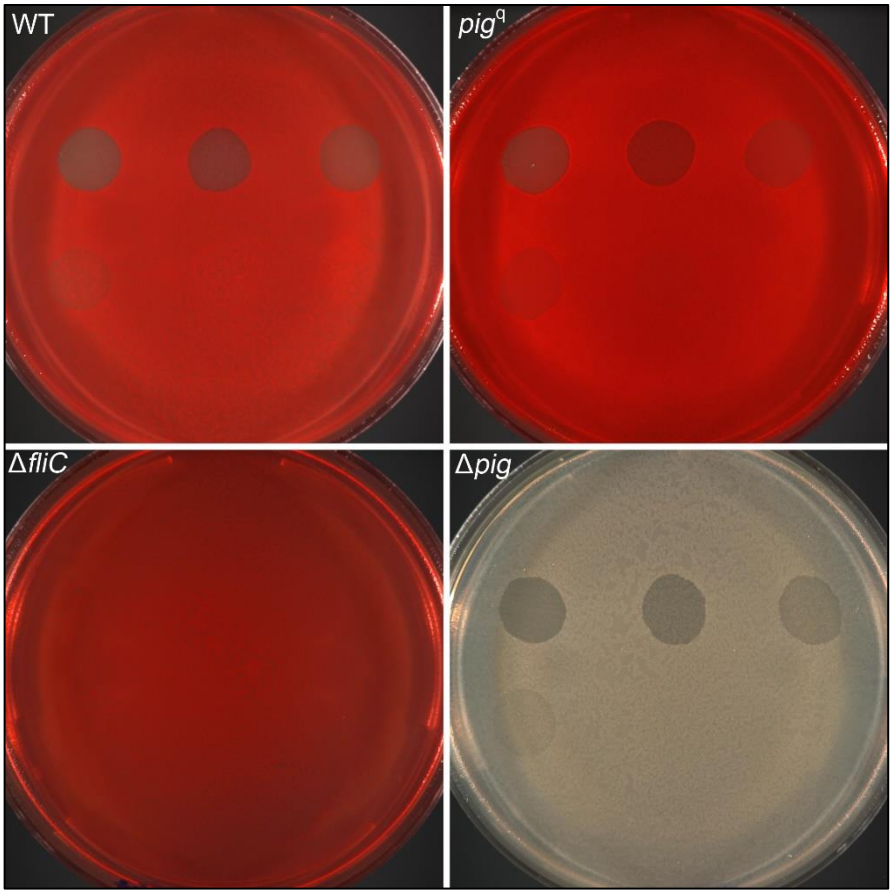


Fig 5.3. Semi-quantitative phage spot assays for determination of phage susceptibility. *S. marcescens* strains were grown in LB to an $OD_{600}$ of 1.0, mixed with molten LB with 0.5% agar, and poured on an LB 1.5% agar plate. Phage χ dilutions in 0.85% NaCl were spotted on the solidified agar surface, and plates were incubated at 25°C overnight and imaged using a Cytiva IQ800 instrument. Zones of clearing indicate lysis and thus χ susceptibility. Dilutions are as follows: top row left to right: $10^{0}$, $10^{-1}$, $10^{-2}$; bottom row left to right: $10^{-4}$, $10^{-5}$, $10^{-6}$.

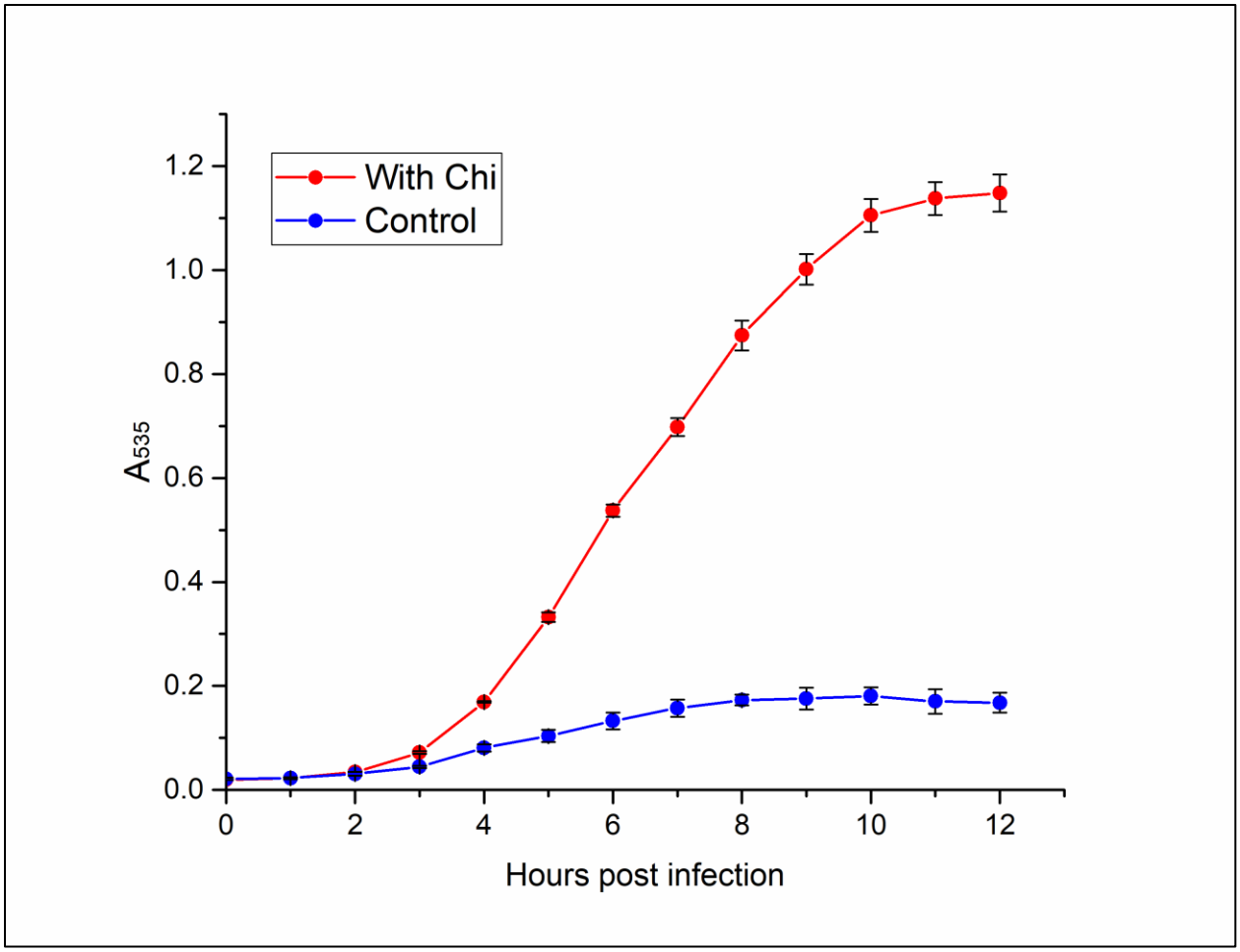


Fig 5.4. Prodigiosin concentration in *S. marcescens* wild type cultures over time after addition of 0.1 MOI χ phage at stationary phase ($OD_{600}$ = 2.0). Values are given as $A_{535}$ measured using a spectrophotometer, which represents prodigiosin concentration in cultures. No phage was added to the control samples. Data points are mean values consisting of n=3 replicates. Error bars indicate standard deviation. Student's T-Test was used to determine statistical significance. The difference in $A_{535}$ between the samples with and without χ is statistically significant ($P<0.05$) at all timepoints 3-12 hours after addition of phage.

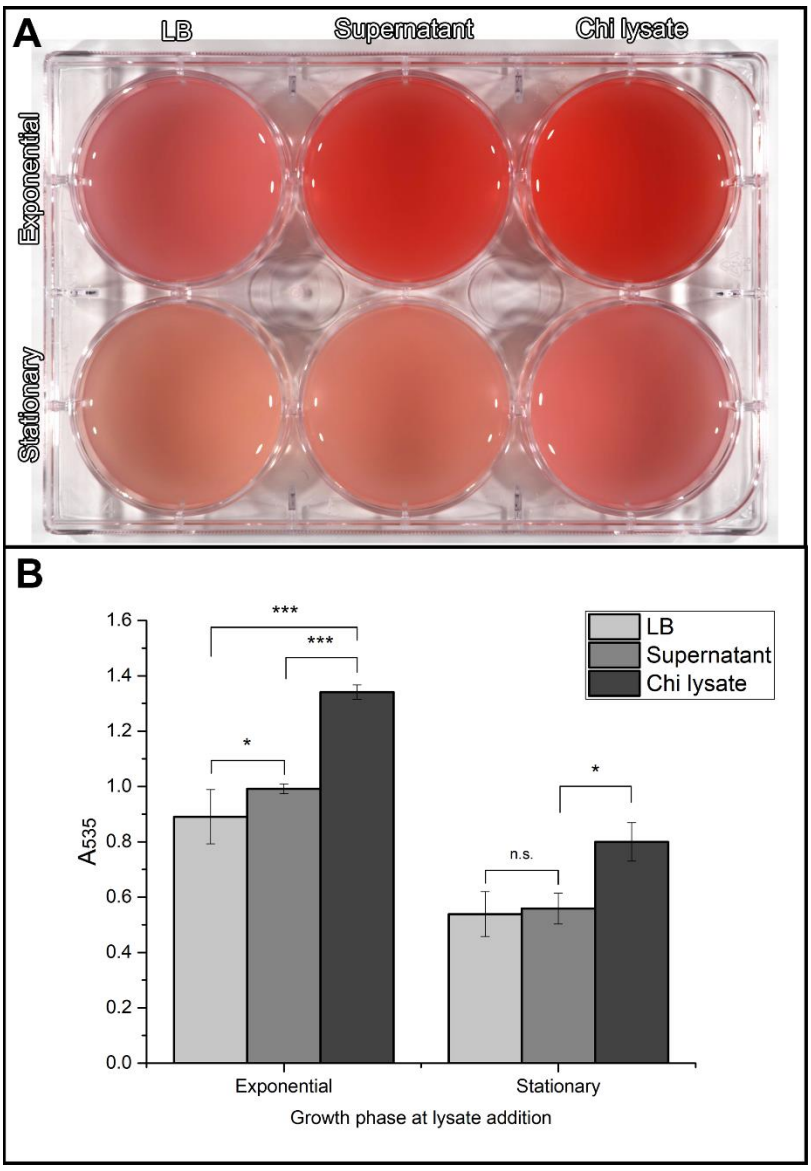


Fig 5.5. (A) Plates of *S. marcescens* Δ*fliC* liquid cultures with added χ phage lysate, Δ*pig* cell supernatant, or fresh LB medium at a ratio of 1:1. After 18 hours of incubation at 25°C with shaking, 5 ml of each culture was pipetted into one well of a 6-well rectangular plate. Plates were imaged with a Cytiva IQ800 instrument. (B) Pigmentation in *S. marcescens* Δ*fliC* cultures as $A_{535}$ quantified via spectrophotometer 18 hours after addition of a χ phage lysate, Δ*pig* cell supernatant, or fresh LB medium to cultures in exponential phase ($OD_{600}$ = 0.5) or stationary phase ($OD_{600}$ = 2.0). Data points are mean values consisting of three replicates. Error bars indicate standard deviation. Student's T-Test was used to determine statistical significance. P values are represented by asterisks: *P<0.05; **P<0.01; ***P<0.001.

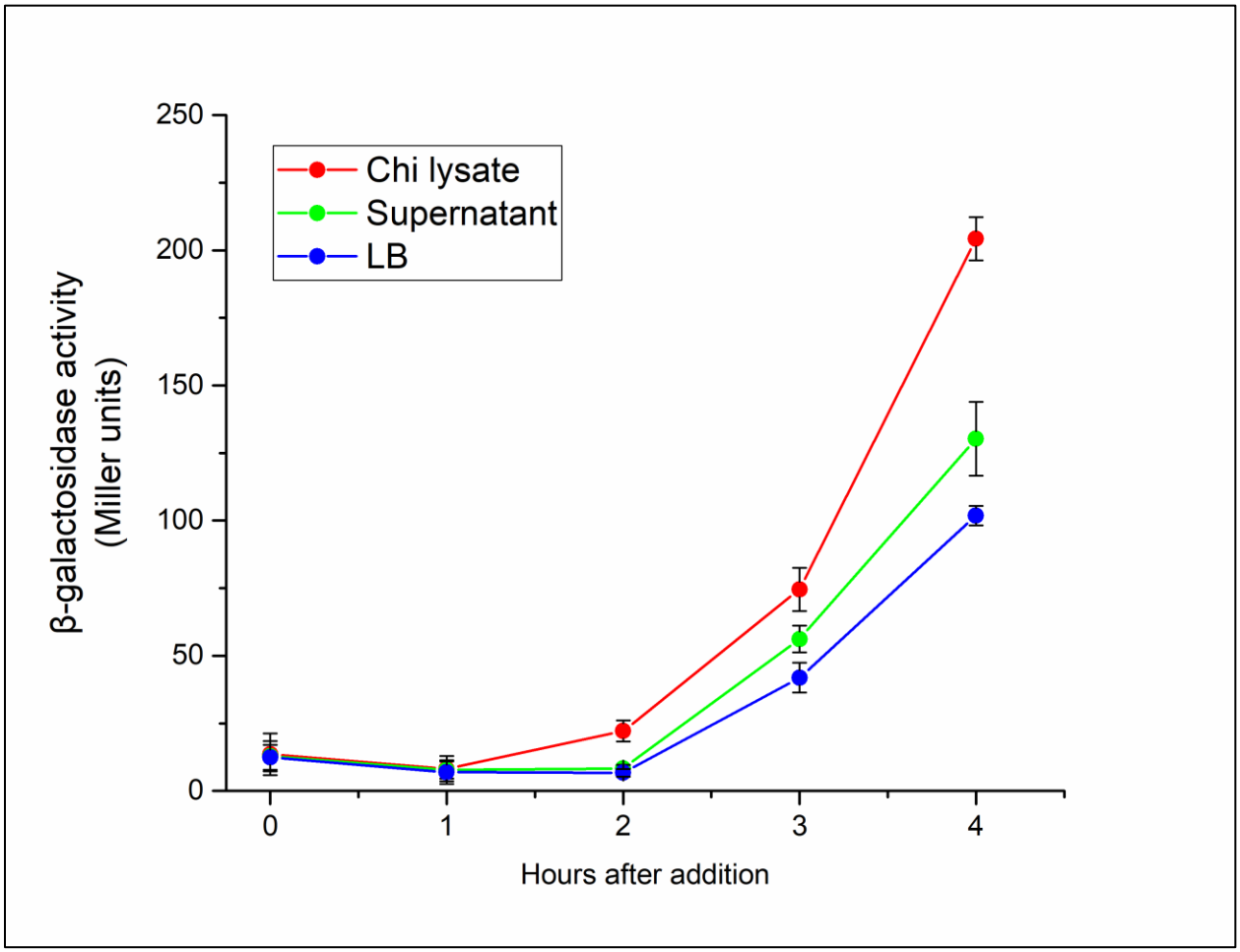


Fig 5.6. Graph of β-galactosidase activity in Miller units measured at 1-hour timepoints after the addition of a χ phage lysate, *S. marcescens* Δ*pig* cell supernatant, or fresh LB medium to an exponential-phase culture of *S. marcescens pig-lacZ* at a ratio of 1:1. Data points are a mean of n=3 replicates, and error bars represent standard deviation. Student's T-Test was used to determine statistical significance. The difference between χ phage lysate and LB control samples is statistically significant ($P<0.05$) 2, 3, and 4 hours after addition of lysate. The difference between cell supernatant and LB control samples is statistically significant ($P<0.05$) 3 and 4 hours after addition.

Chapter VI

# Final Discussion

Nathaniel C. Esteves and Birgit E. Scharf

Virginia Polytechnic Institute and State University, Blacksburg, VA 24061

The three known hosts for χ phage are all organisms of clinical significance. *Salmonella enterica* is a widespread species of enteric pathogens [1, 2], with some serotypes capable of causing typhoid fever [3, 4], a potentially lethal illness that is common in developing countries. Non-typhoidal *Salmonella* serotypes are the leading cause of bacterial gastroenteritis [2, 5], a common problem in both developing and developed countries. While most laboratory strains of *Escherichia coli* are non-pathogenic, highly virulent strains of this species cause widespread illness in humans [6, 7]. In particular, Shiga-toxigenic *E. coli* (STEC) strains like the well-known O157:H7 cause hemorrhagic gastroenteritis due to the production of the Shiga toxin from *Shigella* [6, 8]. The fact that both of these species are foodborne pathogens indicates that χ may be beneficial in a foodservice setting, where phage-based products are already used to prevent bacterial growth on surfaces [9, 10]. *Serratia marcescens* is not generally a foodborne pathogen and does not infect immunocompetent individuals, but can be deadly in the immunocompromised [11]. This organism is commonly multidrug-resistant (MDR) [12] and produces robust biofilms [13]. Phages have been proposed and found to be effective in overcoming biofilms [14, 15] and antibiotic resistance [16, 17]. As χ is an effective predator of *S. marcescens* [18], it could likely be used as a treatment against biofilm-associated infections. Lastly, although χ has only been shown to infect these three bacterial species, the significant differences between them suggest the possibility that χ may infect other species as well. There are undoubtedly many Enterobacterales species that have never been tested for χ susceptibility. As χ phage approaches a century of study, having been discovered in the early 1930s by Sertic and Boulgakov in the laboratory of Felix d'Herelle [19], one can reflect on the relative lack of understanding of this phage system. In-depth research on χ did not begin until the early 1960s

[20] and has been quite sporadic since then. Throughout our research [21-23], many of these unexplored facets of bacteriophage χ, flagellar motility, and interactions between these two systems were explored. While little was previously known about the χ infection cycle past the nut-and-bolt theory of χ moving along the flagellar filament, this is no longer the case. The fact that χ interacts with the multi-substrate efflux system AcrABZ-TolC lends to its potential for future clinical applications [21, 24]. It is likely that a χ host that represses expression of AcrABZ-TolC to avoid χ infection would be increasing its own susceptibility to the pump's substrates. In other phage systems, such as phage OMKO1 of *Pseudomonas aeruginosa*, a similar tradeoff has been explored [16, 25]. An antibiotic efflux system is required for infection of *P. aeruginosa* by OMKO1, and co-administration of antibiotics and this phage resulted in a strong synergistic effect [25]. Similar synergy may be possible with co-administration of χ and an antibiotic substrate of AcrABZ-TolC [26], such as erythromycin, tetracycline, or chloramphenicol. In addition to *S. enterica*, AcrABZ-TolC is also present in the χ host *E. coli* [27], and a homolog named SdeXY is present in *S. marcescens* [28] and is partially responsible for the extensive MDR of this species. This further lends χ to clinical applications against all its known hosts.

Previously, it was only understood that χ binds to flagella and reaches the cell surface due to flagellar rotation [29, 30], but a precise mechanism for binding was not known. Through our research, we have determined through multiple approaches that χ interacts with the D2 domains of *S*. Typhimurium flagellin FliC, and that the structure of these domains determines host range [22]. While the genetic screen in Chapter III was unable to determine reaction partners more specifically than the D2 domains, crosslinking-mass spectrometry outlined in Chapter IV was successful in putatively identifying specific residues participating in interactions, the majority of

which were found in the C-terminal D2 domain. This experiment simultaneously identified gp31, the CHI_31 gene product [31], as the χ receptor binding protein (RBP). After identifying the importance of gp31, we purified this protein to investigate it further. To our knowledge, this represented the first successful purification of a recombinant χ protein. This is an important accomplishment, as the χ genome contains 75 open reading frames, the gene products of which are largely uncharacterized [31]. As the construction of targeted deletions in a virulent phage is much more difficult than in temperate phages and requires a somewhat complex CRISPR-Cas method [32] or in vitro assembly of the phage genome [33], recombinant expression and purification of these proteins may be a more straightforward method of characterization.

The host range of χ can be thought of as simultaneously broad and specific. Despite infecting three separate bacterial genera [18, 20, 29], we have demonstrated that certain *S. enterica* serotypes are resistant due in large part to the structure of their flagellins [22]. This coupled with our findings that the χ tail fiber protein gp31 directly interacts with the flagellum indicates that modification of the tail fiber protein could allow for tailoring of the χ host range. It has been shown in other phage systems that mutagenesis of phage RBPs or construction of chimeric RBPs can be used to modify host range [34, 35]. Targeted phage treatments could avoid disruption of the natural bacterial flora, an issue that can arise during the usage of broad-spectrum antibiotics [36].

Undoubtedly, many transcriptional changes occur within χ-infected cells and in their surroundings. The vibrant pigmentation phenotype we observed in *S. marcescens* seemingly represents a visible consequence of these transcriptional changes. It is likely that transcriptional changes occur in the other χ hosts, which simply lack a visible response. This represents another important facet of χ-host interactions: the ways the host cells respond to infection or lysis. The

concept of the evolutionary arms race between phages and their host bacteria is of great interest and importance for real-world applications [37, 38].

Many important directions for future studies still remain for investigation of χ-host interactions. The specific role of AcrABZ-TolC in χ infection is unknown [21]. We have considered several possible hypotheses: (i) AcrABZ-TolC acts as a cell surface receptor and DNA channel for χ, (ii) AcrB exports an endolysin or small molecule into the periplasm that χ uses to initiate lysis, or (iii) *S.* Typhimurium produces a toxin or toxic metabolite that is normally exported by AcrABZ-TolC and is toxic to χ in the absence of effective efflux. Constructing AcrB point mutations could help explain which hypothesis is correct. If pump function is not required for the role of AcrB in the χ lifecycle, this would be strong evidence against hypotheses (ii) and (iii), both of which should require functional pumps. For AcrABZ-TolC to be an effective cell surface receptor, it might be required to localize near flagellar basal bodies. AcrB and the flagellar basal body could be fluorescently tagged to determine if co-localization occurs. This would potentially support hypothesis (i), as the other two hypotheses would not benefit from co-localization. Hypothesis (iii) could be supported by metabolomic data. Mass spectrometry (MS) could be used to determine any metabolites or toxins that accumulate in an *acrB* deletion strain compared to wild type. The toxic effects of these compounds on χ would then be explored. MS could also be used to determine whether a phage endolysin or similar molecules remain in the cytoplasm in a Δ*acrB* background during active infection, supporting hypothesis (ii).

Our screen also identified the gene *tig*, encoding the molecular chaperone trigger factor [39], as being nearly essential for χ infection [21]. A *tig* deletion mutant exhibits a greater than 99% reduction in plating efficiency, a considerable effect on χ susceptibility. While we hypothesize that trigger factor is involved in proper folding of χ proteins, we do not have direct evidence of

this. However, trigger factor has been shown to be involved in folding of the protein gp20 from phage T4 [40], so similar involvement in the χ lifecycle is a reasonable hypothesis. Exploring this interaction further would increase knowledge of the later stages of the χ lifecycle, when new phage virions are assembled within the cell. Understanding the full lifecycle from flagellar binding to lysis is important for many clinical applications.

Our identification of the importance of the D2 domains in determining χ susceptibility, and the CL-MS data indicating a direct interaction between χ gp31 and CTD2 leads to several logical next steps for experimentation. Similar experiments to those already conducted on FliC could be applied to the phase 2 flagellin FljB [41], to see if the interaction with CTD2 is conserved. Experiments could also be conducted in a $FliB^{+}$ background [42], providing information about the impact of flagellin methylation and how it may alter gp31-flagellin binding. The genetic screen conducted in Chapter III could be continued to further narrow down the regions determining susceptibility. Instead of deleting or altering domains, the entire flagellin *fliC* gene could be mutagenized using one or more random mutagenesis techniques such as chemical mutagenesis [43], error-prone PCR [44], or an *E. coli* mutator strain [45]. Another interesting observation is that expression of a host flagellin in the non-host serotype Enteritidis does not result in a susceptible phenotype [22]. This implies that one or more other factors dictate χ susceptibility. Because of the high level of sequence conservation [22] among flagellar proteins other than flagellin, as well as AcrABZ-TolC, it is likely that the relationship between these other factors and χ is as of yet undiscovered.

To further the future clinical applications of χ, a necessary research direction is in vivo experimentation. Thankfully, many animal models exist for studying phage therapy, and for bacterial infections by pathogens such as *Salmonella*. These include mouse models [46, 47],

*Caenorhabditis elegans* [48], and *Galleria mellonella* [49]. Many of these experiments would be relatively straightforward and could be as simple as determining whether χ is capable of clearing a *Salmonella* infection in one of these model organisms. *Salmonella* Typhimurium is a non-typhoidal serotype in humans, but causes a typhoid-like illness in mice [46], which makes it an effective model for treatment of *Salmonella* Typhi in humans, arguably the most clinically relevant *Salmonella* serotype. Mouse models also exist for *S. marcescens* pneumonia [50] and intraperitoneal infections [51], as well as for pathogenic *E. coli* strains including O157:H7 [52, 53]. Synergistic effects with antibiotics or other phages should also be studied, such as by co-administering χ with a known AcrABZ-TolC substrate antibiotic in an animal model. A therapeutic phage treatment often consists of a cocktail, a mixture of multiple phages typically with different infection pathways, which avoids the issue of development of phage resistance [15, 54]. Bacteriophage χ could be included in a cocktail of other phages that infect via cellular components other than flagella for particularly potent therapy. The logical first step would be to test the effectiveness of χ in a cocktail in an animal model, with the ultimate goal of usage in human patients. The effect of the motility-virulence evolutionary tradeoff also warrants investigation, such as by determining whether exposure to χ reduces virulence in *S. enterica*. Overall, while this research has significantly advanced the field of flagellotropic phages, interactions with the flagellar motility system, and knowledge about a phage with potential clinical applications, considerably more research is required before the proposed applications can be realized. Additionally, many roadblocks exist for the overall usage of phage therapy, including FDA approval and lack of human clinical trials [9, 55, 56]. For this reason, foodservice applications of χ may be more likely to be accomplished in the near future. Products such as ListShield™, a phage-based product for protection against *Listeria*, have paved the way for

novel phage treatments in the food industry [9]. The fact that χ infects two known foodborne pathogens would make it an excellent candidate for inclusion in a phage cocktail.

Overall, bacteriophage χ is a virus with a unique lifecycle, requiring flagellar motility for infection. This factor, and the fact that an antibiotic resistance mechanism is also required for infection, indicates that χ may be of particular interest for phage therapy, the use of the viruses of bacteria as antibacterial treatments. As we approach a post-antibiotic era, phage therapy, including with χ, is an important topic of research. Therefore, the described research has made several important discoveries in the field of χ, but significant work remains before the applications of this phage can be realized.

REFERENCES


1. De Cesare, A., *Salmonella* in Foods: A Reemerging Problem. *Adv Food Nutr Res*, **2018**. 86: p. 137-179.
2. Jajere, S.M., A Review of *Salmonella Enterica* with Particular Focus on the Pathogenicity and Virulence Factors, Host Specificity and Antimicrobial Resistance Including Multidrug Resistance. *Vet World*, **2019**. 12(4): p. 504-521.
3. Marchello, C.S.; Hong, C.Y.; and Crump, J.A., Global Typhoid Fever Incidence: A Systematic Review and Meta-Analysis. *Clin Infect Dis*, **2019**. 68(Suppl 2): p. S105-s116.
4. Zaki, S.A. and Karande, S., Multidrug-Resistant Typhoid Fever: A Review. *J Infect Dev Ctries*, **2011**. 5(5): p. 324-37.
5. Majowicz, S.E.; Musto, J.; Scallan, E.; Angulo, F.J.; Kirk, M.; O'Brien, S.J.; Jones, T.F.; Fazil, A.; and Hoekstra, R.M., The Global Burden of Nontyphoidal *Salmonella* Gastroenteritis. *Clin Infect Dis*, **2010**. 50(6): p. 882-9.
6. Wachsmuth, I.K.; Griffin, P.M.; and Wells, J.G., *Escherichia Coli* O157:H7, a Cause of Hemorrhagic Colitis and Hemolytic Uremic Syndrome. *Acta Paediatr Jpn*, **1991**. 33(5): p. 603-12.
7. Croxen, M.A. and Finlay, B.B., Molecular Mechanisms of Escherichia Coli Pathogenicity. *Nat Rev Microbiol*, **2010**. 8(1): p. 26-38.
8. Newell, D.G. and La Ragione, R.M., Enterohaemorrhagic and Other Shiga Toxin-Producing Escherichia Coli (Stec): Where Are We Now Regarding Diagnostics and Control Strategies? *Transbound Emerg Dis*, **2018**. 65 Suppl 1: p. 49-71.
9. Sarhan, W.A. and Azzazy, H.M., Phage Approved in Food, Why Not as a Therapeutic? *Expert Rev Anti Infect Ther*, **2015**. 13(1): p. 91-101.
10. Sillankorva, S.M.; Oliveira, H.; and Azeredo, J., Bacteriophages and Their Role in Food Safety. *International journal of microbiology*, **2012**. 2012: p. 863945-863945.

11. Hejazi, A. and Falkiner, F.R., *Serratia Marcescens. J Med Microbiol*, **1997**. 46(11): p. 903-912.
12. Zivkovic Zaric, R.; Zaric, M.; Sekulic, M.; Zornic, N.; Nesic, J.; Rosic, V.; Vulovic, T.; Spasic, M.; Vuleta, M.; Jovanovic, J., et al., Antimicrobial Treatment of *Serratia Marcescens* Invasive Infections: Systematic Review. *Antibiotics (Basel)*, **2023**. 12(2).
13. Ray, C.; Shenoy, A.T.; Orihuela, C.J.; and González-Juarbe, N., Killing of *Serratia Marcescens* Biofilms with Chloramphenicol. *Ann Clin Microbiol Antimicrob*, **2017**. 16(1): p. 19.
14. Ferriol-González, C. and Domingo-Calap, P., Phages for Biofilm Removal. *Antibiotics (Basel)*, **2020**. 9(5).
15. Maszewska, A.; Zygmunt, M.; Grzejdziak, I.; and Różalski, A., Use of Polyvalent Bacteriophages to Combat Biofilm of Proteus Mirabilis Causing Catheter-Associated Urinary Tract Infections. *J Appl Microbiol*, **2018**. 125(5): p. 1253-1265.
16. Chan, B.K.; Sistrom, M.; Wertz, J.E.; Kortright, K.E.; Narayan, D.; and Turner, P.E., Phage Selection Restores Antibiotic Sensitivity in Mdr *Pseudomonas Aeruginosa*. *Sci Rep*, **2016**. 6: p. 26717-26717.
17. Kortright, K.E.; Chan, B.K.; Koff, J.L.; and Turner, P.E., Phage Therapy: A Renewed Approach to Combat Antibiotic-Resistant Bacteria. *Cell Host Microbe*, **2019**. 25(2): p. 219-232.
18. Iino, T. and Mitani, M., Infection of *Serratia Marcescens* by Bacteriophage Chi. *J Virol*, **1967**. 1(2): p. 445-447.
19. Sertić, V. and Boulgakov, N.A. *Bacteriophages Specific for Flagellated Forms of Bacteria*. 1936.
20. MEYNELL, E.W., A Phage, *Øχ*, Which Attacks Motile Bacteria. *Microbiology*, **1961**. 25(2): p. 253-290.
21. Esteves, N.C.; Porwollik, S.; McClelland, M.; and Scharf, B.E., The Multi-Drug Efflux System Acrabz-Tolc Is Essential for Infection of *Salmonella* Typhimurium by the Flagellum-Dependent Bacteriophage Chi. *J Virol*, **2021**. 95(11).
22. Esteves, N.C.; Bigham, D.N.; and Scharf, B.E., Phages on Filaments: A Genetic Screen Elucidates the Complex Interactions between *Salmonella Enterica* Flagellin and Bacteriophage Chi. *PLoS Pathog*, **2023**. 19(8): p. e1011537.
23. Li, X.; Gonzalez, F.; Esteves, N.; Scharf, B.E.; and Chen, J., Formation of Phage Lysis Patterns and Implications on Co-Propagation of Phages and Motile Host Bacteria. *PLOS Computational Biology*, **2020**. 16(3): p. e1007236.
24. Esteves, N.C. and Scharf, B.E., Flagellotropic Bacteriophages: Opportunities and Challenges for Antimicrobial Applications. *Int J Mol Sci*, **2022**. 23(13).
25. Chan, B.K.; Turner, P.E.; Kim, S.; Mojibian, H.R.; Elefteriades, J.A.; and Narayan, D., Phage Treatment of an Aortic Graft Infected with Pseudomonas Aeruginosa. *Evolution, Medicine, and Public Health*, **2018**. 2018(1): p. 60-66.
26. Kobylka, J.; Kuth, M.S.; Müller, R.T.; Geertsma, E.R.; and Pos, K.M., Acrb: A Mean, Keen, Drug Efflux Machine. *Annals of the New York Academy of Sciences*, **2020**. 1459(1): p. 38-68.
27. Chowdhury, N.; Suhani, S.; Purkaystha, A.; Begum, M.K.; Raihan, T.; Alam, M.J.; Islam, K.; and Azad, A.K., Identification of Acrab-Tolc Efflux Pump Genes and Detection of Mutation in Efflux Repressor Acrr from Omeprazole Responsive Multidrug-

Resistant Escherichia Coli Isolates Causing Urinary Tract Infections. *Microbiol Insights*, **2019**. 12: p. 1178636119889629.
28. Chen, J.; Kuroda, T.; Huda, M.N.; Mizushima, T.; and Tsuchiya, T., An Rnd-Type Multidrug Efflux Pump Sdexy from Serratia Marcescens. *J Antimicrob Chemother*, **2003**. 52(2): p. 176-9.
29. Schade, S.Z.; Adler, J.; and Ris, H., How Bacteriophage X Attacks Motile Bacteria. *J Virol*, **1967**. 1(3): p. 599.
30. Samuel, A.D.; Pitta, T.P.; Ryu, W.S.; Danese, P.N.; Leung, E.C.; and Berg, H.C., Flagellar Determinants of Bacterial Sensitivity to Chi-Phage. *Proc Natl Acad Sci U S A*, **1999**. 96(17): p. 9863-9866.
31. Hendrix, R.W.; Ko, C.-C.; Jacobs-Sera, D.; Hatfull, G.F.; Erhardt, M.; Hughes, K.T.; and Casjens, S.R., Genome Sequence of *Salmonella* Phage X. *Genome Announc*, **2015**. 3(1): p. e01229-14.
32. Lemay, M.L.; Renaud, A.C.; Rousseau, G.M.; and Moineau, S., Targeted Genome Editing of Virulent Phages Using Crispr-Cas9. *Bio Protoc*, **2018**. 8(1): p. e2674.
33. Pulkkinen, E.M.; Hinkley, T.C.; and Nugen, S.R., Utilizing in Vitro DNA Assembly to Engineer a Synthetic T7 Nanoluc Reporter Phage for Escherichia Coli Detection. *Integr Biol (Camb)*, **2019**. 11(3): p. 63-68.
34. Dunne, M.; Prokhorov, N.S.; Loessner, M.J.; and Leiman, P.G., Reprogramming Bacteriophage Host Range: Design Principles and Strategies for Engineering Receptor Binding Proteins. *Curr Opin Biotechnol*, **2021**. 68: p. 272-281.
35. Dunne, M.; Rupf, B.; Tala, M.; Qabrati, X.; Ernst, P.; Shen, Y.; Sumrall, E.; Heeb, L.; Plückthun, A.; Loessner, M.J., et al., Reprogramming Bacteriophage Host Range through Structure-Guided Design of Chimeric Receptor Binding Proteins. *Cell Rep*, **2019**. 29(5): p. 1336-1350.e4.
36. Yang, J.J.; Wang, J.T.; Cheng, A.; Chuang, Y.C.; and Sheng, W.H., Impact of Broad-Spectrum Antimicrobial Treatment on the Ecology of Intestinal Flora. *J Microbiol Immunol Infect*, **2018**. 51(5): p. 681-687.
37. Stern, A. and Sorek, R., The Phage-Host Arms Race: Shaping the Evolution of Microbes. *Bioessays*, **2011**. 33(1): p. 43-51.
38. Hampton, H.G.; Watson, B.N.J.; and Fineran, P.C., The Arms Race between Bacteria and Their Phage Foes. *Nature*, **2020**. 577(7790): p. 327-336.
39. Haldar, S.; Tapia-Rojo, R.; Eckels, E.C.; Valle-Orero, J.; and Fernandez, J.M., Trigger Factor Chaperone Acts as a Mechanical Foldase. *Nature Communications*, **2017**. 8(1): p. 668.
40. Quinten, T.A. and Kuhn, A., Membrane Interaction of the Portal Protein Gp20 of Bacteriophage T4. *J Virol*, **2012**. 86(20): p. 11107-14.
41. Bonifield, H.R. and Hughes, K.T., Flagellar Phase Variation in *Salmonella Enterica* Is Mediated by a Posttranscriptional Control Mechanism. *J Bacteriol*, **2003**. 185(12): p. 3567-3574.
42. Wang, C.; Nehls, C.; Baabe, D.; Burghaus, O.; Hurwitz, R.; Gutsmann, T.; Bröring, M.; and Kolbe, M., Flagellin Lysine Methyltransferase Flib Catalyzes a [4fe-4s] Mediated Methyl Transfer Reaction. *PLOS Pathog*, **2021**. 17(11): p. e1010052.
43. Pietrzykowska, I.; Krych, M.; and Shugar, D., Mutagenesis Induced by 5-Bromouracil and Methyl Methane Sulfonate: Role of DNA Polymerase I. *Acta Biochim Pol*, **1984**. 31(1): p. 65-75.

44. Wilson, D.S. and Keefe, A.D., Random Mutagenesis by Pcr. *Curr Protoc Mol Biol*, **2001**. Chapter 8: p. Unit8.3.
45. Muteeb, G. and Sen, R., Random Mutagenesis Using a Mutator Strain. *Methods Mol Biol*, **2010**. 634: p. 411-9.
46. Chattopadhyay, A.; Joseph, J.P.; Shyam, S.; and Nandi, D., Characterizing Salmonella Typhimurium-Induced Septic Peritonitis in Mice. *J Vis Exp*, **2022**(185).
47. Wang-Kan, X.; Blair, J.M.A.; Chirullo, B.; Betts, J.; La Ragione, R.M.; Ivens, A.; Ricci, V.; Opperman, T.J.; and Piddock, L.J.V., Lack of Acrb Efflux Function Confers Loss of Virulence on *Salmonella Enterica* Serovar Typhimurium. *mBio*, **2017**. 8(4).
48. Manohar, P.; Loh, B.; Elangovan, N.; Loganathan, A.; Nachimuthu, R.; and Leptihn, S., A Multiwell-Plate Caenorhabditis Elegans Assay for Assessing the Therapeutic Potential of Bacteriophages against Clinical Pathogens. *Microbiol Spectr*, **2022**. 10(1): p. e0139321.
49. Tsai, C.J.; Loh, J.M.; and Proft, T., Galleria Mellonella Infection Models for the Study of Bacterial Diseases and for Antimicrobial Drug Testing. *Virulence*, **2016**. 7(3): p. 214-29.
50. González-Juarbe, N.; Mares, C.A.; Hinojosa, C.A.; Medina, J.L.; Cantwell, A.; Dube, P.H.; Orihuela, C.J.; and Bergman, M.A., Requirement for Serratia Marcescens Cytolysin in a Murine Model of Hemorrhagic Pneumonia. *Infect Immun*, **2015**. 83(2): p. 614-24.
51. Hegazy, W.A.H.; Khayat, M.T.; Ibrahim, T.S.; Youns, M.; Mosbah, R.; and Soliman, W.E., Repurposing of Antidiabetics as Serratia Marcescens Virulence Inhibitors. *Braz J Microbiol*, **2021**. 52(2): p. 627-638.
52. Tontanahal, A.; Sperandio, V.; Kovbasnjuk, O.; Loos, S.; Kristoffersson, A.C.; Karpman, D.; and Arvidsson, I., Igg Binds Escherichia Coli Serine Protease Espp and Protects Mice from E. Coli O157:H7 Infection. *Front Immunol*, **2022**. 13: p. 807959.
53. Bernal, A.M.; Sosa, F.N.; Todero, M.F.; Montagna, D.R.; Vermeulen, M.E.; Fernández-Brando, R.J.; Ramos, M.V.; Errea, A.J.; Rumbo, M.; and Palermo, M.S., Nasal Immunization with H7 Flagellin Protects Mice against Hemolytic Uremic Syndrome Secondary to Escherichia Coli O157:H7 Gastrointestinal Infection. *Front Cell Infect Microbiol*, **2023**. 13: p. 1143918.
54. Chan, B.K. and Abedon, S.T., Phage Therapy Pharmacology Phage Cocktails. *Adv Appl Microbiol*, **2012**. 78: p. 1-23.
55. Wu, S.; Zachary, E.; Wells, K.; and Loc-Carrillo, C., Phage Therapy: Future Inquiries. *Postdoc J*, **2013**. 1(6): p. 24-35.
56. Moelling, K.; Broecker, F.; and Willy, C., A Wake-up Call: We Need Phage Therapy Now. *Viruses*, **2018**. 10(12).

# Appendix A
# Supplemental material for Chapter III

S1 Table. Comprehensive list of *Salmonella enterica* serotypes tested for χ phage susceptibility by spot assay, and their typical phase 1 (FliC), phase 2 (FljB), and phase 3 (FlpA) flagellin (H) antigenic formulae, where applicable, as described by literature sources. The symbol (-) indicates the absence of this specific flagellin gene. Formation of a lysis zone when χ was spotted on a bacterial lawn indicated a susceptible phenotype. No lysis zone formation was interpreted as χ resistance. All are serotypes of *Salmonella enterica*; serotypes that are given names are part of subsp. enterica, while serotypes given only antigenic designations are other *S. enterica* subspecies. Non-motile serotypes are not included. Also included are a ser. Enteritidis *fliC* deletion mutant complemented by pFliC1, a ser. Typhimurium FliC monophasic strain, and a ser. Typhimurium FljB monophasic strain.

| **Serotype/antigenic designation** | **Phase 1 H antigen** | **Phase 2 H antigen** | **Phase 3 H antigen** | **Result** |
|---|---|---|---|---|
| Abortusovis | c | 1,6 | - | Resistant |
| Agona | f,g,s | 1,2 | $z_{27}$,$z_{45}$ | Resistant |
| Anatum | e,h | 1,6 | $z_{64}$ | Resistant |
| Bovismorbificans | r,i | 1,5 | R1 | Susceptible |
| Choleraesuis | c | 1,5 | - | Susceptible |
| Enteritidis | g,m | - | - | Resistant |
| Enteritidis Δ*fliC* pFliC1 | i | - | - | Resistant |
| Hadar | $z_{10}$ | e,n,x | - | Susceptible |
| Hartford | y | e,n,x | $z_{67}$ | Resistant |
| Heidelberg | r | 1,2 | - | Resistant |
| Infantis | r | 1,5 | R1,$z_{37}$,$z_{45}$,$z_{49}$ | Susceptible |
| Java | b | 1,2 | $z_5$,$z_{33}$ | Susceptible |
| Javiana | l,$z_{28}$ | 1,5 | R1 | Susceptible |
| Kottbus | e,h | 1,5 | - | Resistant |
| Meleagridis | e,h | l,w | - | Resistant |
| Miami | a | 1,5 | - | Susceptible |
| Michigan | l,v | 1,5 | - | Resistant |
| Montevideo | g,m,p,s | 1,2,7 | - | Resistant |
| Muenchen | d | 1,2 | $z_{67}$ | Resistant |
| Newport | e,h | 1,2 | $z_{67}$,$z_{78}$ | Susceptible |
| Oranienburg | m,t | z57 | - | Resistant |
| Paratyphi B | b | 1,2 | $z_5$,$z_{33}$ | Susceptible |
| Poona | z | 1,6 | $z_{44}$,$z_{59}$ | Susceptible |
| Rubislaw | r | e,n,x | - | Susceptible |
| Saintpaul | e,h | 1,2 | - | Resistant |
| Schwarzengrund | d | 1,7 | - | Susceptible |
| Seftenberg | g,s,t | - | $z_{27}$,$z_{34}$,$z_{37}$,$z_{43}$, $z_{45}$,$z_{46}$,$z_{82}$ | Resistant |
| Stanley | d | 1,2 | - | Susceptible |
| Thompson | k | 1,5 | R1 | Resistant |
| Typhimurium | i | 1,2 | - | Susceptible |
| Typhimurium FliC-ON | i | - | - | Susceptible |
| Typhimurium FljB-ON | - | 1,2 | - | Susceptible |
| Weltevreden | r | z6 | - | Susceptible |
| 3a:41:$z_4$,$z_{23}$:- | $z_4$,$z_{23}$ | - | - | Susceptible |
| 3a:48:$z_4$,$z_{23}$:- | $z_4$,$z_{23}$ | - | - | Susceptible |
| 3b:61:1,v:1,5 | 1,v | 1,5 | - | Susceptible |
| 6:45:a:e,n,x | a | e,n,x | - | Susceptible |
| 6:11:b:e,n,x | b | e,n,x | - | Resistant |
| 2:47:b:1,5 | b | 1,5 | - | Resistant |
| 2:58:d:$z_6$ | d | z6 | - | Resistant |

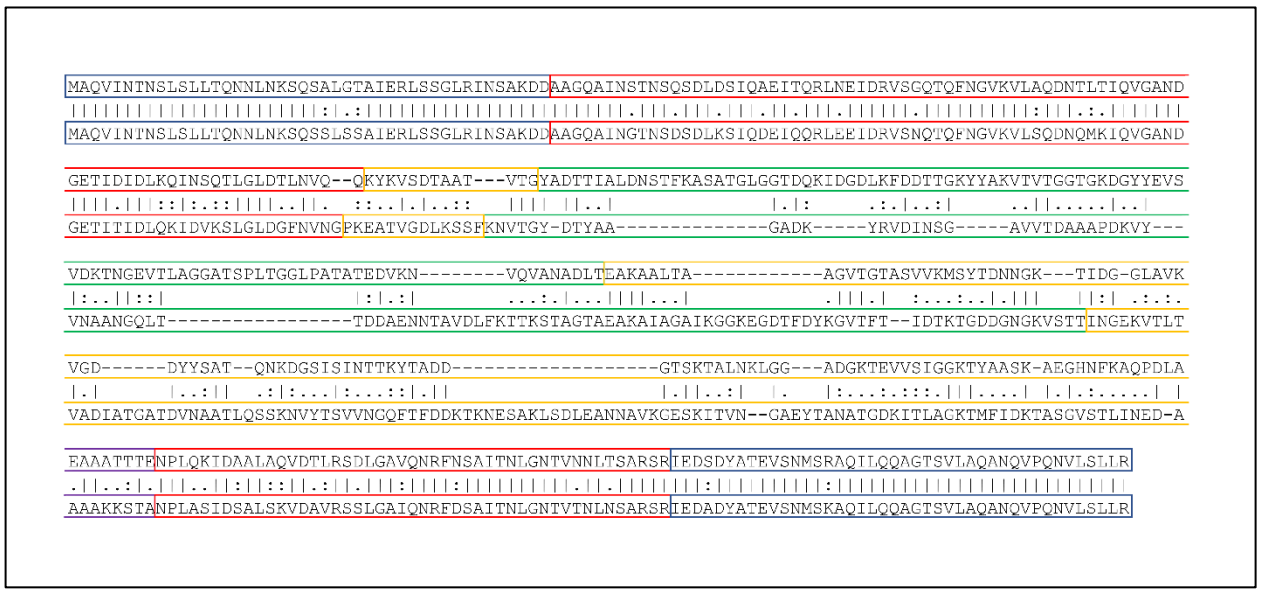


S1 Fig: Amino acid sequence alignment of *Salmonella enterica* flagellin proteins with domains highlighted. Top: ser. Typhimurium flagellin FliC. Bottom: ser. Enteritidis flagellin FliC. D0 domains are highlighted in blue, D1 domains are highlighted in red, D2 domains are highlighted in yellow, and D3 is highlighted in green. Residue numbers, percent identity, and percent similarity are given in Table 3.2. Sequences were aligned using EMBOSS Needleman-Wunsch algorithm.

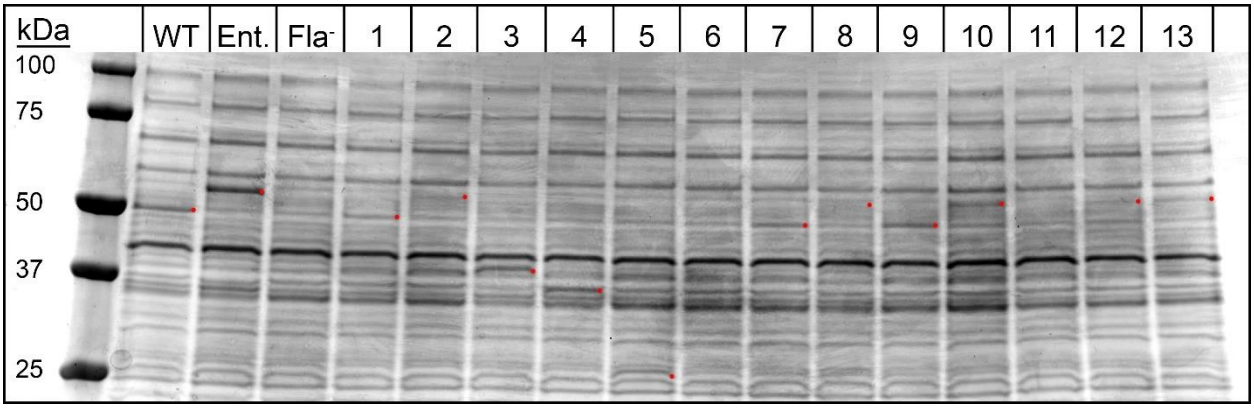


S2 Fig. Coomassie blue-stained denaturing 4-20% polyacrylamide gel of whole cell lysates from pFliC mutants grown to an $OD_{600}$ of 2.0. Ser. Typhimurium 14028s $FliC_{ON}$ Δ*fliB* (chromosomal mutant FliC1) is denoted as "WT." Wild type ser. Enteritidis P125109 is denoted as "Ent." Ser. Typhimurium 14028s Δ*fliC*Δ*fljBA* is denoted as "$Fla^-$." Numbers 1 through 13 refer to the corresponding pFliC plasmid mutants, as described in Fig 1. Bands likely corresponding to flagellin are labelled with a red dot on the rightmost end of the band. Lanes with no marked band do not exhibit a distinct flagellin band or are ambiguous.

## Appendix B
## Full list of strains

Table 1. Strains of *Salmonella enterica*

| Strain number | Serotype | Parental strain | Genotype |
|---|---|---|---|
| NE2001 | Typhimurium | ATCC 14028s | wild type |
| NE2002 | Typhimurium | ATCC 14028s | Δ*fljB* |
| NE2003 | Typhimurium | ATCC 14028s | AcrB F610A |
| NE2004 | Typhimurium | ATCC 14028s | ΔSTM14_0906 (*acrZ*) |
| NE2005 | Typhimurium | ATCC 14028s | Δ*tolC* |
| NE2006 | Typhimurium | ATCC 14028s | Δ*tig* |
| NE2007 | Typhimurium | ATCC 14028s | Δ*acrF* |
| NE2008 | Typhimurium | ATCC 14028s | Δ*fliC* |
| NE2009 | Typhimurium | ATCC 14028s | Δ*acrB* |
| NE2010 | Typhimurium | ATCC 14028s | Δ*acrAB* |
| NE2011 | Typhimurium | ATCC 14028s | *motA*::kan |
| NE2012 | Typhimurium | ATCC 14028s | Δ*acrR* |
| NE2013 | Typhimurium | ATCC 14028s | Δ*gshA* |
| NE2014 | Typhimurium | ATCC 14028s | Δ*ylbA* |
| NE2015 | Typhimurium | ATCC 14028s | Δ*fljBAhin* |
| NE2016 | Typhimurium | ATCC 14028s | Δ*tolC*::tet |
| NE2017 | Typhimurium | ATCC 14028s | FljB-ON |
| NE2018 | Typhimurium | ATCC 14028s | Δ*fliB* |
| NE2019 | Typhimurium | ATCC 14028s | p*fliC*(ΔD3) mot+ mutant |
| NE2020 | Typhimurium | ATCC 14028s | Δ*tig* w/ pTrc99a |
| NE2021 | Typhimurium | ATCC 14028s | Δ*fliL* |
| NE2022 | Typhimurium | ATCC 14028s | Δ*acrB* w/ pKD46 |
| NE2023 | Typhimurium | ATCC 14028s | Δ*tolC* w/pKD46 |
| NE2024 | Typhimurium | JR501 | wild type |
| NE2025 | Typhimurium | JR501 | pKD46 |
| NE2026 | Typhimurium | ATCC 14028s | Δ*acrABtolC* |
| NE2027 | Typhimurium | ATCC 14028s | pWRG730 |
| NE2028 | Typhimurium | ATCC 14028s | Δ*gshB* |
| NE2029 | Typhimurium | ATCC 14028s | Δ*fliB* p*fliB* |
| NE2030 | Typhimurium | ATCC 14028s | Δ*marR* |
| NE2031 | Typhimurium | ATCC 14028s | Δ*fliCfljBA* p*fliC* |
| NE2032 | Typhimurium | ATCC 14028s | Δ*tig* p*tig* |
| NE2033 | Enteritidis | P125109 | wild type |
| NE2034 | Enteritidis | P125109 | Δ*fliB* |
| NE2035 | Typhimurium | VNP20009 | wild type |
| NE2036 | Typhimurium | VNP20009 | CheY+ pKD46 |
| NE2037 | Typhimurium | ATCC 14028s | Δ*fliC*Δ*fljBA* |

| | | | |
|---|---|---|---|
| NE2038 | Typhimurium | ATCC 14028s | Δ*fis* |
| NE2039 | Typhimurium | ATCC 14028s | *fliC*::kan |
| NE2040 | Typhimurium | ATCC 14028s | *fljB*::cm |
| NE2041 | Typhimurium | ATCC 14028s | *fljB*::kan |
| NE2042 | Typhimurium | ATCC 14028s | *fliC*::cm |
| NE2043 | Typhimurium | ATCC 14028s | Δ*crl* |
| NE2044 | Typhimurium | ATCC 14028s | pKD46 |
| NE2045 | Typhimurium | ATCC 14028s | Δ*hfq* |
| NE2046 | Typhimurium | JR501 | pWRG730 |
| NE2047 | Typhimurium | VNP20009 | CheY+ Δ*ompC* |
| NE2048 | Typhimurium | VNP20009 | CheY+ Δ*ompC* pBS630 |
| NE2049 | Typhimurium | VNP20009 | CheY+ Δ*ompC* pBS631 |
| NE2050 | Typhimurium | VNP20009 | CheY+ Δ*ompC* pBS632 |
| NE2051 | Typhimurium | ATCC 14028s | Δ*ssaL* |
| NE2052 | Typhimurium | ATCC 14028s | Δ*dsbB* |
| NE2053 | Typhimurium | ATCC 14028s | Δ*yhfA* |
| NE2054 | Typhimurium | ATCC 14028s | Δ*yaiB* |
| NE2055 | Typhimurium | ATCC 14028s | ΔSTM14_1178 |
| NE2056 | Typhimurium | VNP20009 | CheY+ Δ*ompC* pTrc99a |
| NE2057 | Typhimurium | ATCC 14028s | Δ*yhdA* |
| NE2058 | Typhimurium | ATCC 14028s | Δ*sodC1* |
| NE2059 | Typhimurium | ATCC 14028s | Δgifsy_2 prophage |
| NE2060 | Typhimurium | ATCC 14028s | Δ*fliB* Δ*fljBA*::tet |
| NE2061 | Typhimurium | ATCC 14028s | Fla- w/pFliC chimera C |
| NE2062 | Typhimurium | ATCC 14028s | Fla- w/pFliC3 hypermotile |
| NE2063 | Typhimurium | ATCC 14028s | Fla- w/pFliC13 |
| NE2064 | Typhimurium | ATCC 14028s | Fla- w/pFliC11 |
| NE2065 | Typhimurium | ATCC 14028s | Fla- w/pFliC2 |
| NE2066 | Typhimurium | ATCC 14028s | NE2060 *fliC*::Ent FliC (FliC2) |
| NE2067 | Typhimurium | ATCC 14028s | Fla- w/ pFliC4 |
| NE2068 | Typhimurium | ATCC 14028s | Fla- w/ pFliC8 |
| NE2069 | Typhimurium | ATCC 14028s | Fla- w/pFliC10 |
| NE2070 | Typhimurium | ATCC 14028s | Fla- chim. 1 |
| NE2071 | Typhimurium | ATCC 14028s | Fla- w/pFliC5 |
| NE2072 | Typhimurium | ATCC 14028s | Fla- w/pFliC8 hypermotile |
| NE2073 | Typhimurium | ATCC 14028s | Fla- chimera C hypermotile |
| NE2074 | Typhimurium | ATCC 14028s | Fla- w/pFliC11 hypermotile |
| NE2075 | Typhimurium | ATCC 14028s | Fla- w/pFliC1 |
| NE2076 | Typhimurium | ATCC 14028s | Fla- w/pFliC2 |
| NE2077 | Typhimurium | ATCC 14028s | Δ*fliB* (clean) |
| NE2078 | Typhimurium | ATCC 14028s | Δ*fliB* (clean) w/pWRG730 |
| NE2079 | Typhimurium | ATCC 14028s | Fla- w/pFliC7 |
| NE2080 | Typhimurium | ATCC 14028s | NE2060 *fliC* D3 swap (FliC6) |

| | | | |
|---|---|---|---|
| NE2081 | Typhimurium | ATCC 14028s | Δ*fliB* Δ*fljBA* |
| NE2082 | Typhimurium | ATCC 14028s | Fla- pFliC DGKTEVV->GGGGGGG |
| NE2083 | Typhimurium | ATCC 14028s | NE2060 *fliC* ΔD3 (FliC3) |
| NE2084 | Typhimurium | ATCC 14028s | Fla- w/pFliC7 |
| NE2085 | Typhimurium | ATCC 14028s | Fla- w/pFliC ΔDGKTEVV |
| NE2086 | Typhimurium | ATCC 14028s | Fla- w/pFliC ΔDGKTEVV flare |
| NE2087 | Typhimurium | ATCC 14028s | NE2060 FliC11 |
| NE2088 | Typhimurium | ATCC 14028s | Fla- w/pFliC3 |
| NE2089 | Typhimurium | ATCC 14028s | NE2060 FliC8 |
| NE2090 | Typhimurium | ATCC 14028s | NE2060 FliC7 |
| NE2091 | Typhimurium | ATCC 14028s | NE2060 FliC4 |
| NE2092 | Typhimurium | ATCC 14028s | Δ*fliB* Δ*fljBA fliC*:kan w/pWRG730 |
| NE2093 | Typhimurium | ATCC 14028s | Fla- w/pFliC12 |
| NE2094 | Typhimurium | ATCC 14028s | Fla- w/pFliC9 |
| NE2095 | Typhimurium | ATCC 14028s | NE2060 FliC5 |
| NE2096 | Typhimurium | ATCC 14028s | Δ*fliB fliC*::kan w/pWRG730 |

Table 2. Strains of *Serratia marcescens*

| **Strain number** | **Parental strain** | **Genotype** |
|---|---|---|
| NE3001 | ATCC 274 | wild type |
| NE3002 | ATCC 274 | Δ*cpxRA* |
| NE3003 | ATCC 274 | Δ*fliC* |
| NE3004 | ATCC 274 | *pig*$^{q}$ |
| NE3005 | ATCC 274 | Δ*pigABCDEFGHIJKLMN* |
| NE3006 | ATCC 274 | *lacZ-pigA* fusion |
| NE3007 | ATCC 274 | spontaneous hypermotile (M37) |
| NE3008 | ATCC 274 | *lacZ-pigA* fusion, Δ*fliC* |
| NE3009 | ATCC 274 | Δ*luxS* |
| NE3010 | ATCC 274 | ΔSMATCC274_08100 |
| NE3011 | ATCC 274 | Δ*pigP* |